THESIS

FACIES ARCHITECTURE AND DEPOSITIONAL PROCESSES INCFLUENCING CARBONATE FACIES BELT DEVELOPMENT ALONG A LOW-INCLINED SHELF, HUK FORMATION, NORWAY, AND KOMSTAD FORMATION, SWEDEN

Submitted by

James J. Van Hook

Department of Geosciences

In partial fulfillment of the requirements

For the Degree of Master of Science

Colorado State University

Fort Collins, Colorado

Spring 2022

Master's Committee:

Advisor: Sven Egenhoff

Lisa Stright
Michelle Stanley

Copyright by James J. Van Hook 2022

All Rights Reserved

ABSTRACT

FACIES ARCHITECTURE AND DEPOSITIONAL PROCESSES INCFLUENCING CARBONATE FACIES BELT DEVELOPMENT ALONG A LOW-INCLINED SHELF, HUK FORMATION, NORWAY, AND KOMSTAD FORMATION, SWEDEN

Heterozoan, or temperate to cool water, carbonate successions can provide unique obstacles to establishing a typical depositional model that can be universally applied. Unlike their tropical realm counterparts, these carbonates are typically highly heterogeneous, occurring across a wide range of oceanographic and climatic settings, thus requiring a case-by-case approach to interpret any given depositional system. One such example is displayed in the Middle Ordovician aged Huk Formation of southern Norway, and Komstad Formation of Scania, Sweden. These formations are approximately 8m thick, corresponding to the Baltoscandian “Orthoceratite Limestone.” This study aims to explore the depositional processes influencing the facies development along a temperate-water, low-inclined carbonate shelf environment by characterizing and interpreting two formations along the shelf profile representing varying positions along the transect.

The Huk Formation consists of the lower Hukodden Member composed of mostly massive wackestone, a middle Lysaker Member composed of interbedded nodular to semi-nodular wackestone and carbonate mudstone, and an upper Svartodden Member composed of mostly massive packstone and some massive wackestone. The Komstad Formation is composed of an informal lower member, composed of mostly massive

wackestone, and an informal upper member composed of interbedded nodular and semi-nodular wackestone and carbonate mudstone with some massive wackestone beds. The facies of these formations can be grouped into seven carbonate facies: massive trilobite- and brachiopod-bearing calcareous mudstone (facies 1), bioturbated carbonate mud-wackestone (facies 2), planar-bedded fossiliferous wackestone (facies 3a), nodular to lenticular fossiliferous wackestone (facies 3b), mud-rich carbonate wacke- to packstone (facies 3c), massive fossiliferous packstone (facies 4a), and fossiliferous carbonate packstone pockets (facies 4b). These facies are ordered by increasing grain size as well as relative grain biodiversity, reflecting an overall increase in energy regime and subsequent decrease in water depth. These facies are further interpreted to represent the various processes and facies development on a low-inclined carbonate shelf, with massive packstones and wackestones occupying the proximal middle shelf environment, thin beds of nodular to semi-nodular wackestone in the distal middle shelf, and carbonate mudstone in the deep shelf environment.

Despite the overall decrease in energy regime at depth, the energetic influences on the carbonate facies changes indicate that storms had a prominent impact on their development throughout the succession. This along with the presence of bioturbation and burrowing throughout the succession indicate that even the distal most reaches of this succession was deposited above storm wave base in a well oxygenated and hospitable environment. These formations further reflect a relatively drastic sea-level fall compared to the over- and underlying dark graptolitic shales. Regional sea-level reconstructions identify a largely scale regression during the deposition of these carbonate successions relative to the overlying and underlying graptolitic siliciclastic

mudstones, identifying a relative sea-level low point within the middle of the succession at the transition from the Volkhov to the Kunda stage. Paleoenvironmental and paleoclimatic reconstructions of Middle Ordovician Baltoscandia indicate that environmental conditions during this time were generally relatively stable, suggesting that the fine-scale interbedded wackestone and mudstone characteristic of these formations could serve as excellent indicators of the fine-scale climatic and environmental fluctuations.

AKNOWLEDGEMENTS

First, I would like to thank my advisor, Dr. Sven Egenhoff for his guidance, enthusiasm, support, and mentorship throughout this project, as well as the countless hours spent advising me and thoroughly reviewing and counseling of this thesis. I would also like to thank the members of my committee, Dr. Sven Egenhoff, Dr. Lisa Stright, and Dr. Michelle Stanley, for their comments, feedback, and support of this project. I would also like to thank Dr. Per Ahlberg at the University of Lund for providing access to the Fågelsång-3 drill core for this project, as well as Dr. Gene Rankey at the University of Kansas for his review of an earlier version of the introduction

I would also like to thank my office mates in the sedimentology and stratigraphy working group that I had the absolute pleasure of working with during my time at Colorado State University, including Joel Spansel, Dr. Aleksandra Novak, Lindsay Mota, Ahmed Ali Abukhtwa, along with the many lifelong friends that I have made here at CSU. I would also like to thank my family for their incredible love and support in me taking on this project so far from home. Finally, I would like to thank my wife Emily, for her continued love, support, and encouragement throughout this project and our future endeavors.

TABLE OF CONTENTS

ABSTRACT…………………………………………………………………………………..…. ii
AKNOWLEDGEMENTS……………………………………………………………………….. v
LIST OF FIGURES………………………………………………………………………… vii
1.0 INTRODUCTION…………………………………………………………………….... 1
2.0 GEOLOGICAL SETTING……………………………………………………………. 5
3.0 METHODS…………………………………………………………………………… 13
4.0 SEDIMENTOLOGY…………………………………………………………………. 20
5.0 HARDGROUNDS…………………………………………………………………… 34
6.0 FACIES ARCHITECTURE…………………………………………………………. 36
7.0 DEPOSITIONAL MODEL…………………………………………………………... 40
8.0 DISCUSSION……………………………………………………………………….... 45
9.0 CONCLUSIONS……………………………………………………………………….. 59
REFERENCES…………………………………………………………………………... 62
APPENDIX A: INDIVIDUAL HUK OUTCROP AND KOMSTAD CORE LOGS…………. 71
APPENDIX B: THIN SECTIONS AND DESCRIPTIONS…………………………………. 77

LIST OF FIGURES

FIGURE 1: Location Map……………………………………………………………….………... 3
FIGURE 2: Paleogeographic Map……………………………………………………..……… 6
FIGURE 3: Stratigraphic Overview………………………………………………………… 8
FIGURE 4: Geological Map of Southern Norway…………………………………………… 9
FIGURE 5: Geological Map of Southern Sweden………………………………………….. 11
FIGURE 6: Composite Huk Formation Stratigraphic Column…………………………….. 14
FIGURE 7: Fågelsång-3 Drill Core Stratigraphic Column………………………………… 15
FIGURE 8: Outcrop Overview Photographs………………………………………………... 17
FIGURE 9: Paleocurrent Analysis…………………………………………………………… 19
FIGURE 10: Thin Section Photo-Micrographs……………………………………………... 21
FIGURE 11: Outcrop Example Photographs……………………………………………….. 35
FIGURE 12: Depositional Model……………………………………………………………….. 47
FIGURE 13: Comparative Sea-Level Reconstructions…………………………………… 54

1.0 INTRODUCTION

Early Paleozoic temperate-water carbonates, as with most heterozoan carbonates, present a unique obstacle to the established classification and interpretation of “typical” carbonate environments (Michel et al. 2018). Heterozoan carbonates refer to carbonate deposition in cool- to temperate water (Mutti and Hallock 2003; Pomar et al. 2004), dominated by skeletal grains and phototrophic red algae (Hallock 2015). In contrast to photozoan carbonates, which occur in the tropical realm, restricted to low latitudes (Ehrenberg et al. 2002; Dryer et al. 2018; Matonti et al. 2021), heterozoan carbonate deposits are typically highly heterogenous, occurring across a wide breadth of climatic and oceanographic conditions, thus limiting our ability to make predictive interpretations based on a schematic model. These types of carbonates are readily found in the rock record in the Upper Oligocene Attard member of the lower Coralline Limestone (Brando et al. 2009), and the Late Cretaceous Ensues-la Redonne syncline of southeastern France (Philip and Gari 2005), as well as in modern settings, for example, the rocky, coral dominated reefs of the Galápagos Archipelago (Reymond et al. 2015) and the red algae deposits of the Norwegian Fjord, (Sjøtun et al. 2015).

Another prime example of this is beautifully displayed in the Middle Ordovician succession of southern Scandinavia forming part of the microcontinent Baltica during the Early Paleozoic. Located approximately 40 - 45°S (Torsvik and Rehnström 2003; Cocks and Torsvik 2005), the microcontinent of Baltica was surrounded by cool to temperate water during this time (e.g. Cocks and Torsvik 2005). This is further reflected in the graptolite populations of this succession which is most similar to cool-water settings (Maletz and Egenhoff 2001; Maletz et al. 2011), in contrast to, for example, the time-equivalent populations of Laurentia (e.g. Cooper et al. 2001; Štorch et al. 2011). The present study will focus on two time-equivalent formations of the "Orthoceratite Limestone": the Middle Ordovician Huk Formation of the Oslo-Asker region of southern Norway, and the time-equivalent Komstad Formation of the Scania region of Sweden (Figure 1).

The Huk and Komstad formations of southern Scandinavia exhibit such temperate-water carbonates, and present an excellent case study into further developing and understanding the mechanisms governing these highly heterogeneous deposits. These formations present as mud-rich, fine-grained, skeletal grain dominated units, with few if any sedimentary structures preserved due to intense bioturbation (Owen et al. 1990). The sedimentary characteristics of these two carbonate units were investigated, describing in centimeter-scale detail a total of five outcrops of the Huk Formation in the Oslo-Asker region of southern Norway, along with a drill core of the time-equivalent Komstad Limestone recovered from the village of Fågelsång, Sweden (Figure 1). The facies documentations are supported by forty-five samples, twenty-five of which have been made into thin sections showing key intervals of the succession. Additionally, the orientations of two elongate nautiloid species found throughout the formation, orthocerid and endocerid cephalopods (Størmer 1953), were measured in order to reconstruct regional paleocurrent orientations.

The primary objective of this study is to enhance our understanding of the mechanisms governing and shaping an Early-Paleozoic temperate-water, low-inclined carbonate system as reflected by the Huk and Komstad Formations. This study will

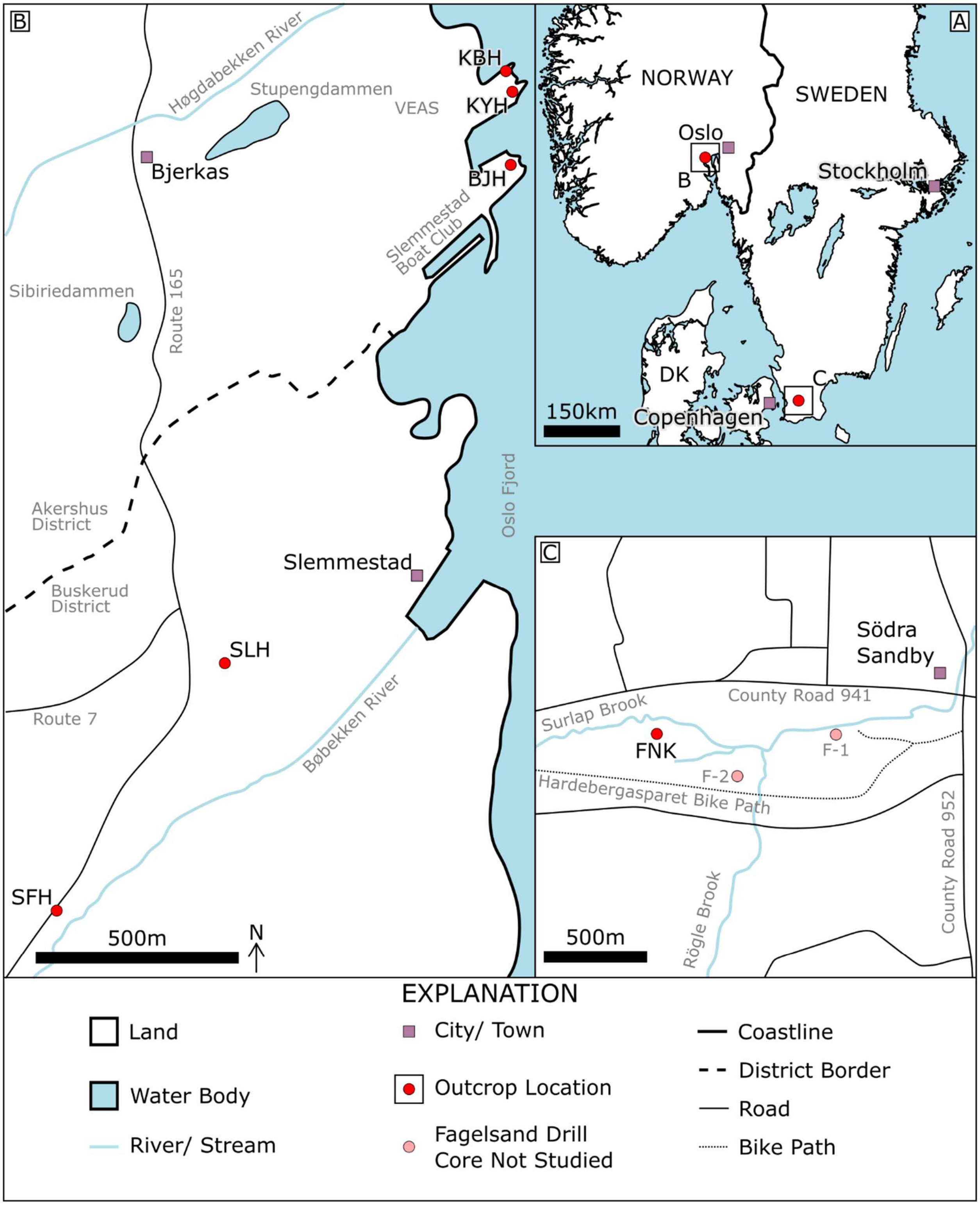

Figure 1. Location maps showing the localities studied in southern Scandanavia (A), the Huk Formation outcrop locations in the Asker region, Norway (B), and the Komstad Formation drill core location in Scania, Sweden (C). Locations F-1 and F-2 represent cores recovered from the same location as FNK, but not studied here. Komstad Formation map (C) modified from Maletz and Ahlberg (2018). Southern Scandanavia (A) and Oslo-Asker region (B) maps modified from Google Earth.

identify and describe the facies and facies architecture of the Huk and Komstad Formations in order to determine the primary climatic, oceanographic, and ecological mechanisms governing carbonate deposition in this sedimentary environment. Further, this study will determine the primary depositional processes at work in these formations in order to develop a depositional model that can inform heterozoan carbonate deposition within sedimentary systems similar to the Middle Ordovician succession of southern Scandinavia.

2.0 GEOLOGICAL SETTING

The Ordovician is a critical time interval in Earth history: it saw the initial breakup of the southern supercontinent Gondwana (Cooper et al. 2013), one of the largest biodiversification events during Earth's evolution (Cooper 2004), the maximum Paleozoic sea-level position (Cocks and Torsvik, 2002) as well as its subsequent drastic fall and related major extinction event at the end of this period (Schmitz et al. 2008). Baltica, one of the smaller continents during this time positioned approximately 40-45°S, consisted of large parts of present-day Scandinavia, the Baltic States, Poland, Belarus, and western Russia (Torsvik et al. 1991; Cocks and Torsvik 2005). Having moved north-eastwards during the Late Cambrian, Baltica continued this journey during the Ordovician and underwent an approximately 120° rotation (Torsvik and Rehnström 2003). It is assumed that a large portion of the Ordovician represented greenhouse climate conditions, nevertheless, most of the Upper Ordovician saw icehouse climatic conditions and the formation of polar ice caps culminating in the Hirnantian glaciation on the southern continents (Young et al. 2010).

During much of the Ordovician, Baltica was flooded by an epicontinental sea (Lindström 1971) with only a small part of the microcontinent above sea-level (Cocks and Torsvik 2005). The widespread marine shelf region surrounding this central exposed part of the continent was characterized by a local sandstone facies belt forming the shoreline, an adjacent carbonate facies belt further offshore, and a siliciclastic mudstone facies belt on the deep shelf (Figure 2) (Jaanusson 1976; Cocks and Trosvik 2002; Àlvaro et al. 2010). Climatic conditions during the Ordovician on

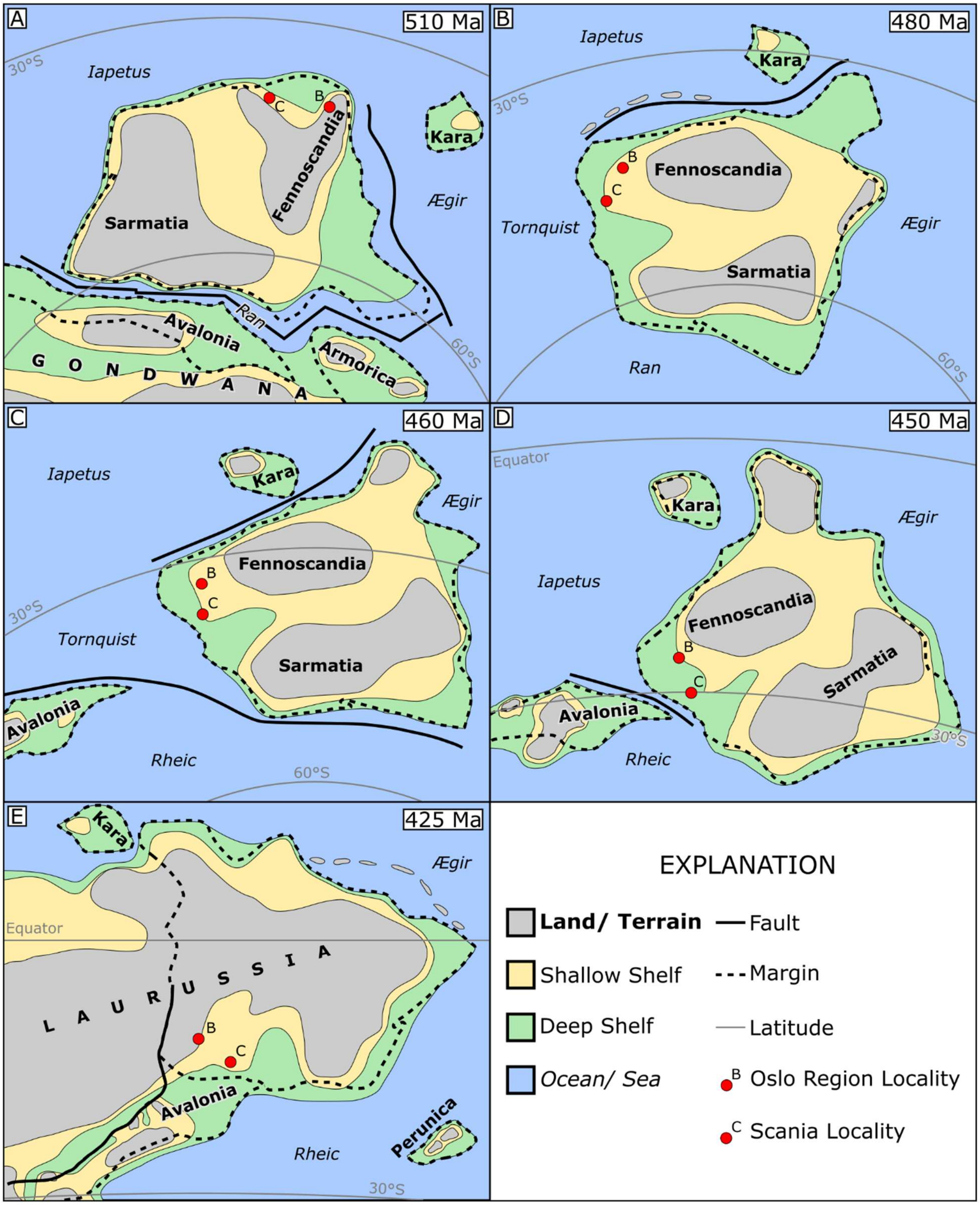

Figure 2. Paleogeographic maps of Baltica at 510 Ma (A), 480 Ma (B), 460 Ma (C), 450 Ma (D), and 425 Ma (E). These maps highlight the movement of Baltica and adjacent terranes from the Lower Cambrian through the Middle Silurian, as well as the aerial distribution of the exposed land and shelf development. Oslo region locality (B) and Scania region locality (C) are referenced as they are in Figure 1. Modified from Cocks and Torsvik (2005).

Baltica are envisioned to have been temperate to warm and relatively wet; however, temperatures likely increased towards the Late Ordovician as Baltica was migrating into the tropical realm (e.g. Munnecke et al. 2010).

In the Oslo-Asker region of Norway, the bulk of the Ordovician succession sits on top of the Middle Cambrian to Lower Ordovician Alum Shale and consists of alternating units showing mostly siliciclastic mudstones and carbonates (Figure 3) (Owen et al. 1990). The Alum Shale is overlain by the carbonate dominated Bjørkåsholmen Formation which lies below the Tøyen Shale, a dark, graptolitic siliciclastic mudstone unit (e.g. Egenhoff et al. 2010). The overlying Huk Formation consists of carbonate mudstone-wackestone alternations and is the focus of the present study; it shows a conformable contact with the Tøyen Shale and is in turn overlain by another graptolitic siliclastic mudstone unit in the Elnes Formation (e.g. Maletz et al. 2011). While the designation “Huk Formation” is limited to the Norwegian part of the succession, adjacent Swedish carbonate units that are approximately age-equivalent with the Huk Formation are referred to as the “Komstad Limestone” (e.g. Nielsen 1995). It has been interpreted that the alternating packages of carbonates in the Oslo-Asker region of Norway reflects changing sea-level throughout Ordovician times on the Baltica shelf (Jaanusson 1976).

The Huk Formation, between 6m and 8m in thickness in the Oslo-Asker region (Figure 4), is generally subdivided into three members: the basal Hukodden Member, the middle Lysaker Member, and the upper Svartodden Member (Owen et al. 1990). The Hukodden Member is a carbonate unit and consists of mostly carbonate mudstones and wackestones with minor packstones and very thin, dark mudstone laminae, showing some significant hardground development. This sub-unit is interpreted as

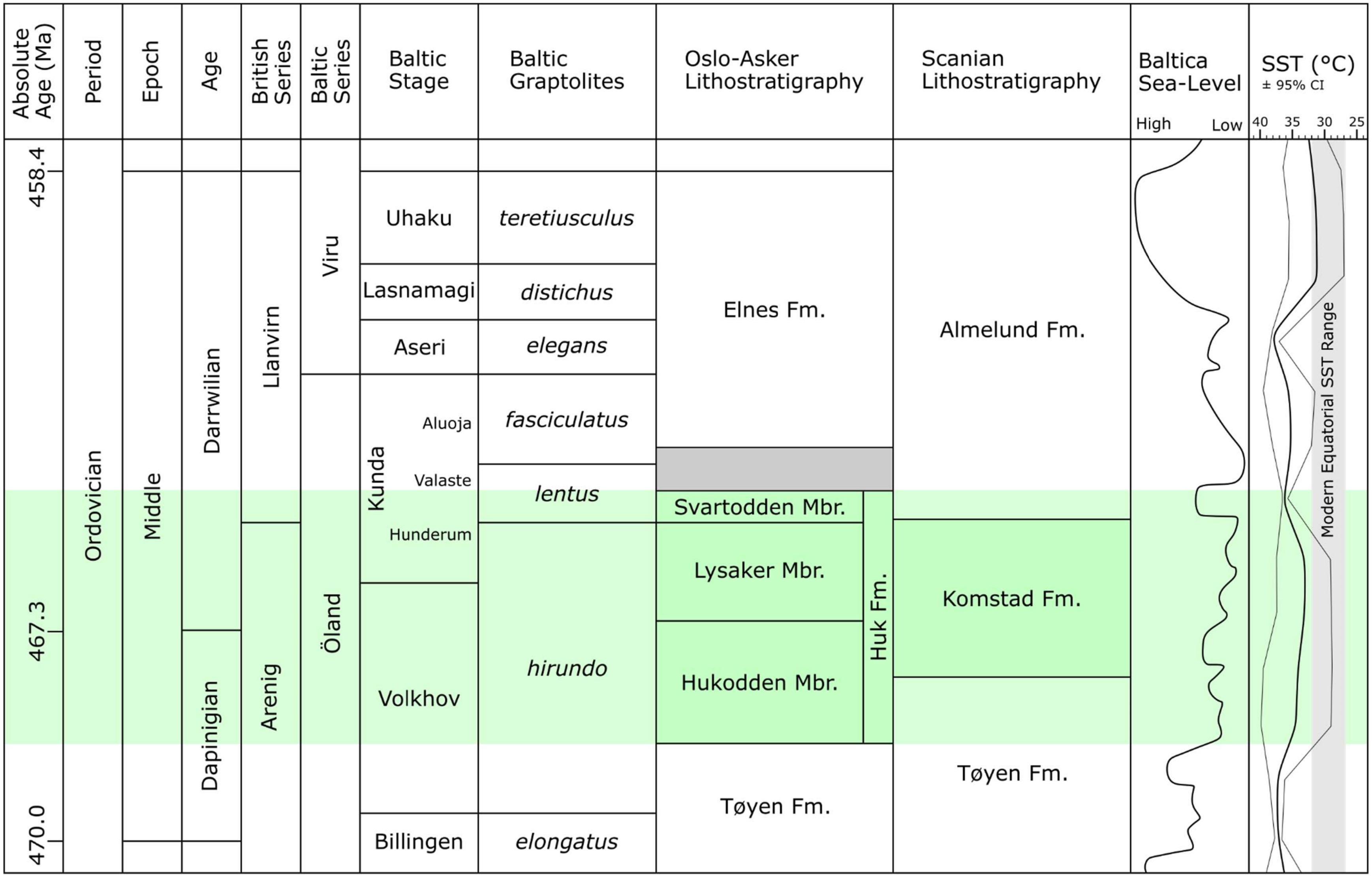

Figure 3. Stratigraphic overview chart showing the Middle Ordovician stratigraphy of the Oslo-Asker region, Norway, and Scania region, Sweden. Modified from Bruton et al. (2010), Nielsen (1995), Maletz and Ahlberg (2018), and Wu et al. (2018). Baltoscandian sea-level curve from Nielsen (2004). Sea surface temperature (SST) curve from Song et al. (2019). Absolute age dates modified from Walker et el. (2018). Huk Formation and Komstad Formation ranges highlighted in green for reference.

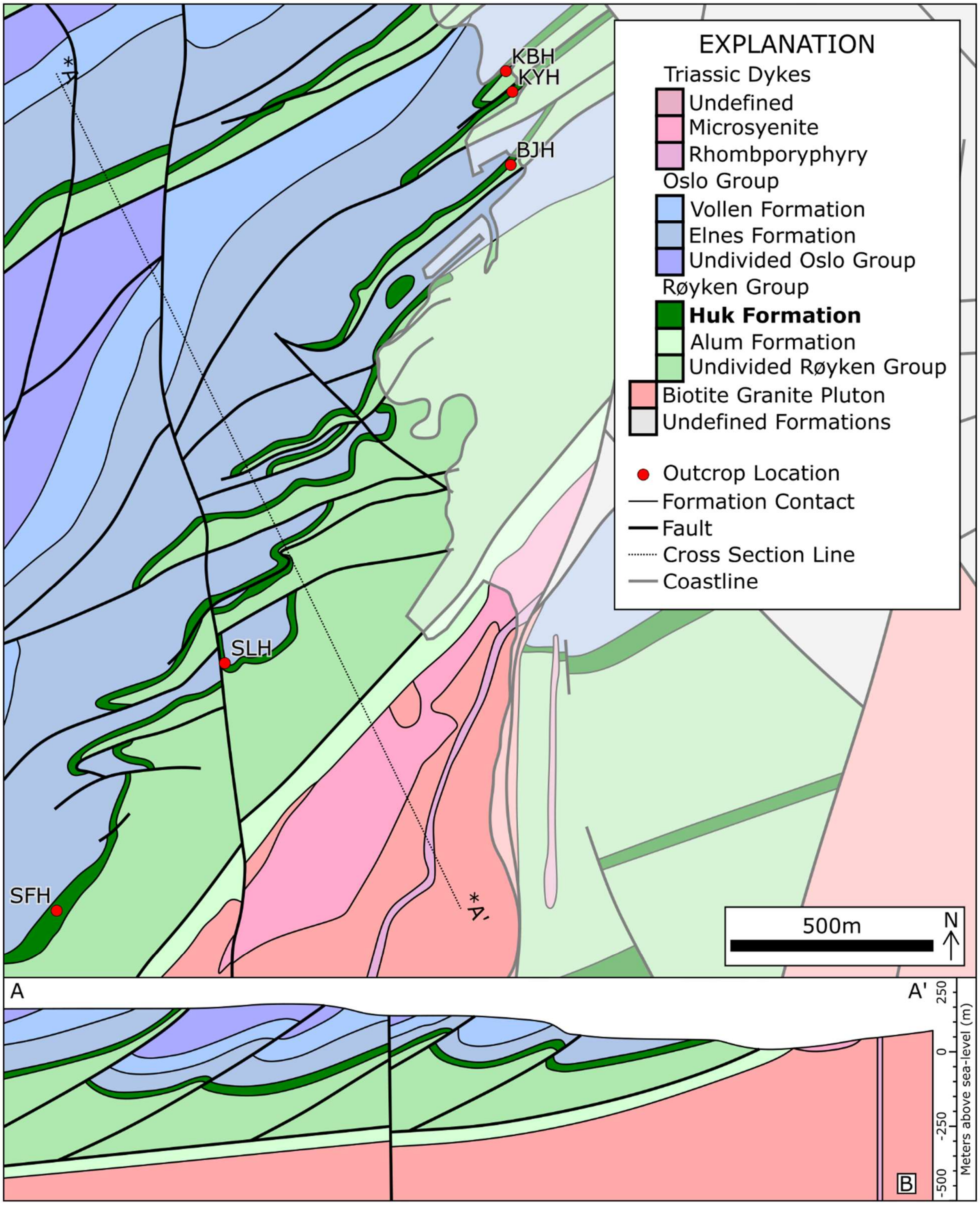

Figure 4. Geological bedrock map (A) and cross section (B) of the Asker region, Norway, modified from Lutro et al. (2017). Cross section should be used as approximate reference only. Transect line here is translated 1km NE from original position in Lutro et al. (2017). Undivided Oslo Group includes the Solvang Fm. the Nakkholmen Fm., the Frognerkilen Fm., and the Arnestad Fm. Undivided Røyken Group includes the Tøyen Fm., the Bjørkåsholmen Fm, and the Alum Fm.

carbonate deposition on a shelf transitional zone, with periods of non-deposition represented by the hardgrounds (e.g. Nordlund 1989; Ekdale et al. 2002). The middle Lysaker Member is formed by dominantly centimeter- to decimeter-thick dark greenish-grey to grey carbonate mudstones intercalated with beds of nodular wackestone. It is interpreted as representing a sea-level rise showing higher amounts of deep-water carbonate mudstones (Rasmussen 1991). The Svartodden Member, forming the top of the Huk Formation, is dominated by thick beds of wackestone and packstone, many preserving orthocerid and endocerid cephalopods (Kohut 1972), which gave the Huk its former name of “Orthoceras Limestone”, as well as other fossil fragments and evidence of burrowing. The Svartodden Member also contains some interbedded carbonate mudstones and is envisioned to represent a renewed sea-level fall in comparison to the underlying Lysaker Member. The sporadic high content of grains within this member has been interpreted by Hansen et al. (2011) to reflect deposition in a high-energy, shallow sea.

The Komstad Limestone, largely a time-equivalent of the Huk Formation found in southern Sweden (Tinn and Meidla 1999), was defined by Jaanusson (1960) as a southern, isolated extension of the Orthoceras Limestone, residing in a deep section of the Baltoscandian basin (Wu et al 2018) (Figure 5). Very similar to the Huk Formation, the Komstad Formation largely consists of carbonate mudstones and wackestones, with significantly less packstones than the Norwegian Huk Formation, containing beds of dark carbonate mudstone intercalated with nodular wackestones, and an abundance of glauconite that impregnates hardground surfaces throughout (Nielsen 1995). The formation is thought to represent several important sea-level fluctuations with an overall

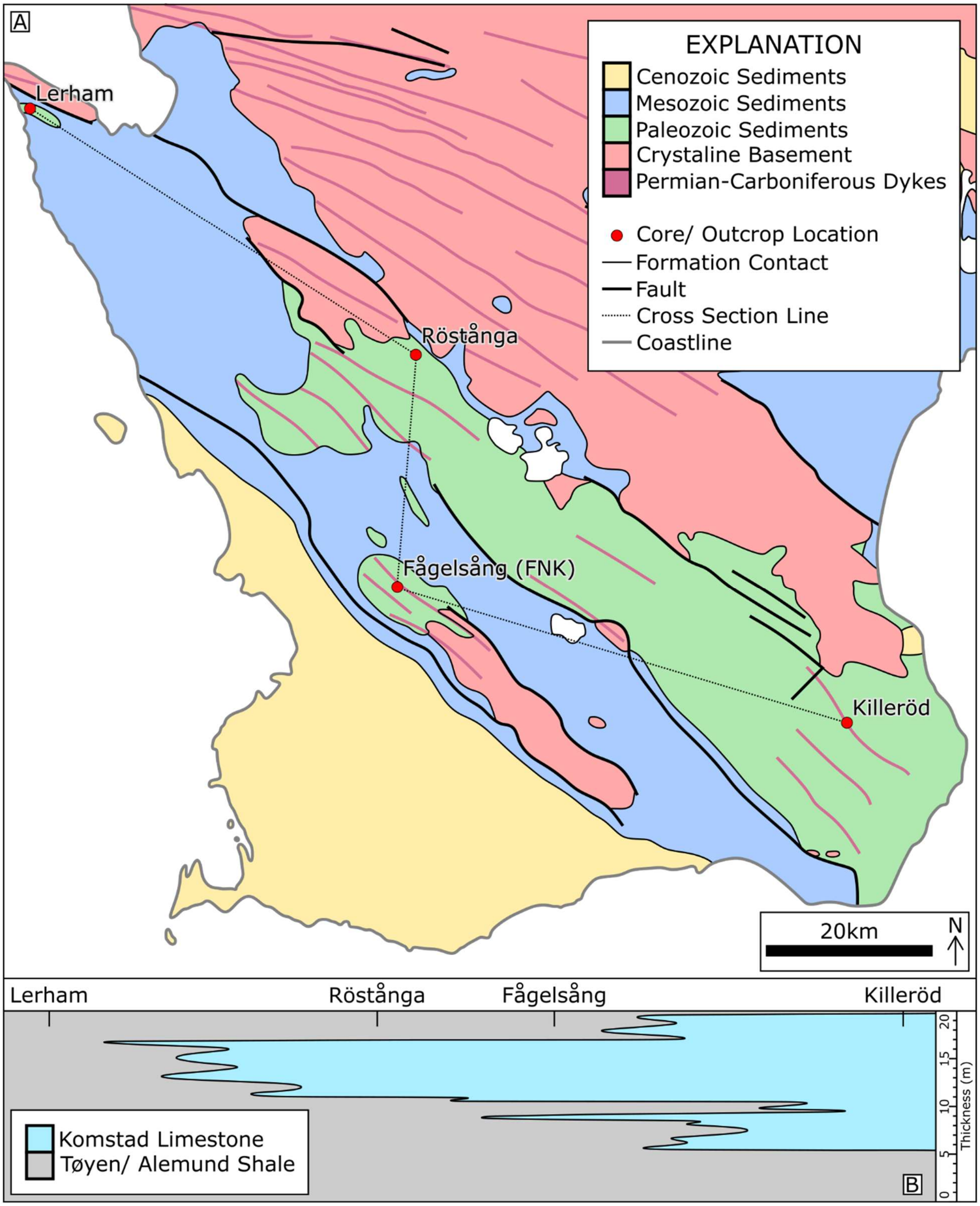

Figure 5. Simplified geological bedrock map of the Scania region of Sweden (A) and cross section of the thickness of the Komstad Formation throughout the region (B). Bedrock map modified from Martin (2014) and Erström et al. (1999) and shows sediments lumped by era. Cross Section modified from Nielsen (1995) to do thickness and distribution patterns of the Komstad Formation, and adjacent shale formations throughout the region. Komstad Formation is part of the Paleozoic Sediments on map A. FNK drill core recovery site located at Fågelsång

fall in sea-level relative to the over- and underlying siliciclastic mudstone-dominated units (Wu et al 2018).

3.0 METHODS

3.1 Outcrops and Core

Outcrop locations for the Huk Formation were chosen based on accessibility, exposure, and the identifiability of contacts both with the overlying and underlying formations. All outcrops were measured at centimeter-scale detail, with special attention to changes in lithology, fossil content and distribution, grain size changes, burrowing and burrowing intensity, or other significant changes in the rock (Figure 6) (Figure 7). A total of forty-five samples were collected from the five outcrops investigated in Norway, as well as six samples from the Komstad Limestone core. The five outcrops making up the Oslo-Asker region study location were composited together by averaging the thickness, quantity, and other key common features identified throughout this study location for the Huk Formation

The three northernmost outcrops are located on the northern side of the Djuptrekkodden Penninsula (KBH) and on the southern side of the same peninsula just north of the Vollen Båtservice shipyard (KYH), as well as on the Bjerkåsholmen peninsula, adjacent to the Slemmestad båtforening boat club (BJH) (Figure 1). These well exposed sections show all three members of the Huk Formation, as well as the contacts with the overlying Elnes Formation and the underlying Tøyen Formation. Further south, an incomplete exposure of the Huk was documented at a road cut near the Slemmestad Barneskole (SLH) (Figure 1). This outcrop preserves the lower Hukkoden member and middle Lysaker member of the Huk Formation, as well as the contacts with the underlying Tøyen Formation and the basal contact with the upper

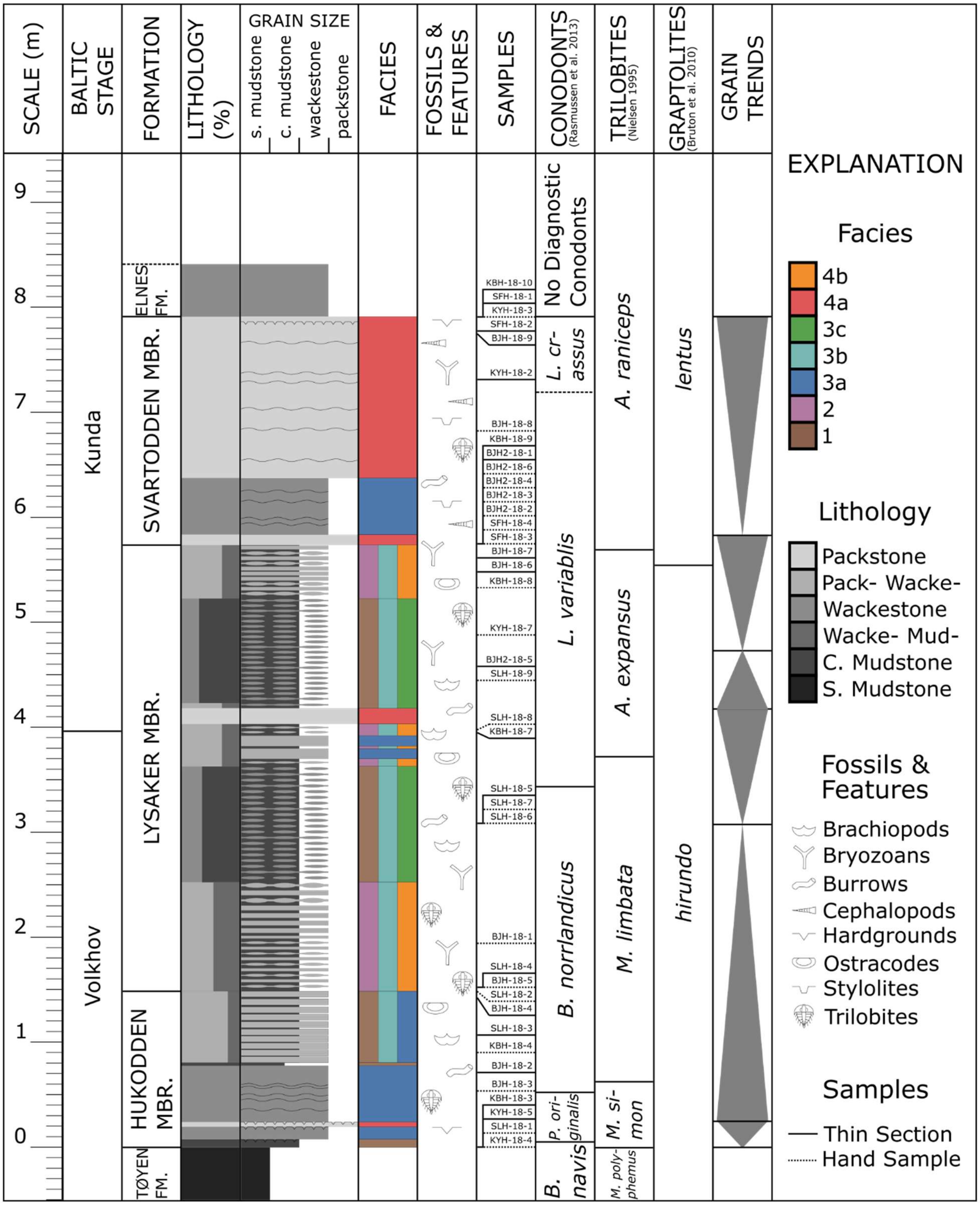

Figure 6. Composite log of the Huk Formation, combining the measured sections from all 5 locations in the Asker region. Compositing includes 3 complete sections of the Huk Formation (KBH, KYH, and BJH), one section missing the Svartodden Member (SLH), and one section where only the Svartodden Member is exposed (SFH). Conodont biostratigraphy from Rasmussen et al. 2013. Trilobite biostratigraphy from Nielsen (1995). Graptolite biostratigraphy Bruton et al. (2010). Carbonate mudstone is abbreviated to "c. mudstone" and siliciclastic mudstone is abbreviated to "s. mudstone."

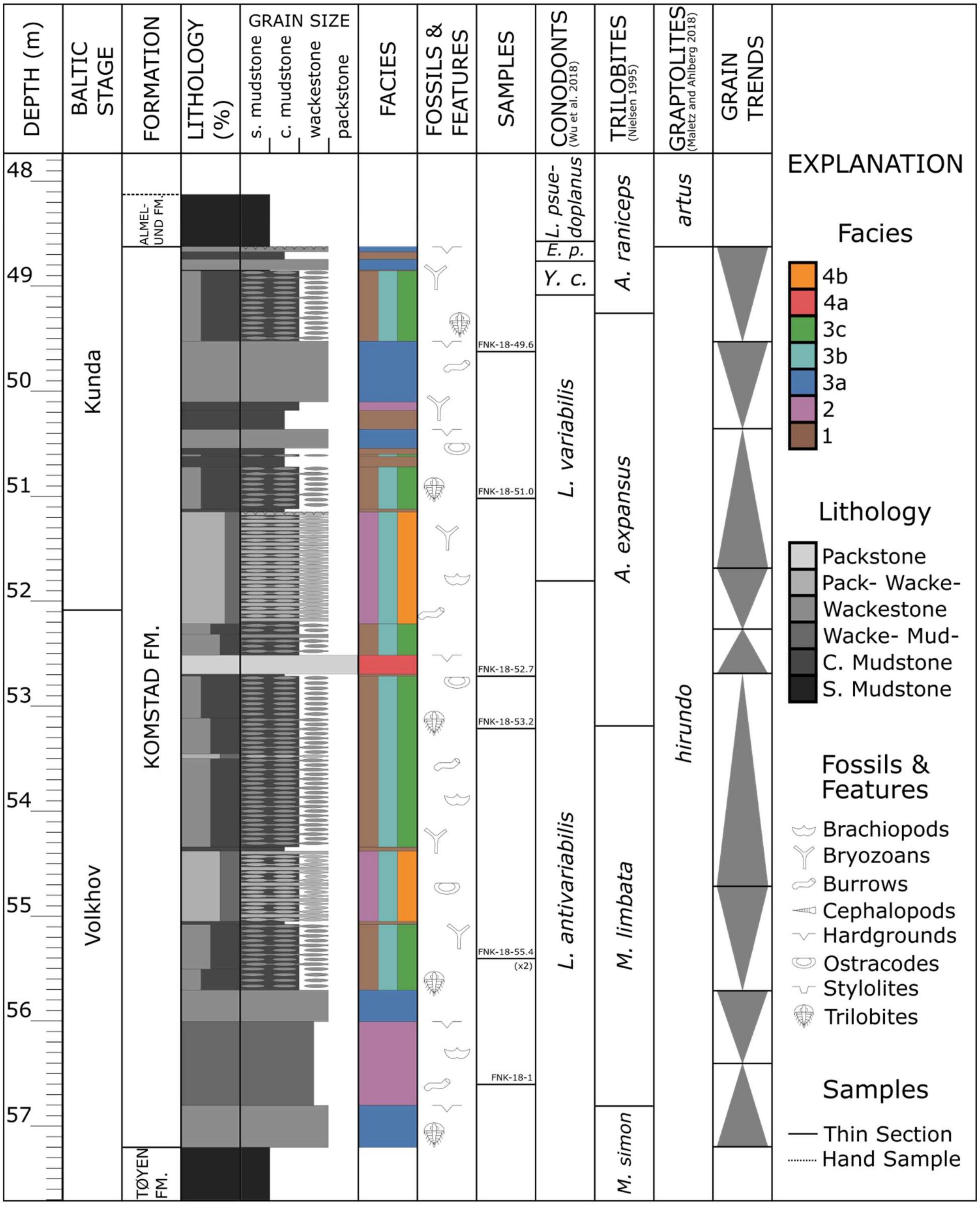

Figure 7. Log of the Komstad Formation section of the Fågelsång-3 drill core recovered from Scania, Sweden. Conodont biostratigraphy from Wu et al. (2018). Trilobite biostratigraphy from Nielsen (1995). Graptolite biostratigraphy from Maletz and Ahlberg (2018). Here, the E. pseudoplanus conodont zone is abbreviated to "E. p.", and the Y. crassus conodont zone is abbreviated to "Y. c." Carbonate mudstone is abbreviated to "c. mudstone" and siliciclastic mudstone is abbreviated to "s. mudstone." Duplicate samples were taken from FNK-18-55.4 for thin section.

Svartodden member. The fifth outcrop in the Oslo-Asker region is located at the Slemmestad Football Arena (SFH) (Figure 1). This outcrop, while it only contains the upper Svartodden member of the Huk, is widely regarded as a world-class outcrop and one of the largest fossil exposures in the country (Trilobites of Norway 2020). The Fågelsång-3 drill core was recovered near the village of Fågelsång in southern Sweden (FNK) (Figure 1) and provided by Lund University. The core contains a complete succession of the Komstad Limestone, along with the contacts of the underlying Tøyen Formation and the overlying Almelund Formation (Bergström et al. 2018). (Figure 8) For field logs of the individual outcrops in the Oslo-Asker region, and the Fågelsång-3 drill core, see appendix A.

3.2 Thin Sections

Of the forty-five samples of the Huk Formation and Komstad Limestone, twenty-five samples were glued, cut, and prepared for thin section analysis; eighteen of the samples originated from the outcrops in the Oslo-Asker region and seven samples were prepared from the Fågelsång-3 drill core. Thin sections consisting primarily of carbonate wacksetone and packstone were prepared to a thickness of 30µm, while samples consisting primarily of carbonate mudstone were made thinner to a thickness of 20µm in order to observe fine details in these rocks. All thin sections were cut to a standard size of 27mm by 46mm and were prepared to show one polished surface. Thin sections were described and classified according to the Dunham (1962) carbonate classification scheme modified by Embry and Klovan (1971), and visual estimations of component compositions were made following Baccelle and Bosellini (1965). All samples were analyzed in plain polarized light and cross polarized light using a Nikon Eclipse Ci

Figure 8. Photographs of outcrop loactions and core. Complete exposures of the Huk Formation are found at KBH (A), KYH (B), BJH (C). Incomplete exposures are found at SLH (D) where the upper Svartodden Member is missing, and at SFH (E) where only the Svartodden Member is exposed. Photos of the complete Komstad Formation core recovered from FNK (F) are also shown.

Microscope and accompanying Nikon DS-Fi2 microscope camera for capturing photomicrographs. For photo micrographs of all thin sections, see appendix B.

3.3 Paleocurrent Analysis

The Huk Formation contains a number of fossils, but it is best known for the orthocerid and endocerid cephalopods, having given the formation the local stratigraphic terms "Orthocerite Limestone" and "Endoceras Limestone" (Størmer 1953). These fossils have a relatively straight conical shape that allows them to orient themselves in the direction of paleocurrent during deposition. Following the death of the cephalopod, and subsequent deposition on the sea-floor, the thicker and heavier end of the conch serves as the anchor point, allowing the thinner and lighter end to move and point in the direction of flow (Figure 9) (Dixon 1970). To analyze the direction of paleocurrent at the time of deposition, seventy-five orientation measurements were made of the orthocerid and endocerid cephalopod fossils within the Huk Formation outcrops in the Oslo-Asker region. These data points were then plotted on rose diagrams to determine primary paleocurrent orientation (Figure 9) using the GeoRose rose diagram software.

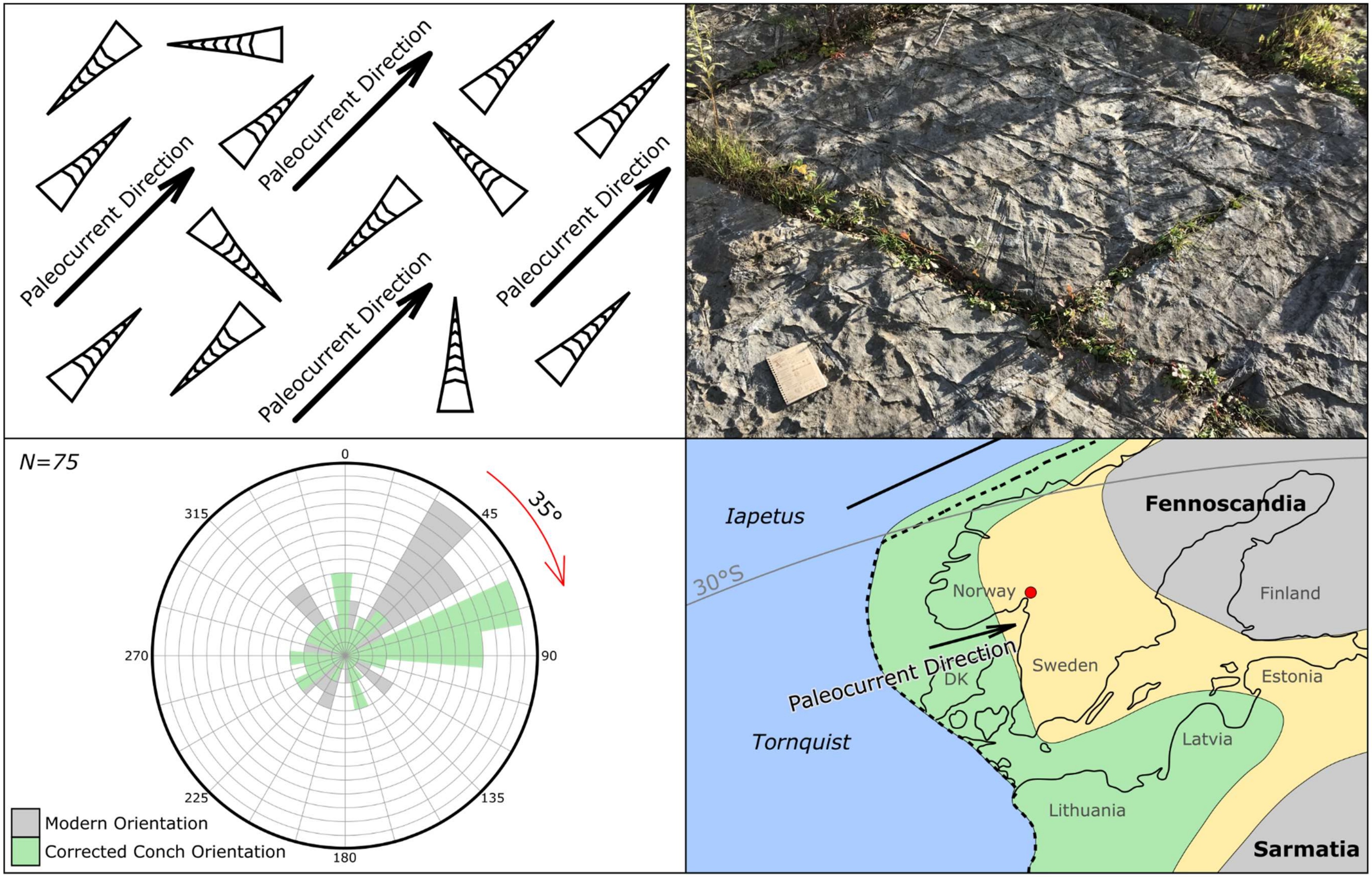

Figure 9. Diagrammatic representing of Cephalopod coch orientation relative to current, with the apex oriented into the direction of the current (A). Photograph of the upper surface of the Svartodden Member at SFH showing abundant Endocerid Cephalopods (B). Rose diagram reults of the conch orientation analysis (C) which has been rotated clockwise by 35° to reflect current direction relative to the time of deposition. Paleogeographic map showing the location of the Huk Formation outcrops studied for this analysis, and the direction of the prevailing paleocurrent relative to the continental arrangement 460 Ma (D), modified from Cocks and Torsvik (2005).

4.0 SEDIMENTOLOGY

4.1 Facies 1: Massive Trilobite- and Brachiopod-Bearing Calcareous Mudstone

Facies 1 is a carbonate mudstone containing some broken biogenes and bioclasts that are predominantly carbonate in composition (Figure 10A), mostly between 0.1mm and 0.2mm in size and have a maximum length of 0.5mm. The biogenes are predominantly trilobite and brachiopod debris that preserve characteristic internal shell structures as well as outer relief. Less than 5% of biogenes are remnants of crinoid stems, bryozoans, and conodonts, the latter ones phosphatic in composition. Rarely, other phosphatic bioclastic grains occur, are sub-millimeter in size and make up less than 0.1 vol% of the rock. Beds of facies 1 are between 10mm and 200mm thick. All grains are angular to sub-angular and only appear rounded if their original form was roundish already. The grains are swimming in a fine-grained carbonate mud matrix that contains varying amounts of clay minerals (as much as 10 vol%) with the grains either appearing in clusters or isolated. Facies 1 is massive and devoid of sedimentary structures. Its color varies between light brownish grey to dark grey in both outcrop and thin section. Contacts to over- and underlying facies are sharp. The orientation of all particles is generally random; however, some of the elongate grains show a sub-parallel to parallel arrangement to bedding. There are two types of distinct burrows in this facies: *Skolithos* isp. and *Thalassinoides* isp .Burrows in thin section are up to 1.5 mm in height and 3 mm in width (Figure 10); they have a matrix that is generally finer-grained than the matrix of the rock but contains significantly more carbonate debris. In most cases carbonate grains are arranged concentrically in the outer parts of the

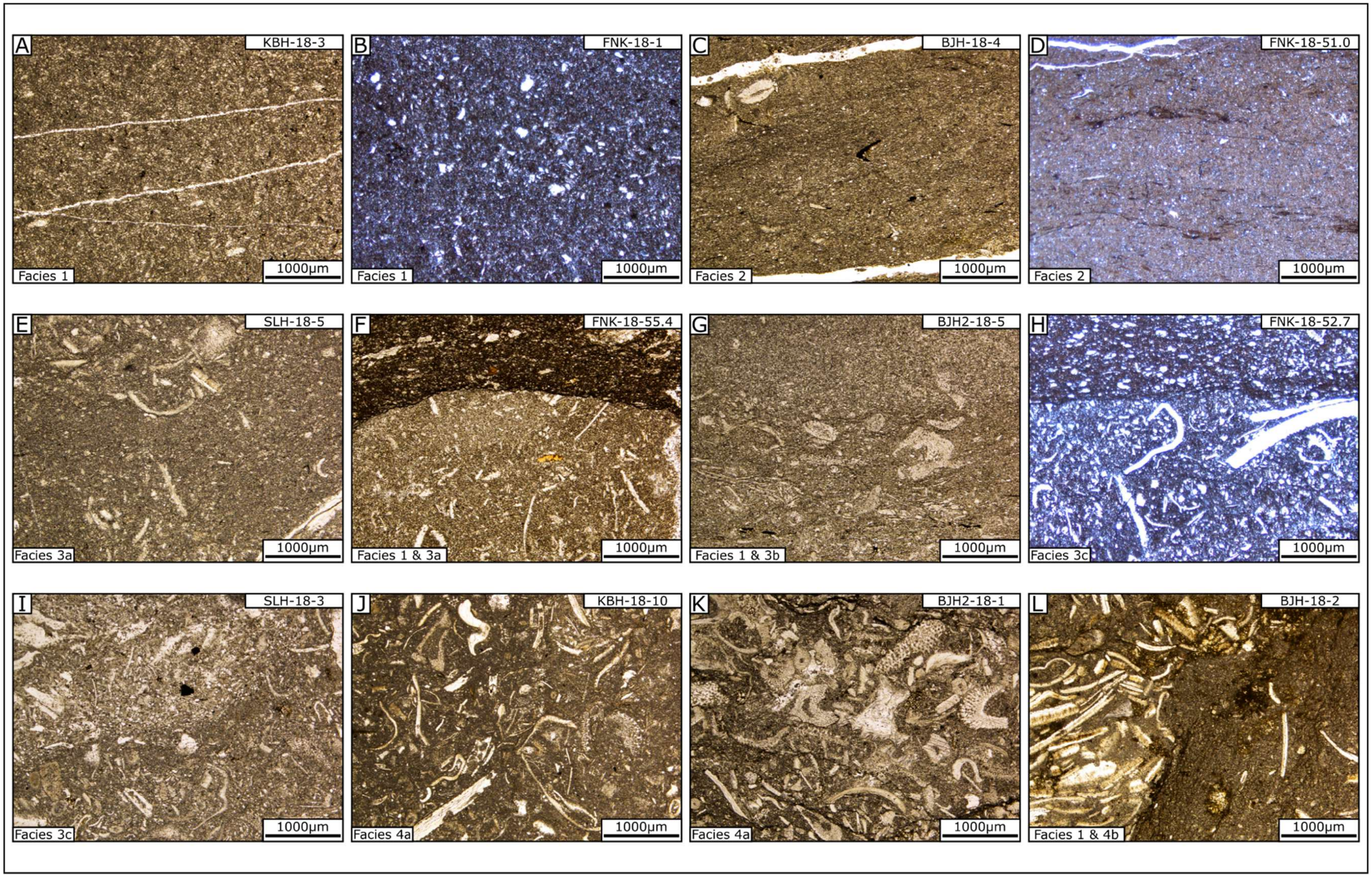

Figure 10. Photomicrograph examples of the facies identified in this study. Facies 1 with calcite seams (A) and heavily recrystalized facies 1 (B). Facies 2 with calcite seams (C, D). Facies 3a biogene bearing massive carbonate wackestone (E). Contact between facies 1 and facies 3a (F). Contact between facies 1 and the nodular wackestone of facies 3b (G). Facies 3c wacke- and packstone with bioclasts and trilobite and brachiopod fragments (H, I). Facies 4a mud-rich carbonate packstone with varying amounts of fossil content (J, K). Facies 4b packstone scoured into carbonate mudstone (L). See appendix A for more detailed descriptions.

burrow structure. Phycosiphonid fecal strings are present throughout facies 1 and show a matrix and clay-rich fill (Figure 10B). The bioturbation index (BI) index of this facies is 6 following Taylor and Goldring (1993). In places, facies 1 can be strongly recrystallized and contain pyritized biogenic grains. Some thin sections show calcite-filled fractures that have angles parallel to about 45° to bedding; only few of them show an orientation perpendicular to bedding. They are laterally continuous, do not show thickness changes and vary in thickness between 50µm and 3 mm. In places, calcite filled veins can be observed, in places cross cutting each other (Figure 10A)

4.1.1 Facies 1 Interpretation

The mudstones of facies 1 reflect an overall tranquil setting based on their generally small grain size. However, the presence of some broken biogenes and the generally fragmented bioclasts indicate some amount of energy that was at play during deposition of this facies; similarly, the sharp bases of facies 1 deposits reflect relatively high rather than low energy conditions during sedimentation of the carbonate mudstones. Both of these observations together indicate that changing energy conditions were most likely responsible for the deposition of facies 1. During most of its sedimentation history conditions at the seafloor must have been quiet as indicated by the mudstone (e.g. Schieber et al. 2013). Nevertheless, at times high energy events, likely storms, stirred up the mud, concentrated and transported the large biogenic grains and thereby broke a fair amount of them. After deposition, burrowing distributed the grains and destroyed most if not all evidence of storm related influence.

The composition of the grains reflects a somewhat diminished variety in comparison to other over- and underlying facies; however, the environment must have been hospitable as is also reflected in the bioturbation intensity and amount of clearly recognizable burrows; similarly, the random distribution of grains reflects the high degree of bioturbation. This facies also record minor amounts of sediment starvation which is indicated in the phosphates (e.g. Nordlund 1989). As all the other grains, also the phosphates were re-distributed by burrowing. While the *Thalassinoides* burrows can be indicative of relatively shallow as well as deep water (Benton and Harper 1997) the *Skolithos* burrows are exclusive to a very shallow water environment (Seilacher 1967; Bromley 1996). It is therefore likely that at least some of this facies was deposited in relatively shallow waters. Subsequent to sedimentation and induration facies 1 deposits were subjected to brittle deformation which resulted in at least three generations of fracture formation reflected in their cross-cutting relationships.

4.2 Facies 2: Bioturbated Carbonate Mud- Wackestone

This facies consists of mostly carbonate mud with some amount of siliciclastic fine-grained components in the matrix. The grains are brachiopod and other shell debris of unknown organisms, recrystallized carbonate coarse silt to fine sand-size grains, silt-size quartz grains, conodonts, and organic matter flakes that are generally sub-millimeter but can be up to a millimeter long. The grains make up between 7 and 15 vol% of the rock (visual estimation). All grains are angular to sub-angular except the quartz grains that are generally well-rounded. The sediment is moderately well sorted with especially the larger grains often arranged along bedding planes. All grains are matrix-supported (Figure 10C, Figure 10D). The thickness of beds of this facies is several centimeters to some decimeters. The matrix makes up between 93 and 85 vol% of the rock and consists mainly of carbonate mud with varying amounts of clay and organic matter. Bedding is visible in parts of this facies and generally paralleled by the organic matter flakes. Grading is absent in these mud- to wackestones, and so are sedimentary structures. This facies shows irregular patches in which burrowing is absent, which are slightly darker in color and contain higher amounts of organic matter flakes than neighboring parts of the rock. The color of this facies in outcrop is dark brown to black, and it is medium grey to tan/brown in thin section. Contacts to over- and underlying facies are generally sharp. Large fossil pieces are always broken; small fossils such as conodonts are generally intact. The orientation of fossils can be random but in other places they form bed-parallel accumulations of shells and shell debris. Distinct burrows are rare, diffuse burrowing ubiquitous; however, some *Planolites isp*. are present and contain a fill that is slightly lighter-colored tan the matrix. The BI index is about 3. Porosity is exclusively present as minus-cement porosity in recrystallized biogenic fragments. Pyrite is present as sub-millimeter crystals and generally associated to the organic matter flakes.

4.2.1 Facies 2 Interpretation

The two grain sizes present in this facies deliver opposing views on the energy level that this facies reflects. The dominance of carbonate mud, the presence of some amounts of siliciclastic mud and the fact that this facies is mud-supported all indicate relatively quiet depositional conditions for this lithology. However, both the carbonate mud (Schieber et al. 2013) as well as the siliciclastic mud (Schieber 2003; Schieber et al. 2007; Egenhoff and Fishman 2013) may as well have been transported by currents and therefore show the opposite – energetic conditions during sedimentation. Similarly, the sand-size well-rounded quartz grains ubiquitous in this facies indicate some amount of transport energy and not entirely quiet conditions. However, the non-bioturbated portions of this facies which are fine-grained as well as the amount of organic matter especially abundant in non-bioturbated patches reflects tranquil sedimentary conditions. In order to integrate both of these observations it is most likely that this facies was deposited by some high-energy events, likely storms, with periods of quiescence representing fair-weather deposition in-between.

The source of the sediment is interpreted as being very different for the carbonates and the siliciclastic components: the carbonates likely originated in this marine setting itself, using the Bahamas as one possible comparison (e.g. Dryer et al. 2018) likely in the shallow portion of the Baltica shelf. The siliciclastics, however, probably stem from the exposed part of the Baltic Shield and must have been transported into the marine realm mostly by rivers. This is also reflected in their excellent rounding indicating a significant transport distance from their place of origin to where they were deposited. The depositional environment of this facies must have been well oxygenated. This is reflected in the amount of fossil remains including *Planolites isp*. as well as the abundance of bioturbation reflected in both fecal strings and the random orientation of shells interpreted as being displaced by burrowing organisms.

4.3 Facies 3: Wacke- and Wacke- to Packstones

The carbonate wackestones of facies 3 contain between 10 vol% and 25 vol% of biogenes and bioclasts. Grains are generally intact and do not show rounding or sorting. Basal contacts with this facies are sharp and abrupt with facies 4a; however, top contacts with the same facies can be gradational. Any other contact of facies 3 with e.g. facies 1 or 2 at the base or top, are generally somewhat gradational. The matrix of facies 3 consists mostly of carbonate mud and some amount of clay (between 3 vol% and 5 vol%) which accounts for the massive nature of the rock. This facies does not contain any internal laminations, grading, or sedimentary structures. It is light grey to light tannish grey in outcrop and core, and tan to brown in thin section. In places, elongate phosphatic grains occur that make up between half and 1 vol% of this facies; they are between 50μm to 200μm in diameter, structureless, and sub-angular to sub-rounded. Throughout this facies, irregular zones of dark-colored, preferentially carbonate mud-filled sediment are visible in thin section that contain mostly bioclasts and only some biogenes; they are overall much less particle-rich with only about 15 vol% grains than the bulk of this facies. Their width varies from sub-millimeter to about 3mm. The bioturbation index of facies 3 is 5 to 6 (based on Taylor and Goldring 1993). The irregular, carbonate mud-rich zones also contain the bulk of dissolution seams (Bathurst 1982) in this facies. Facies 3 contains some euhedral pyrite preferentially but not exclusively in the irregular carbonate mud-rich zones. The carbonate wackestones are here subdivided into two sub-facies: sub-facies 3a – planar-bedded fossiliferous wackestone, and sub-facies 3b – nodular to lenticular fossiliferous wackestone.

4.3.1 Sub Facies 3a: Massive Fossiliferous Wackestone

The biogenes in these rocks are primarily brachiopod and trilobite shells, with <5 vol% of crinoids (Figure 10E, Figure 10F). In general, biogenes are more common than bioclasts in this sub-facies; nevertheless, most of the biogenes and all bioclasts are broken. Beds of this sub-facies are between 100mm and 500mm thick and do not show any or very little lateral variability in their thicknesses within an outcrop or core. The matrix consists primarily of carbonate mud but is often strongly recrystallized. In general, all elongate grains display a weak preferential orientation parallel to bedding with most of them being oriented at 5° to 40° relative to bedding. Distinct roundish burrow cross-sections have not been observed in this sub-facies.

4.3.2 Sub Facies 3b: Nodular to Lenticular Fossiliferous Wackestone

The biodiversity of this sub-facies is low, biogenes consist primarily of trilobites and brachiopods with minor amounts of bryozoans and conodonts. The majority of organism-derived grains are bioclasts which make up between 80 vol% to 85 vol% of grains in this sub-facies. Most biogenes and all bioclasts are fragmented in nature (Figure 10G). The matrix is generally carbonate mud that is not recrystallized. All grains are oriented at various angles to bedding, with no apparent preferential orientation. *Thalassinoides* isp. burrows occur in this facies and are typically 0.4mm in height and 0.8mm in width. They appear in a slightly flattened, elliptical shape parallel to bedding, with thin (>5μm) halos of dark, clay-sized material surrounding the rims of the burrows.

4.3.3 Sub Facies 3c: Mud-Rich Carbonate Wacke- to Packstone

The dark-colored wacke- to packstone consists of medium silt to sand-size components, the largest one several millimeters in size that are composed of calcite and generally make up between 20 and 30% of the rock volume; in places, the grain abundance is below 15 vol%. All grains are either poorly or not rounded, and sorting is also poor. Grains are organized into irregular several millimeter-thick laminae containing packstones with streaks of carbonate wackestones in-between (Figure 10H). The thickness of beds of this facies is in the range of several centimeters to some decimeters. This facies is primarily mud-supported, and in places grain-supported. The matrix is dark brown in color and consists of predominantly carbonate mud; it contains a small percentage of clay and other impurities that account for the dark color of the sediment. The matrix generally makes up between 70 and 80 vol% and only in places up to 85 vol% of the rock. Despite the stringers of carbonate wackestones, most of this facies is massive and shows neither grading nor any sedimentary structures (Figure 10I). However, it is organized into several millimeter to centimeter-size roundish to irregular features that are often bound by dissolution seams.

While in thin section this facies is dark brown, it is black in core and fresh hand samples. Contacts to over- and underlying facies are sharp. Carbonate wacke- to packstone grains of this facies consists mostly of recrystallized pieces of biogenic particles that are unrecognizable (bioclasts). However, the larger grains often preserve their inner or outer structure and are crinoids and other echinoderms, shell debris, either of unknown origin or from brachiopods, bryozoans, and some trilobites. All grains are randomly oriented and are, with few exceptions, broken. Distinct burrow cross sections are uncommon but are around one millimeter in diameter; they are filled with carbonate mud. The BI index is estimated at 3-4. Cement-filled porosity is absent in many thin sections; however, it may be present as part of burrow fills in places. Up to one millimeter-thick roughly bedding-parallel cement-filled features that are up to 15 millimeters in length occur; they are generally filled with at least one, mostly two generations of cement: a cloudy outer rim which is often the only cement filling these features, and in places a clear cement containing large crystals (up to several hundred micrometers in size). All carbonate particles are recrystallized to some degree. This facies contains dissolution seams every few centimeters throughout the succession.

4.3.4 Facies 3 Interpretation

The relative abundance of biogenic grains, particularly the shelly remains, in this facies is interpreted to reflect that a certain amount of energy was likely involved in depositing this facies. A relatively high-energy deposition of the biogenic hard parts is also indicated in their generally broken nature and the in places sharp contacts to underlying facies; gradational top contacts, even though at the bed level, are typical for tempestites (e.g. Aigner 1985). Nevertheless, deposition of the carbonate wackestones also experienced quiet conditions in which the carbonate mud could settle in-between the grains; this was likely a settling from suspension, but this cannot be reconstructed because of later overprint of the texture by intense burrowing. This discrepancy in interpretation of facies 3 sedimentation based on the grain size is most likely a reflection of its episodic deposition: during high-energy events, likely storms, the coarse grains were deposited, probably in laminae. Once these storms calmed down the carbonate mud was laid down on top and in-between the grains. Fair-weather sedimentation resumed which was likely also characterized majorly by carbonate mud. Nevertheless, the environment was probably well oxygenated; this is reflected in the relatively high biodiversity, the abundance of organism hard parts in this facies, and the irregular zones filled with mostly carbonate mud that are here interpreted as oblique cuts through burrow structures. The phosphatic grains probably indicate time of little sediment delivery and sediment starvation (Nordlund 1989); however, as they only occur reworked it is likely that at least some amount of transport was involved prior to deposition. This transport maybe from a site very close by or further away; the mixing may also mainly reflect the burrowing which may be responsible for their random occurrence in the sediment.

4.4 Facies 4: Packstones

This facies is a massive, biogene- and bioclast-rich carbonate packstones. Its grains are calcitic in composition and make up between 40 vol% and 50 vol% of the rock. All grains display poor or no rounding, and sorting is equally poor. This facies is entirely grain-supported although nearly all pore spaces are filled with carbonate mud. The matrix consists exclusively of carbonate mud and contains little (less than 3 vol%) clay-sized minerals. Grading is absent, and so are sedimentary structures. In outcrop and core, this facies generally appears as light grey to light orangish grey, and in thin section as light orangish brown to dark brown, with grains appearing as light grey. Contacts with this facies are abrupt and sharp; beds over- and underlying this facies are generally mud-rich (facies 2 to 3). The majority of grains in this facies are bioclasts that range from sub-millimeter to about one millimeter in size. Most biogenes and all bioclasts are broken; some are sub-rounded but most of them are angular to sub-angular. Dissolution seams (Bathurst 1982) are somewhat common within this facies. They are constituted of thin (>1mm), undulating features and are outlined by clay and iron oxide particles. In places, these dissolution seams grade into stylolites. This facies contains minor amounts of sub-millimeter-size euhedral pyrite crystals.

4.4.1 Sub Facies 4a: Massive Fossiliferous Packstone

This sub-facies forms beds that are between 10cm and 18cm thick and do not show significant thickness changes laterally in outcrop. The biogenic composition of sub-facies 4a is diverse: it comprises brachiopods, trilobites, echinoderms, cephalopods, bryozoans, and ostracods (Figure 10J); these grains are sub-millimeter to several millimeters in size. In places, this sub-facies contains large Endocerid cephalopods which range in size from 50mm to as large as 250mm. The biogenes make up between 20 vol% and 40 vol% of the grains. Orientation of biogenes and bioclasts is always random, and only in places where distinct burrows occur may take a circular shape (Figure 10K). Rarely, this sub-facies exhibits microbial overgrowth. Burrows are ubiquitous in this sub-facies and comprise *Thalassinoides* isp. and *Skolithos* isp. types; *Skolithos* is generally between 10mm and 40mm in length. In thin section, the tangential arrangement of carbonate particles around a central, carbonate mud-dominated part of a burrow are between 2mm and 5mm in diameter; in places, also elongate cross sections through burrows are present. Most burrows are filled with carbonate mud and carbonate grains; however, some show a partial fill with carbonate cement. The BI index of this sub-facies (following Taylor and Goldring 1993) is likely about 6.

4.4.2 Sub Facies 4b: Trilobite- and Brachiopod-Bearing Packstone Pockets

Sub-facies 4b forms lens-like “pockets” of packstone with sharp basal and top contacts to other facies (Figure 10L). These “pockets” are typically 8mm to 9mm in width, and 3mm to 4mm in height, with some measuring as large as 150mm width and height. They often have a slightly elongate shape, appearing to taper on either end, with a flattened top and bulbous base. These “pockets” also show in thin section to be surrounded by a thin rim of oxidation that continues laterally as an extension from the tapered edge of the deposit. The biogenes in these “pockets” are trilobites and brachiopod fragments, as well as the dominant bioclasts. Orientation of the grains in these pockets is mostly sub-parallel or at low angles to bedding; from measuring all grain orientations relative to bedding in two of the “pockets” an average of 27° from all elongate biogenes and bioclasts was determined. Distinct burrowing in this facies is absent; in places, minor suspected burrows are observed. The BI index of this facies (Taylor and Goldring 1993) is likely about 1.

4.4.3 Facies 4 Interpretation

The high amount of grains in this facies and their size up to several millimeters (not including the Endocerid cephalopods) indicates high energy during deposition; a high-energy setting is also indicated by the fact that nearly all grains are broken, and the basal surfaces of this facies are sharp. It is most likely that the grains which form a framework were deposited independently, or largely independently from the carbonate mud; the mud filling all pore spaces reflects significantly less energy than the grains and was likely introduced into the rock after the grains have been deposited. Nevertheless, transport of the grains cannot have been very far as few of them show rounding, and if some rounding is present then only poor rounding of edges which also speaks to little transport prior to deposition. Facies 4 rocks are interpreted to reflect a two-phase deposition with the biogenes and bioclasts deposited first during high-energetic conditions, and the carbonate mud subsequently when depositional energy was overall very low. Facies 4 sediments therefore likely represent event or storm deposition but probably not in an area that was constantly well agitated as that would have prevented the carbonate mud to settle.

Sub-facies 4a indicates that living conditions at and below the sea-floor must have been favorable during its sedimentation. This is reflected in the diversity of grains as well as in the intensity and the amount of burrowing (BI of about 6 Following Taylor and Goldring 1993). The burrowing is also seen as responsible for a complete homogenization of the sediment leading to the massive nature of these packstones, and the random orientation of all grains. The occurrence of *Skolithos* in these facies (following Seilacher 1967) indicates that where this trace fossil occurs these rocks were most likely deposited in a very shallow-marine settling. In this context, the alternation of high-energy deposition of shells versus the low-energy sedimentation of the carbonate mud would suggest deposition in a transitional zone setting just around normal wave base.

Sub-facies 4b is interpreted to record episodic deposition of preferentially shell debris and some biogenic components subsequent to an erosional event scouring into mud-rich strata. The scour at the base of these “pockets” represents the height of the energetic event, most likely a storm that exclusively eroded during this time. When this storm calmed down it started to fill the scours with the coarsest sediment it transported which were the biogenic fragments. Once the storm had largely given way to fair-weather conditions the carbonate mud settled out and filled the voids between the biogenic particles. The orientation of the elongate grains still reflects the dominant transport process of these carbonate particles which was probably largely as bed load close to the ocean floor.

5.0 HARDGROUNDS

Hardgrounds are prominent discontinuity surfaces, known to represent a period of non-deposition and subsequent in-situ lithification of the sea floor. This can be a result of sediment starvation, sediment condensation, or changes in seawater chemistry, with the resultant sedimentary hiatus potentially spanning anywhere from 10s of year to millions of years (Christ et al. 2015). Here, these surfaces appear in outcrop as clear discontinuity surfaces, with pyritized and phosphatized crusts, as well as borings. The borings into these hardgrounds are typically narrow and cylindrical, extending as far a 3cm below the surface, giving these hardgrounds their characteristic undulating appearance (Figure 11A, Figure 11B). The specific hardgrounds here have been interpreted to represent regressive surfaces (e.g. Lindström 1979; Nordlund 1989; Guttormsen 2012). This is supported by evidence of graded infilling of bioeroded pits (Lindström 1979), phosphatized surfaces (Nordlund 1989), bioerosion, erosion, and dissolution of cephalopod conchs (Guttormsen 2012), loose-sediment surface abrasion (Ekdale and Bromley 2001), and further by sea level reconstructions (Nielson 2004) suggesting significant sea level rise following the end-stages of Huk deposition. The basal hardground complex in particular has been correlated to the “Blodläget,” or Bloody Layer (Figure 11A, Figure 11B), a hardground complex widely distributed and recognizable throughout the Ordovician succession of Scandinavia (Lindström 1979), and first recognized in the Huk Formation of the Oslo-Asker region by Pétterfy (2015).

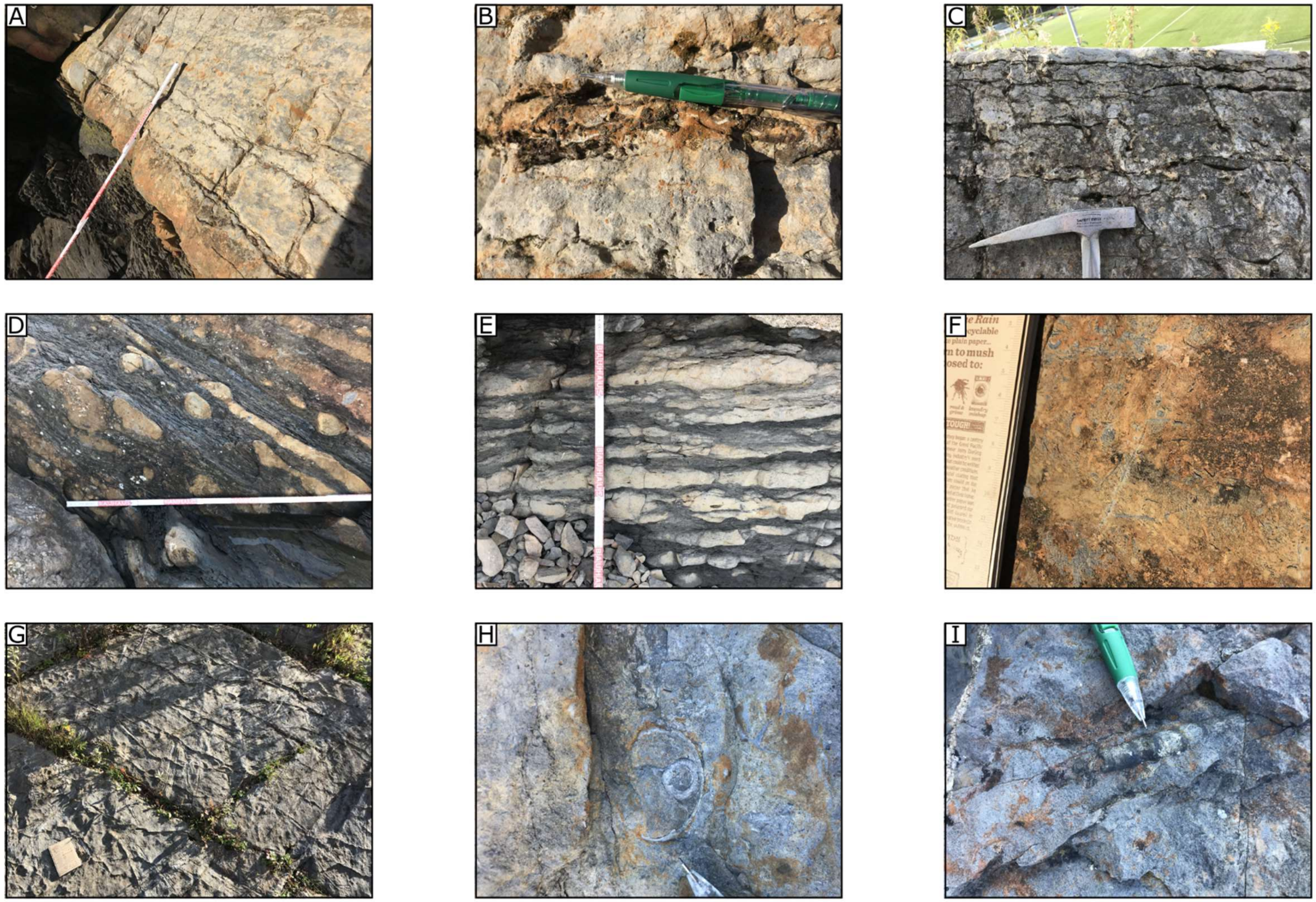

Figure 11. Outcrop photo of the Blodläget hardground complex at the base of the Huk Formation (A), and close-up of the pyrite impregnations of those hardgrounds (B). Possible secondary hardground complex at the top of the Huk Formation (C). Example of relative more carbonate mudstone rich (D) and wackestone rich (E) units, and the Volkhov-Kunda packstone boundary bed (F) within the middle member of the Huk Formation. Upper surface of the Huk Formation showing abundant Orthocerids (G) as well as close-up cross sectional (H) and longitudinal (I) exposure of these key fossils.

6.0 FACIES ARCHITECTURE

The facies distribution and architecture of the Norwegian Huk Formation is largely reflective of the previously defined tripartite division of the formation (Owen et al. 1990). According to that source, the Huk Formation consists of the basal Hukodden Member, overlain by the Lysaker Member and topped by the Svartodden Member. Generally, the formation consists of fine-grained wackestone deposits at the base, overlain by alternating wackestones and carbonate mudstones, with beds of mostly massive packstones and some wackestones making up the uppermost part of the formation. The Swedish Komstad Formation largely mimics the facies architecture of the Huk Formation, characterized by wackestone beds at the base, and overlain by alternating beds of wackestones and carbonate mudstones. In contrast to the mostly massive packstones of the Svartodden Member of the Huk Formation, the upper Komstad Formation is characterized by more nodular wackestone and carbonate mudstone beds that are intercalated with lenticular massive wackestones. In general, the massive fine-grained carbonate mudstones, characteristic of the middle portions of both formations, make up a larger component of the Komstad Formation than in the Huk Formation.

The lower 0.8m of the Hukodden Member shows a weakly developed overall fining-upward succession. While it consists predominantly of facies 3a, it also includes a 0.1m thick bed of heavily recrystallized facies 2 at its base. Immediately above this bed is the first hardground complex in the Huk Formation; a series of 3 hardground surfaces 20cm from the basal contact with the Tøyen Formation. The upper 0.7m of the

Hukodden Member consists of alternating beds of facies 2 and 3b with intercalated deposits of facies 4b, the latter forming small pockets within the wackestone beds. The alternating beds of the Lysaker Member shows three maxima of wackestone occurrence (Figure 11D, Figure 11E). These packages comprise the basal 1.0m of the member, the central 0.6m, and the uppermost 0.5m. These wackestone maxima are separated by a 1.1m thick lower and 1.0m thick upper package where the relative content of carbonate mudstone is greater than the wackestone content. In the wackestone-rich portions of the succession, wackestone beds are more frequently semi-nodular to nearly lenticular while in the mudstone-rich packages, wackestone beds are generally more nodular. The pockets of facies 4b here are generally more abundant in parts of the succession with a higher content of wackestone. Amongst the alternating wackestone and carbonate mudstone beds, a single 0.15m thick bed of facies 4a (Figure 11F) packstones can be found in the middle of the member, with a prominent discontinuity surface at the upper contact of this packstone bed. Topping the formation, the upper Svartodden Member shows a distinct coarsening-upward succession with the lower 0.6m of the member consisting mostly of facies 3a, while the upper 1.5m and basal 0.1m consist overwhelmingly of facies 4a. Additionally, the second major hardground complex occurs near the top of the Svartodden Member, approximately 10cm from the contact with the overlying Elnes Formation.

The tri-partite subdivision apparent in the Huk Formation can be roughly translated to the Komstad Formation. Although not previously formally proposed, the equivalent to the lower package of the Huk Formation is 1.5m thick in the Komstad Formation. It shows a weakly defined coarsening-upward succession, its upper 0.3m and lower 0.4m portions comprised mostly of facies 3a with the bulk of its middle 0.8m thick portion consisting of facies 1. Above the 0.4m thick bed of facies 3a is the lowermost prominent hardground surface at the contact with the overlying bed of facies 1. Additionally, a less well developed hardground can be identified 1.2m from the base of the formation. The central part of the Komstad Formation is approximately 5.3m thick, and similar to the Lysaker Member, consists of alternations of facies 2 and 3b. While alternations of carbonate mudstone-rich and wackestone-rich units are apparent in the Komstad Formation as they are in the Huk Formation, these packages are not as clearly defined. Here, carbonate mudstone is dominant in the basal 0.6m, the central 1.8m, and the uppermost 0.4m, separated by a lower 0.7m thick and an upper 1.3m thick package where wackestone dominates. This pattern is generally opposite to the Huk Formation: whereas in the Huk Formation, three wackestone-rich packages are separated by two carbonate mudstone-rich packages, the Komstad Formation consists of three carbonate mudstone-rich packages separated by two wackestone-rich packages. The pockets of facies 4b occur in the Komstad Formation preferentially enclosed in the wackestones, however, they are less frequent in comparison to their occurrences in the Huk Formation. As in the Huk Formation, a single 0.18m thick bed of facies 4a appears in the middle of the Komstad Formation amongst the intercalations of facies 2 and facies 3b and is the only appearance of facies 4a within the formation. A prominent discontinuity surface can be identified at the upper contact of this packstone bed, similarly to the equivalent bed found in the Huk Formation. The top part of the Komstad Formation is 2.5m thick and characterized by alternations of facies 2 and 3b, with the middle consisting of a 0.6m thick unit of facies 3a, and scattered centimeter-thick beds of facies 1 distributed throughout this upper portion of the formation. A prominent discontinuity surface forms at the very top of the Komstad Formation at the contact with the overlying Almelund Formation.

7.0 DEPOSITIONAL MODEL

7.1 Vertical Facies Succession

The stacking of the facies in the Huk Formation is largely reflective of the relative water depth during deposition, influencing the character of the sediment facies belt developed. This formation can be separated into two large scale stacking patterns: a fining upward sequence from the base of the formation at the contact with the underlying Tøyen Formation, up through the Volkhov-Kunda boundary bed 4.1m from the base, and a coarsening upward sequence from that marker bed up through the fossiliferous packstone beds of the upper Svartodden Member. In the lower of the large-scale stacking patterns, the thick wackestone beds transition into intercalated beds of wackestone and carbonate mudstone, with the relative mudstone content increasing upwards. This is interpreted as reflecting increasing water depth, first depositing sediments from a medial middle shelf environment, overlain by distal middle shelf, and ultimately deep shelf sediments (Burchette and Wright 1992). The upper half of the succession mirrors what is seen in the lower half of the succession, with interbedded wackestone and carbonate mudstone beds decreasing in relative mudstone content upwards, overlain by thick beds of wackestone. However, above these beds, the uppermost deposits contain thick beds of packstone, reflecting a more proximal position than at the base of the formation (Burchette and Wright 1992). Between these two large scale sequences, the Volkhov-Kunda boundary bed is reflective of a large-scale drop in sea level, representing the proximal-most deposits recorded in the Huk Formation (Owen et al. 1990; Calner et al. 2013).

Whereas in the Huk Formation, where a clear overall coarsening upwards sequence could be observed, the pattern in the Komstad is not as clear. Above the Volkhov-Kunda boundary bed, there is a very weakly defined coarsening upward sequence observable, grading from interbedded wackestone and packstone into thick beds of wackestone 1m from the upper contact of the formation. This again reflects a gradual rising in water depth, depositing first sediments from the proximal middle shelf, followed by distal middle shelf and ultimately deep shelf sediments (Burchette and Wright 1992; Harris et al. 2004). Whereas in the Huk Formation, where a clear overall coarsening upwards sequence could be observed, the pattern in the Komstad is not as clear. Above the Volkhov-Kunda boundary bed, there is a very weakly defined coarsening upward sequence observable, grading from interbedded wackestone and packstone into thick beds of wackestone 1m from the upper contact of the formation. This is interpretated similarly to the upper portions of the Huk Formation, as deposition of distal shelf sediments, followed by distal to proximal middle shelf deposition. Counter to the Huk, the Komstad is topped by a package of interbedded wackestone and carbonate mudstone, with the mudstone making up the majority of the composition. This grading into the carbonate mudstone and siliciclastic mudstones of the Almelund Formation is interpreted as the onset of sea level rise during the end stages of Komstad deposition (Tinn and Meidla 1999; Bergström et al. 2004; Nielsen 2004).

7.2 Lateral Facies Succession

The Huk and Komstad Formations are interpreted here as representing varying positions along a low-inclined carbonate shelf system, similar to a carbonate ramp, with the facies changes of the formations representing changes in sea-level and energy regime. The seven facies identified in this study characterize a variety of depositional sub-settings within this low-inclined shelf environment. In the classical model for deposition on low-inclined carbonate depositional systems (Burchette and Wright 1992), as is the prevailing interpretation of the depositional model for the Ordovician succession of Scandinavia (e.g. Owen et al. 1990; Egenhoff et al. 2010; Hansen et al. 2011; Calner et al. 2013), high energy and shallow water lends to the deposition of coarse-grained sediment, while relatively low energy and deeper water lends to the deposition of fine-grained sediments. This model is applied, among others, by Harris et al. (2004) for the Ordovician succession of Estonia which is an extension of the Scandinavian succession to the east within the same basin. Their model shows a shallow shelf with grain-supported sediments in proximal areas, a middle shelf setting containing mixed grain-supported and mud-supported sediments, a deep shelf environment consisting exclusively of mud-supported carbonates, and a basin environment characterized by organic rich siliciclastic mudstones. Following this model, the facies identified in this study can be grouped into three zones, proximal middle shelf, the distal middle shelf, and deep shelf environments

The proximal middle shelf facies belt represents the most proximal deposition recorded in the Huk and Komstad Formations. This zone consists of massive fossiliferous packestones (facies 4a) and wackestone (facies 3a), representing the more grain-supported portion of the “mixed” middle shelf (Harris et al. 2004). This depositional environment is characterized as being heavily influenced by the frequent but episodic reworking of storm events between periods of relatively low energy (e.g. Sanders and Höfling 2000; Rankey 2004). The fossiliferous nature of the facies found within this belt, combined with the biodiversity and non-preferential orientation of the grains, are indicative of a relatively high energy regime. The mud content, however, indicates an energy regime less than that characteristic of nearshore and shoreface environments, where the constant agitation of wave action would prevent mud deposition. The hardground development observed within this facies belt are excellent indicators of sediment starvation or condensation, potentially caused by high-order marine transgressions (Lindström 1979; Nordlund 1989; Guttormsen 2012).

Adjacent to the proximal middle shelf deposits lie the distal middle shelf facies, consisting of the thin beds of nodular to semi-nodular wackestone (facies 3b) with distributed pockets of packstone (facies 4b), and thin beds of carbonate wacke- to packstone (facies 3c). The wackestone and carbonate mudstone facies of this belt, making up the majority of deposits on the deep shelf, can be generally characterized as incredibly mud-rich, with biogenic grains making up a relatively minor component, but are nonetheless present and largely whole and unbroken. While packstones (facies 4b) are not typical of this environment, the occurrence of facies 4b here are treated as a feature of the wackestone beds, being less mud-rich, but significantly more fossiliferous. Bioturbation is also high within the wackestone and mudstones, primarily containing *Thalassinoides* isp. burrows, and a BI index around 5 or 6 (Taylor and Goldring 1993).

This depositional environment is traditionally characterized as representing relatively tranquil conditions, mostly beyond the frequent agitation of fair-weather wave base, but within the reach of high energy events (Coe et al. 2003). The majority of the sediments here reflect a classically defined deep shelf facies belt, with grains being generally sparse or absent, reflective of mostly tranquil conditions. While less abundant than in other parts of the succession, the packstone pockets of facies 4b indicate the occasional influence of higher energy events than typical storms. It is therefore likely that the packstone deposits represent deposition at the very distal end of the middle shelf facies belt, near the lower reaches of episodic storm related influence. The mud-rich wackestones not containing pockets of packstone lie adjacent to the prior, representing a proximal to medial position within the deep shelf.

Adjacent to the distal middle shelf facies lie the dark, grain-poor carbonate mudstones (facies 1) and bioturbated carbonate mud- to wackestone (facies 2), representing the distal-most facies belt recorded in the Huk and Komstad Formations. The deep shelf sediments here are largely defined as fine-grained, silt-bearing carbonate mudstones with some amount of siliclastic mud in the matrix. Grains are fine-silt to clay sized, and biogenic grains are largely lacking. Bioturbation in this facies belt is relatively low. This depositional environment in traditionally characterized as a relatively low energy and tranquil conditions, classically outside of the direct influence of typical storm related events (e.g. Phelps et al. 2008; Zeller et al. 2015). Both the carbonate mud and the siliciclastic mud were likely transported by way of current transport and subsequent settling out of suspension, however, the presence of well-rounded quartz grains amongst the high content of organic matter likely indicate a largely tranquil environment episodically influenced by high energy events. (Schieber 2003; Schieber et al. 2007; Egenhoff and Fishman 2013; Schieber et al. 2013).

8.0 DISCUSSION

8.1 Depositional Processes of a Medial Carbonate Shelf Transitional Zone

The lithostratigraphic depositional model presented in this study for the Huk and Komstad formartions can be used to generally understand and reconstruct similar Early Paleozoic temperate water carbonate platforms. This model is entirely based on facies characteristics and shows the processes that were active on this medial carbonate shelf. The transition from the proximal to the distal medial shelf is thought to have been where highly fossiliferous mud-rich carbonate packstones transition into relatively fossil-poor fine-grained carbonate mudstones. This lines up exactly with the transition from the outer ramp to basin facies according to Burchette and Wright (1992), or deep shelf to basin environments according to Harris et al. (2004). The classical interpretation of this environment characterizes the middle shelf as being heavily influenced by frequent storm reworking, suspension fall-out of terrigenous and lime mud, and pervasive bioturbation (Burchette and Wright 1992; Zeller et al. 2015). The distal portion of the middle shelf environment is interpreted classically as being below storm wave base and characterized by suboxic conditions (Burchette and Wright 1992; Phelps et al. 2008) shows very different characteristics on the Huk shelf. While the classical models suggest infrequent reworking of this part of the shelf (Burchette and Wright 1992; Harris et al. 2004) the wackestones and mudstones attributed to a distal middle shelf environment in the Huk Formation show frequent storm wave influence which is first and foremost reflected in presence of facies 4b pockets of packstone (Figure 6, Figure 7) and could also be a cause for the rounding of grains observed in distal mid-shelf sediments. Suboxic conditions during sedimentation are also not confirmed by the Huk deposits: bioturbation is quite frequent in this depositional zone, with bioturbation indices being nearly or as high as in the proximal middle shelf. It is therefore likely that the process that influence middle shelf deposition are largely the same as on the deep shelf, yet high-energy processes become less common on the distal middle shelf in comparison to the deep middle shelf.

It seems reasonable to assume that this study confused zonation on the shelf: what we call proximal and distal middle shelf are simply middle ramp/ middle shelf deposits in all other papers which would then, rightfully so as the environment gets deeper, show a decrease in burrowing and storm intensity going downslope. Nevertheless, this would assume that a distal slope consisting entirely of carbonates would form the facies belt adjacent to the ones described here as distal shelf. But that is not the case. The facies belt adjacent to the most mud rich Huk carbonates is most likely a siliciclastic mudstone (Figure 12). A confusion of facies zonation (facies belts) on the shelf is therefore very unlikely. These two discrepancies between the classical models and the findings of this study suggest a modification of our view on medial shelf environments: storms did reach down into the distal medial shelf setting, eroded, modified and transported sediment in that zone, which was strongly modified by burrowing organisms, to a degree that processes are not easily recognizable anymore.

The facies distribution, however, is also influenced by small-scale sea-level fluctuations. These sea-level fluctuations resulted in an alternation of grain-rich facies 3a and grain-poor facies 1 deposits which are thought to mirror ups and down of sea-level. However, Amberg et al. (2016) suggested that the alternations of grain-rich and

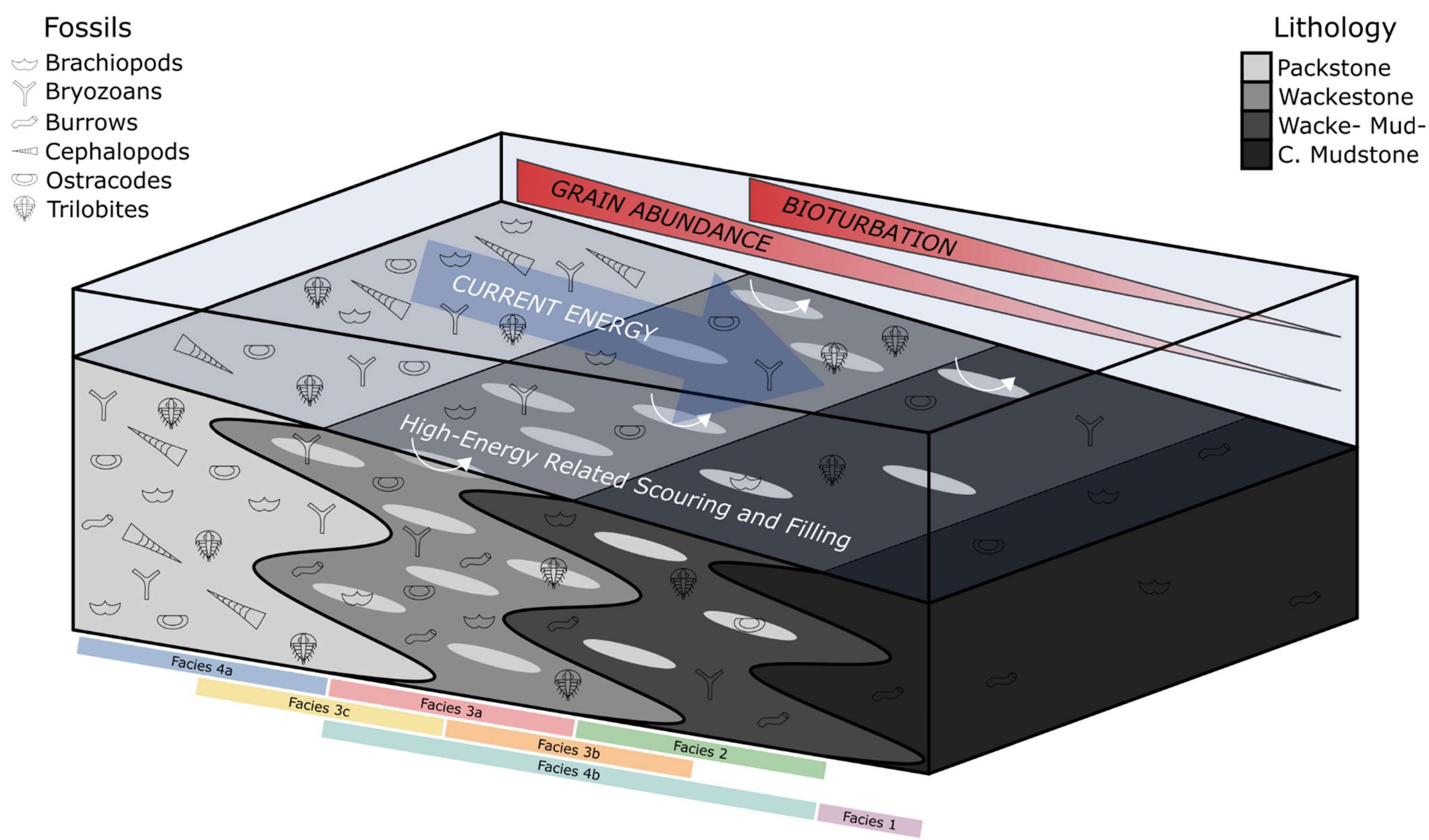

Figure 12. Block diagramatic depositional model of the low-inclined carbonate shelf depositional system as recorded in the Huk and Komstad Formations. Grain abundance and bioturbation generally decreases with increasing water depth and bottom current energy, with mud content increasing along the same track. The oblong "pockets" of packstone of facies 4b are generally absent in the proximal most positions of the shelf, and gradually decrease in abundance with decreasing grain size from the wackstone dominated facies to the carbonate mudstone dominated facies. These deposits are generally described to have been the product of high-energy storm events.

grain-poor lithologies are not a reflection of sea-level variations but instead are a sign of diagenetic alteration of one grain-rich lithology that originally characterized this rock. This model is essentially a modification of Westphal et al. (2004) with the difference that in this case these are alterations of grain-rich and grain-poor lithologies, not limestones and marls. However, assuming that Amberg et al. (2016) are correct and the carbonate mudstones were originally grain-rich, then this would make the depositional model for the Huk Formation even more problematic. In that case, grain-rich lithologies would border directly on siliciclastic mud-rich lithologies in the sedimentary transect through the shelf. This does not only contradict all sedimentological models of low-inclined carbonate depositional systems but also be questionable from the perspective of depositional energy. It would mean that relatively high-energy deposition reflected in the shell-rich packstones would directly transition laterally into overall low energy transition of siliciclastic mudstones. This has never been proposed in any depositional model before, neither for the recent nor the geological past. This suggestion therefore seems unlikely.

8.2 Relative Positioning of the Huk and Komstad and Wave Base Influences

This study suggests that the Norwegian Huk Formation was positioned more proximally on the shelf than the Swedish Komstad Formation, which was positioned more distally (Figure 2). This interpretation is due in large part to the relatively higher content of packstones in the Huk Formation, and the relatively higher content of carbonate mudstones in the Komstad Formation. This generally matches with paleogeographic reconstructions of Baltica during the Ordovician (Cocks and Torsvik 2005), however, of note is that the positions of these formations represent a more transverse view of the shelf, rather than a strict coastline-perpendicular transect. While the localities investigated in this study are separated by nearly 500km, their positioning on the shelf relative to the shoreline was likely only separated by 10’s of kilometers (Figure 2), which is reflected in the relatively similar characteristics of the two formations.

The most significant adjustment to the traditional depositional model is the relative positions of fair-weather and storm wave base. The proposed depositional model of the Huk and Komstad formations in this study is based primarily on the lithological characteristics typical of the middle shelf, and deep shelf depositional models. The traditional model of carbonate ramp depositional environments (Burchette and Wright 1992) places fair-weather wave base at the transition from the inner ramp to the mid-ramp, and storm wave base at the transition from the mid-ramp to the outer ramp. The carbonate shelf depositional model developed by Harris et al. (2004), which is adapted from the Burchette and Wright (1992) model, places fair-weather wave base at the transition from the shallow shelf to the middle shelf, and storm wave base at the transition from the middle shelf to the deep shelf. These definitions, however, are called into question by the findings of this study of the Huk and Komstad Formations.

It is relatively logical to interpret fair-weather wave base as being positioned near the top or above the depositional model presented here. The mud-rich character of the massive packstones, interpreted to represent the most proximal depositional environment of the Huk and Komstad Formations, indicates periods of quiescent conditions, allowing mud to deposit between the grains. This would not be likely under the constant agitation of wave energy. However, specifically relating to the positioning of storm wave base, both these and other models (e.g. Read 1985; Tucker 1985; Sanders and Höfling 2000; Zeller et al. 2015) characterize mudstones as almost exclusively falling below the reaches of storm waves, with only the largest and most catastrophic events reworking these carbonate mudstone deposits. This study shows that storm related reworking is common within the carbonate mudstones, evident in the broken bioclastic grains and sharp contacts with over- and underlying facies.

A study by Peters and Loss (2012) argues that the positioning of these stratigraphic boundaries is not actually strict, but rather that the capability of a certain wave influencing and interacting with the seafloor is a function of the relative event that formed any given wave. This study investigated the depth of influence of waves, both during fair-weather and storm conditions of the modern ocean and found that the probability of any given wave interacting with the sea-floor is a function of water depth, rather than strict water depth boundaries. Deep shelf facies, for example, have the possibility being influenced be extreme waves, up to a depth of approximately 250m. This model largely agrees with what is observed in the Huk and Komstad Formation. While the carbonate mudstones generally reflect mostly tranquil conditions, they still exhibit clear evidence of at least episodic energy conditions. Strictly in terms of lithology, the distribution of proximal coarse-grained and distal fine-grained sediments fit within the classical depositional models, but the vast influence of wave related reworking observed throughout the succession should be treated more as a measure of the frequency and relative strength with which wave-generating events impacted the seafloor during the deposition of the Huk and Komstad Formations. Therefore, this study postulates that storm wave base as defined, is neither recorded in this succession, nor is it likely applicable.

8.3 Paleoenvironmental and Paleoclimatic Implications

Facies changes within carbonate successions can be caused by numerous factors, including but not limited to changes in water depth, water chemistry, and biological productivity (Read 1985; Tucker 1985; Lucia et al. 2003). In the shallow epicratonic sea that covered Baltica during the Ordovician (Lindström 1971), it is likely that the facies changes recorded in the Huk and Komstad Formations are likely the product of fluctuations in sea-level, potential as a result of glacio-eustasy (Nielsen 2004). Sea-surface temperatures in Baltica during the late Dapinigian and early Darwillian are estimated to have been around 35°C (Song et al. 2019) with atmospheric O_2 and CO_2 levels estimated to be around 15% to 10% (Edwards et al. 2017) and 2500ppm (Cocks and Trosvik 2020) respectively. While the sea-level curve for Baltoscandia by Nielsen (2004) is on a relative scale, global sea-level at the same time is estimated to have ranged between 150m and 250m above modern day sea levels (Rasmussen et al. 2019).

Likely the most environmentally sensitive part of the succession lies within the Lysaker Member of the Huk Formation and the middle and parts of the upper portions of the Komstad Formation. These parts of the succession are characterized by repetitive interbeds of wackestone (facies 3b & 3c) and carbonate mudstone (facies 1 & 2) within the Komstad Formation. These thin beds indicate a position on the shelf straddling the boundary between the distal middle shelf (facies 3b & 3c) and the proximal deep shelf (facies 1 & 2). The sea-level fluctuations on Baltica during the Ordovician have been interpreted to be glacio-eustatic in nature (e.g. Brenchley and Newall 1980; Nielsen 2004; Hints et al. 2010), and thus, the sea-level fluctuations are dependent on the paleoclimatic conditions, with higher temperatures leading to glacial decline and oceanic thermal expansion (Schulz and Schäfer-Neth 1997), subsequently leading to rising sea-levels, with cooler temperatures leading to glacial growth and oceanic thermal contraction, resulting in falling sea-levels (Elrick et al. 2013). However, as noted by Egenhoff et al. (2010), the cause of these sea-level fluctuations as observed in the Bjørkåsholmen Formation may not be strictly glacio-eustatic. They note that the amplitude of modeled sea-level changes (e.g. Nielsen 2004; Haq and Schutter 2008; Dronov et al. 2011) does not match the drastic change in lithology of the underlying Alum Formation, to the carbonate Bjørkåsholmen Formation, and the overlying Tøyen Formation. A drastic change in lithology, if eustatic in nature, should be reflected in sea-level reconstructions, and show a rather large-scale fall that can be globally correlated. Such as in the Bjørkåsholmen Formation, both the Huk and Komstad formations represent a stark drop in sea-level relative to the under- and overlying shale formations. So, while these small-scale fluctuations may have a certain eustatic component to them, it is also likely that regional Scandinavia tectonism played a significant role.

A paleocurrent reconstruction, following the methods of Dixon (1970) is shown recreating current direction during the end stages of the Huk Formation deposition, utilizing the orientations of cephalopod conchs, found abundantly on the upper surface of the Svartodden Member in the Oslo-Asker region (Figure 11G, Figure 11H, Figure 11I). This analysis shows that the prevailing paleocurrent direction originated from the north-east (Figure 9). This orientation, however, is relative to the modern-day orientation of Norway, and needs to be corrected to reflect the current direction relative to Baltica during the time that the uppermost portions of the Svartodden Member were deposited. Paleogeographical reconstructions (Cocks and Trosvik 2002) estimate that Baltica was oriented approximately 180° relative to its current orientation while sutured to Gondwana and rotated counterclockwise by approximately 35° by the end of the Arenig stage, which approximately corresponds to the end of Svartodden deposition (Calner et al. 2013). Therefore, this approximates the paleocurrent orientation as originating from the east north-east, which is approximately from the interior of what is now the Oslo Fjord (Figure 9).

8.4 Comparison of Facies to Regional Sea-Level Reconstructions

While regional relative sea-level reconstructions (e.g. Nielsen 1995; Nielsen 2004; Dronov et al. 2011; Rasmussen et al. 2019) generally capture the larger scale sea-level patterns within the middle Ordovician succession of Southern Scandinavia, the finer-scale details are largely missing. Perhaps the most widely cited such reconstruction is the Ordovician Baltoscandian sea-level curve as proposed by Nielsen (2004). This reconstruction adequately captures the relative sea-level highs as recorded in graptolictic siliciclastic mudstones of the underlying Tøyen Formation and the overlying Elnes Formation in southern Norway and Almelund in southern Sweden, as well as the relative fall in sea-level as recorded in the carbonate Huk and Komstad Formations (Figure 3). However, the fine scale details as well as the depositional trends recorded in these formations are either largely unaccounted for or absent in this reconstruction (Figure 13). What is suggested by the sea-level curve proposed by Nielsen (2004) is, overall, as slow and gradual rise in water depths throughout the

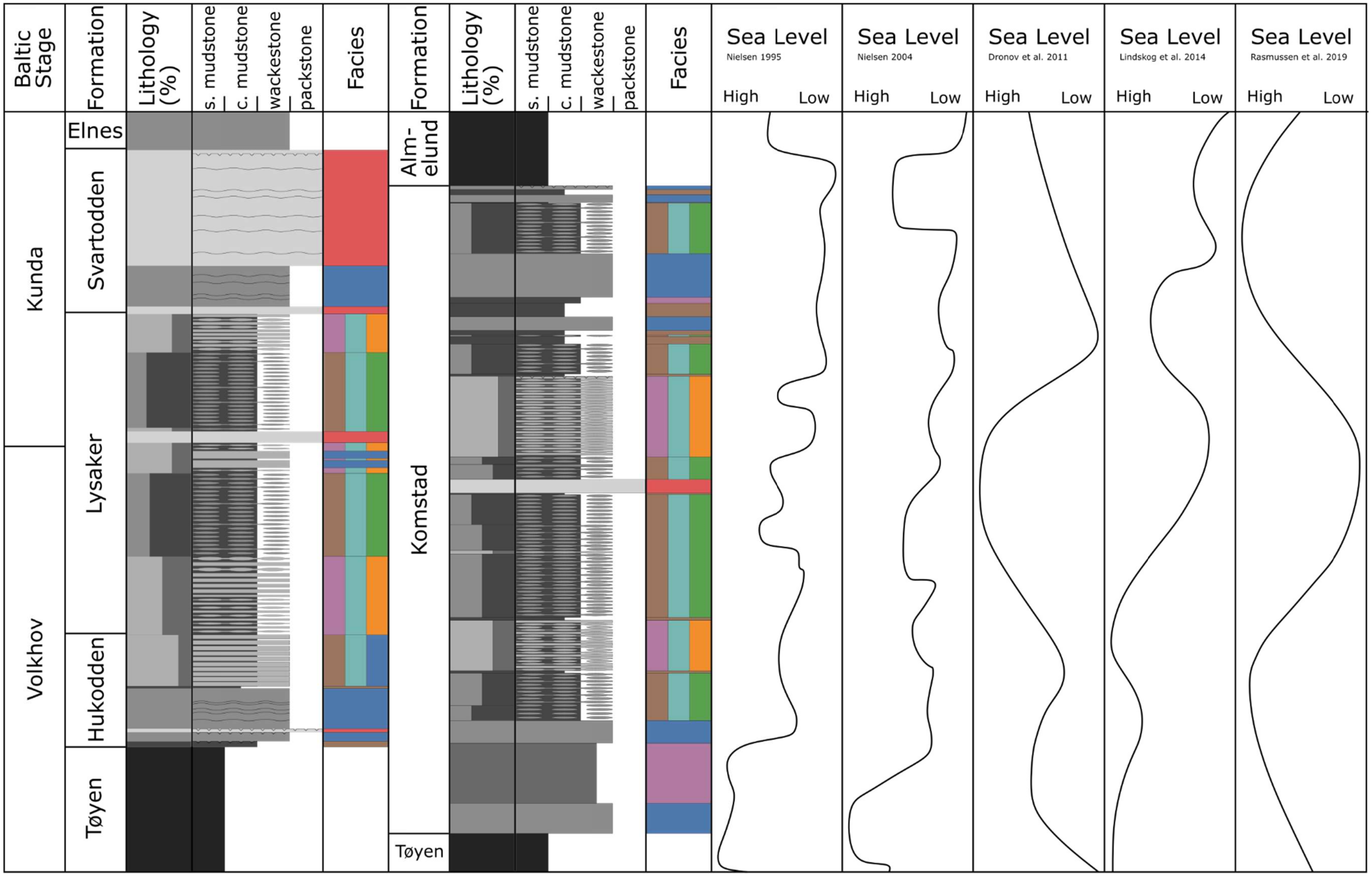

Figure 13. Comparison of the facies identified in the Huk and Komstad Formations to regional relative sea-level reconstructions from Nielsen 1995, Nielsen 2004, Dronov et al. 2011, Lindskog et al. 2014, and Rasmussen et al. 2019. All curves are are reconstructions of relative sea-level during the Middle Ordovician, and have been cropped to reflect the specific time during the Volkhov and Kunda Baltic stages during which the Huk and Komstad formations were deposited. Measured sections have been alligned along the Volkhov-Kunda Stage boundary

second half of the Volkhov Baltic Stage to the Hunderum and Early Valaste substages of the Kunda Baltic Stage (Nielsen 1995, Bruton et al. 2010, Maletz and Ahlberg 2018, Wu et al. 2018). Additionally, several small peaks in this reconstruction estimate rapid falls and subsequent rises in sea-level, primarily in the interbedded carbonate mudstone and wackestone of the middle of both the Huk and Komstad successions.

Within the Huk Formation, the large-scale stacking pattern can largely be described as a roughly fining upward sequence from the base of the succession up to the middle of the Lysaker member, where relative carbonate mudstone content is approximately its highest. From this point, the relative carbonate mudstone content within the middle of the Huk Formation gradually decreases to the base of the upper Svartodden member, where the interbedded mudstone and wackestone is overlain by fossiliferous massive wackestone (Facies 3b), and itself overlain by fossiliferous packstone (Facies 4a) (Figure 13). These facies would suggest a sea-level curve to reflect a rapid fall in sea-level following the end stages of Tøyen deposition, followed by a gradual rise and subsequent gradual fall in sea-level throughout Huk deposition, and finally topped by a rapid rise following the end stages of Huk deposition.

Within the Komstad Formation, the large scale stacking pattern is largely reflective of the Huk Formation, with a relatively more grain-rich lithology overlying the Tøyen Formation, itself overlain by interbedded carbonate mudstone and wackestone which rapidly decrease in relative wackestone composition before the relative carbonate mudstone increase to the middle of the succession. Counter the Huk, from the middle of the formation, the overall relative carbonate mudstone content can be seen to increate gradually, from a wackestone rich package near the middle of the formation, fining upwards to increasingly mudstone rich intercalations and thick beds of nearly entirely carbonate mudstone near the top. Finally, near the top of the Komstad Formation, a thick ~70cm bed of fossiliferous carbonate wackestone likely represents the approximate sea-level minimum preceding the onset of siliciclastic mudstone deposition of the Almelund Formation. These facies would suggest a sea-level curve to reflect a gradual fall in sea-level following the end-stages of Tøyen Formation deposition, followed by a gradually and relatively consistent increase in relative water depth. Two key points, near the base of the succession where the relative carbonate mudstone content, and near the top of the formation where the tick bed of fossiliferous wackestone is recorded, likely represent brief, small-scale regressions, allowing for brief deposition of characteristically more shallow facies (e.g. Van Wagoner et al. 1988, Zecchin and Catuneau 2013)

Finally, what is unaccounted for in the sea-level reconstruction relative to the facies recorded in both the Huk and Komstad Formations is the likely forced regression (Zecchin and Catuneanu 2013) as recorded in the 15cm to 20cm thick bed of fossiliferous carbonate packstone (facies 4a) found in the middle of both successions at roughly the same stratigraphic position. This bed of relatively more grain-rich composition has been identified in these formations to represent a significant, but brief, sea-level fall at the boundary between the Volkhov and Kunda Baltic Stages (e.g. Harris et al. 2004; Meidla et al. 2014; Lindskog et al. 2014; Lindskog et al. 2018). The sea-level curve proposed by Nielsen (2004), while it does roughly account for relatively small regressions throughout the deposition of the Huk and Komstad Formations, does not do so adequately. The presence of these incredibly grain-rich lithologies amongst intercalated beds of carbonate mudstone and wackestone where the relative carbonate mudstone composition is at or near a maximum, suggests a rapid and substantial fall in sea-level, followed by relative rise in sea-level of roughly equal magnitude.

8.5 Suggested Further Investigation

While this study provides some insight into the heterozoan, low-inclined carbonate shelf environment of the Huk and Komstad formations, our understanding could be further bolstered by additional investigations. Given the apparent sensitivity to oceanic and climate conditions of the Lysaker Member and upper parts of the Komstad Formation, they may serve as an excellent record of large-scale climate changes. However, the model proposed by Amberg et al. (2016) indicates that these alternating packages of wackestone and carbonate mudstone may not be primary depositional records of small-scale climate and sea-level fluctuations through the Middle Ordovician. This could be further investigated following the methods proposed by Ghosh et al. (2006) and refined by Eiler (2011) and Zaarur et al. (2013) with clumped isotope thermometry. This method would attempt to bypass the traditional problems related to paleothermometry of ancient rocks by directly measuring the ratio of ^{13}C-^{18}O bonds and ^{12}C-^{16}O bonds to recreate sea surface temperature. This method could then be further applied to time equivalent formations throughout Scandinavia including the Holen and Lanna Formations of central Sweden (Lindskog et al. 2018), and further east into Estonia and Russia (Harris et al. 2004; Meidla et al. 2014). Applications to these formations would allow for the depositional model to be further refined at a larger scale, more strongly valid to similar temperate water heterozoan systems. This study does, however, provide significant and new insight into this exemplary record of such a depositional system, setting forth the necessary building blocks on which to expand.

9.0 CONCLUSIONS

1. The Huk and Komstad Formations consist of 7 carbonate facies: massive trilobite- and brachiopod-bearing calcareous mudstone (facies 1), bioturbated carbonate mud-wackestone (facies 2), planar-bedded fossiliferous wackestone (facies 3a), nodular to lenticular fossiliferous wackestone (facies 3b), mud-rich carbonate wacke- to packstone (facies 3c), massive fossiliferous packstone (facies 4a), and fossiliferous carbonate packstone pockets (facies 4b).

2. The Norwegian Huk Formation and the Swedish Komstad Formation represent varying positions of carbonate facies development along the Ordovician Baltoscandian paleo-basin. Positionally, the Huk Formation represents more proximal deposition, while the Komstad Formation represents more distal deposition. Paleogeographic reconstructions, however, estimate that these formations likely only represent 10’s of kilometers of separation along the shelf profile, their transect being mostly parallel to the shoreline.

3. These seven facies make up 2 distinct facies belts and 4 sub-facies belts: the proximal middle shelf environment, the distal middle shelf environment, the proximal deep shelf environment, and the distal deep shelf environment. The proximal middle shelf is characterized by massive fossiliferous packstones, the distal middle shelf is characterized by planar bedded massive fossiliferous wackestones, the proximal deep shelf is characterized by intercalations of thinly bedded nodular fossiliferous wackestone with pockets of trilobite and brachiopod bearing packstone pockets, silty fossil poor

carbonate wacksetone and carbonate mudstone, and the distal deep shelf is characterized by fossil-poor calcareous mudstone.

4. Fair-weather wave base in this succession is interpreted to have been well above the facies recorded in these formations, with the constant agitation of fair-weather not appearing to have influenced the deposition of these facies. This mostly agrees with the traditional positioning of fair-weather wave base on a low-inclined shelf. Storm waves, however, appears to have had periodic to episodic influence throughout the succession, which largely disagrees with the traditional interpretation of storm wave base at the transition from the middle shelf to the deep shelf. This study therefore suggests that storm-wave base was positioned below the facies of this succession, and likely was positioned at least at the very distal end of the deep shelf, or within the basin realm of this low-inclined carbonate shelf, beneath the facies recorded in this succession.

5. Comparison to well-cited sea-level reconstructions reflect that while the large scale pattern of relatively high sea-level during the deposition of the underlying and overlying graptolitic siliciclastic mudstone deposition, with sea-level reflecting a relative sea-level low during the deposition of these carbonate successions. However, the

6. While the interbedded wackestone and carbonate mudstone characteristic of the Lysaker Member and portions of the Komstad Formation are often regarded as primary records of small-scale sea-level fluctuations, alternative interpretations have suggested the true nature of these beds are of diagenetic origin. Several factors, prime amongst them being the lateral traceability of these small-scale intercalations leads this study to favor the interpretation of these being primary records of sea-level fluctuations.

7. Potential future investigations of the Middle Ordovician Baltoscandian carbonate shelf could focus more heavily on the middle Lysaker Member of the Huk Formation and the middle and upper portions of the Komstad Formation. This investigation would apply the model proposed by Amberg et al. (2016) to evaluate the climatic and oceanic sensitivity of the intercalated wackestone and carbonate mudstone via clumped isotope paleothermometry reconstructions. Additionally, a similar investigation could be applied to the time equivalent counterparts of these formations throughout the Baltoscandian Basin to further develop the depositional model of these Early Paleozoic heterozoan carbonate successions.

REFERENCES

Aigner, T., 1985, Biofabrics as Dynamic Indicators in Nummulite Accumulations, Journal of Sedimentary Petrology, v. 55, n. 1, p. 131-134.

Àlvaro, J. J., Ahlberg, P., and Axheimer, N., 2010, Skeletal Carbonate Productivity and Phosphogenesis at the Lower-Middle Cambrian Transition of Scania, Southern Sweden, Geological Magazine, v. 147, p. 59-76.

Amberg, C. E. A., Collart, T., Salenbien, W., Egger, L. M., Munnecke, A., Nielsen, A. T., Monnet, C., Hammer, Ø., and Vandenbroucke, T. R. A., 2016, The Nature of Ordovician Limestone-Marl Alternations in the Oslo-Asker District (Norway): Witness of Primary Glacio-Eustasy or Diagenetic Rhythms? Nature Scientific Reports, v. 6, n. 18787, 13 p.

Baccelle, L., and Bosellini, A., 1965, Diagrammi per la stima visive della composizione percentuale nelle rocche sedimentarie – Annali dell'Universitá di Ferrara (Nuova Serie), Sezione 9, Scienze geologiche e paleontologiche, v. 1, n. 3, p. 59-62.

Basset, M. G. (ed), 1976, The Ordovician System: Proceedings from the Palaelontological Association Symposium, p. 301-326.

Bathurst, R. G., C., 1982, Genesis of Stromatactic Cavities Between Submarine Crusts in Paleozoic Carbonate Mud Buildups, Journal of the Geological Society of London, v. 139, p. 165-181.

Benton, M. J., and Harper, D. A. T., 1997, Basic Palaeontology, Geological Magazine, v. 135, n. 6, p. 819-842.

Bergström, S. M., Larsson, K., Pålsson, C., and Ahlberg, P., 2002, The Almelund Shale, a Replacement Name for the Upper Didymograptus Shale and the Lower Dicellograptus Shale in the Lithostratigraphical Classification of the Ordovician Succession in Scania, Southern Sweden: Bulletin of the Geological Society of Denmark, v. 49, p. 41-47.

Bergström, S. M., Ahlberg, P., Maletz, J., Lundberg, F., and Joachimski, M. M., 2018, Darwilian (Middle Ordovician,) Chemoostratigraphy linked to Graptolite, Conodont, and Trilobite Biostratigrapht in the Fågelsång-3 Drill Core, Scania, Sweden, Geologiska Föreningen, v. 140, n. 3, p. 229-240.

Birkeland, C., ed., 20115, Coral Reefs in the Anthropocene: New York, Springer, 271 p.

Brando, M., Frezza, V., Tomassetti, L., and Cuffaro, M., 2009, Heterozoan Carbonates in Oligotrophic Tropical Waters: The Attard Member of the Lower Coralline Limestone Formation (Upper Oligocene, Malta), Palaeogeography, Palaeoclimatology, Palaeoecology, v. 274, p. 54-63.

Brenchley, P. J., and Newall, G., 1980, A Facies Analysis of Upper Ordovician Regressive Sequences in the Oslo Region, Norway – A Record of Glacio-Eustatic Changes, Palaeogeography, Palaeoclimatology, Palaeoecology, v. 31, p. 1-38.

Bromley, R. G., 1996, Trace Fossils. Biology, Taphonomy and Applications, Geological Magazine, v. 134, n. 4, p. 409-421.

Bruton, D. L., Gabrielsen, R. H., and Larsen, B., 2010, The Caledonides of the Oslo Region, Norway – Stratigraphy and Structural Elements, Norwegian Journal of Geology, v. 90, p. 93-121.

Burchette, T. P., and Wright, V. P., 1992, Carbonate Ramp Depositional Systems, Sedimentary Geology, v. 79, p. 3-57.

Calner, M., Ahlberg, P., Lehnert, O., and Erlström, M., 2013, The Lower Paleozoic of Southern Sweden and the Oslo Region, Norway, Field Guide for the 3rd Annual Meeting of the IGCP Project 591: Geological Survey of Sweden, v. 133, 96 p.

Christ, N., Immenhauser, A., Wood, R.A., Darwich, K., and Niedermayer, A., 2015, Petrography and Environmental Controls on the Formation of Phanerozoic Marine Carbonate Hardgrounds: Earth-Science Reviews, v. 151, p. 176-226.

Cocks, L. R. M., and Torsvik, T. H., 2002, Earth Geography from 500 to 400 Million Years Ago: A Faunal and Palaeomagnetic Review: Journal of the Geological Society, London, v. 159, p. 631-644.

Cocks, L. R., and Torsvik, T. H., 2005, Baltica from the Late Precambrian to Mid-Palaeozoic Times: The Gain and Loss of a Terrane's Identity: Earth-Science Reviews, v. 72, p. 39-66.

Cocks, L. R. M., and Torsvik, T. H., 2020, Ordovician Palaeogeography and Climate Change, Gondwana Research, doi: 10.1016/j.gr.2020.09.008 (in press), 20 p.

Coe, A. L., Bosence, D. W. J., Church, K. D., Flint, S. S., Howell, J. A., and Wilson, R. C. L., eds., 2003, The Sedimentary Record of Sea-Level Change: New York: Cambridge University Press, 287 p.

Cooper, R. A., 2004, Measures of Diversity, *in* Webby, D. B., Paris, F., Droser, M. L., and Percival, I. G., eds., 2004, The Great Ordovician Biodiversification Event: New York, Columbia University Press, p. 52-57.

Cooper, R. A., Nowlan, G. S., and Williams, S. H., 2001, Global Stratotype Section and Point for Base of the Ordovician System, Episodes, v. 24, n. 1, p. 19-28.

Cooper, R. A., Sadler, P. M., Munnecke, A., and Crampton, J. S., 2013, Graptoloid Evolutional Rates Track Ordovician-Silurian Global Climate Change: Geological Magazine, v. 151, no. 2, p. 349-364.

Dixon, O. A., 1970, Nautiloids and Current Ripples as Paleocurrent Indicators in Upper Ordovician Limestones, Anticosti Island, Canada, Journal of Sedimentary Petrology, v. 40, n. 2, p. 682-687.

Dronov, A. V., Ainsaar, L., Kaljo, D., Meidla, T., and Einasto, R., 2011, Ordovician of Baltoscandia: Facies, Sequences and Sea-Level Changes: Cuandernos del Museo Geominero, v. 14, p. 143-150.

Dyer, B., Maloof, A. C., Purkis, S. J., and Harris, P. M., 2018, Quantifying the Relationship Between Water Depth and Carbonate Facies, Sedimentary Geology, v. 373, p. 1-10.

Dunham, R. J., 1962, Classification of Carbonate Rocks According to Depositional Textures, Memoirs of the American Association of Petroleum Geologists, v. 1, p. 108-121.

Edwards, C. T., Saltzman, M. R., Royer, D. L., and Fike, D. A., 2017, Oxygenation as a Driver of the Great Ordovician Biodiversification Event, Nature Geosciences, v. 10, p. 925-929.

Egenhoff, S. O., and Fishman, N. S., 2013, Traces in the Dark - Sedimentary Processes and Facies Gradients in the Upper Shale Member of the Upper Devonian-Lower Mississippian Bakken Formation, Williston Basin, North Dakota, U.S.A., Journal of Sedimentary Research, v. 83, p. 803-824.

Egenhoff, S., Cassle, C., Maletz, J., Frisk, A.M., Ebbestad, J.O.R., and Stübner, K., 2010, Sedimentology and Sequence Stratigraphy of a Pronounced Early Ordovician Sea-Level Fall on Baltica – The Bjørkåsholmen Formation in Norway and Sweden: Sedimentary Geology, v. 224, p. 1-14.

Ehrenberg, S. N., Pickard, N. A. H., Svånå, T. A., and Oxtoby, N. H., 2002, Cement Geochemistry of Photozoan Carbonate Strata (Upper Carboniferous-Lower Permian), Finnmark Carbonate Platform, Barents Sea, Journal of Sedimentary Research, v. 72, n. 1, p. 95-115.

Eiler, J. M., 2011, Paleoclimate Reconstructions Using Carbonate Clumped Isotope Thermometry: Quaternary Science Reviews, v. 30, p. 3575-3588.

Ekdale, A. A., and Bromley, R. G., 2001, Bioerosional Innovation for Living in Carbonate Hardgrounds in the Early Ordovician of Sweden, Lethaia, v. 34, 12 p.

Ekdale, A. A., Benner, J. S., Bromley, R. G., and de Gibert, J. M., 2002, Bioerosion of Lower Ordovician Hardgrounds in Southern Scandinavia and Western North America, Acta Geologica Hispanica, v. 37, n. 1, p. 9-13.

Elrick, M., Reardon, D., Labor, W., Martin, J., Desrochers, A., and Pope, M., 2013, Orbital-Scale Climate Change and Glacioeustasy During the Early Late

Ordovician (pre-Hirnantian) Determined from δ18O Values in Marine Apatite, Geology, v. 41, n. 7, p. 775-778.

Embry, A. F., and Klovan, J. E., 1971, A Late Devonian Reef Tract on Northeastern Banks Island, N.W.T., Bulletin of Canadian Petroleum Geology, v. 19, n. 4, p. 730-781.

Erlström, M., Sivhed, U., and Wilkman, H., 1999, Skånes Berggund, *in* Germundsson, T. and Schlyter, P., eds., 1999, Atlas över Skåne, Sveriges Nationalatlas Förlag.

Germundsson, T. and Schlyter, P., eds., 1999, Atlas över Skåne, Sveriges Nationalatlas Förlag.

Ghosh, P., Adkins, J., Affek, H., Balta, B., Guo, W., Schauble, D., and Eiler, J. M., 2006, ^{13}C-^{18}O Bonds in Carbonate Minerals: A New Kind of Paleothermometer, Geochimica et Cosmochimica Acta, v. 70, p. 1439-1456.

Guttormsen, J., 2012, Sedimentology, Palaeontology and Diagenesis of the Ordovician (Darriwilian) Svartodden Member (Huk Formation), Slemmestad, Oslo Region [Master's Thesis]: University of Oslo, Oslo, Norway, 174 p.

Hallock, P., 2015, Changing Influences Between Life and Limestones in Earth History, *in* Birkeland, C., ed., 2015, Coral Reefs in the Anthropocene: New York, Springer, p. 17-42.

Hansen, T., Nielsen, A. T., and Bruton, D. L., 2011, Palaeocology in a Mud-Dominated Epicontinental Sea: A Case Study of the Ordovician Elnes Formation, Southern Norway: Palaeogeography, Palaeoclimatology, Palaeoecology, v. 299, p. 348-362.

Haq, B. U., and Schutter, S. R., 2008, A Chronology of Paleozoic Sea-Level Changes, Science Research Article, v. 322, p. 64-68.

Harris, M. T., Ainsaar, S. L., Hints, L., Männik, P., Nõlvak, J., and Rubel, M., 2004, Upper Ordovician Sequences of Western Estonia, Palaeogeography, Palaeoclimatology, Palaeoecology, v. 210, p. 135-148.

Hints, O., Delabroye, A., Nõlvak, J., Servais, T., Uutela, A., and Wallin, Å., 2010, Biodiversity Patterns of Ordovician Marine Microphytoplankton from Baltica: Comparison with Other Fossil Groups and Sea-Level Changes, Palaeogeography, Palaeoclimatology, Palaeoecology, v. 294, p. 161-173.

Jaanusson, V., 1960, Graptoloids from the Ontikan and Viruan (Ordov.) Limestones of Estonia and Sweden, Bulletin of the Geological Institutions of the University of Uppsala, v. 38, p. 289-366.

Jaanusson, V., 1976, Faunal Dynamics in the Middle Ordovician (Viruan) of Balto-Scandia, *in* Basset, M. G. (ed), 1976, The Ordovician System: Proceedings from the Palaelontological Association Symposium, p. 301-326.

Kohut, J. J., 1972, Conodont Biostratigraphy of the Lower Ordovician Orthoceras and Stein Limestones (3c), Norway: Norsk Geologisk Tidsskrift, v. 52, p. 427-445.

Lindskog, A., Eriksson, M. E., and Pettersson, A. M. L., 2014, The Volkhov-Kunda Transition and the Base of the Holen Limestone at Kinnekulle, Västergotland, Sweden, Geologiska Föreningen, v. 136, p. 167-171.

Lindskog, A., Lindskog, A. M. L., Johansson, J. V., Ahlberg, P., and Eriksson, M. E., 2018, The Cambrian-Ordovician Succession at Lanna, Sweden: Stratigraphy and Depositional Environmnets, Estonian Journal of Earth Sciences, v. 67, n. 2, p. 133-148.

Lindström, M., 1971, Lower Ordovician Conodonts of Europe, Geological Society of America Symposium on Conodont Biostratigraphy, v. 127, p. 21-62.

Lindström, M., 1979, Diagenesis of Lower Ordovician Hardgrounds in Sweden, Geologica et Palaeontologiva, v. 13, p. 9-30.

Lucia, F. J., Kearns, C., and Jennings Jr., J., W., 2003, Carbonate Reservoir Characterization, Journal of Petroleum Technology, v. 55, n. 6, p. 70-72.

Lutro, O., Graversen, O., Larset, B. T., Naterstad, J., and Bockelie, T., 2017, Bedrock Map Asker 1814-1, Norges Geologiske Undersøklse, scale 1:50,000.

Maletz, J., and Ahlberg, P., 2018, The Lower Ordovician Tøyen Shale Succession in the Fågelsång-3 Drill Core, Scania, Sweden, Geologiska Föreningen, v. 140, n. 4, p. 293-305.

Maletz, J., and Egenhoff, S. O., 2001, Larte Tremadoc to Early Arenig Graptolite Faunas of Southern Bolivia and their Implications for a Worldwide Biozonation, Lethaia, v. 34, p. 47-62.

Maletz, J., Egenhoff, S., Böhme, M., Asch, R., Borowski, K., Höntzsch, S., Kirsch, M., and Werner, M., 2011, A Tale of Both Sides of Iapetus – Upper Darriwilian (Ordovician) Graptolite Faunal Dynamics on the Edges of Two Continents, Canadian Journal of Earth Sciences, v. 48, p. 841-859.

Martin, E., 2014, Komstad Limestone Formation, Killeröd, Southern Sweden: A High-Resolution Study of an Increaded Meteorite Flus in the Middle Ordovician, [Master's Thesis]: Lund University, Lund, Sweden, 66 p.

Matonti, C., Bourget, J., Fournier, F., Håkansson, E., Pellerin, M., Hong, F., and Reijmer, J., 2021, Distinct Petroacoustic Signature in Heterozoan and Photozoan

Carbonates Resulting from Combined Depositional and Diagenetic Processes, Marine and Petroleum Geology, v. 128, 21 p.

Meidla, T., Ainsaar, L., Hints, O., 2014, The Ordovician System in Estonia, Field Guide for the 4th Annual Meeting of IGCP 591, Estonia, 8 p.

Michel, J., Borgomano, J., and Reijmer, J. J. G., 2018, Heterozoan Carbonates: When, Where, and Why? A Synthesis on Parameters Controlling Carbonate Production and Occurrences, Earth-Science Reviews, v. 182, p. 50-67.

Multti, M., and Hallock, P., 2003, Carbonate Systems Along Nutrient and Temperature Gradients: Some Sedimentological and Geochemical Constraints, International Journal of Earth Science, v. 92, p. 465-475.

Munnecke, A., Calner, M., Harper, D. A. T., and Servais, T., 2010, Ordovician and Silurian Sea-Water Chemistry, Sea Level, and Climate: A Synopsis: Palaeogeography, Palaeoclimatology, Palaeoecology, v. 296, p. 389-413.

Nielsen, A. T., 1995, Trilobite Systematics, Biostratigraphy and Palaeoecology of the Lower Ordovician Komstad Limestone and Huk Formations, Southern Scandinavia, Fossils and Strata, p. 1-374.

Nielsen, A. T., 2004, Ordovician Sea Level Changes: A Baltoscandian Perspective, *in* Webby, D. B., Paris, F., Droser, M. L., and Percival, I. G., eds., 2004, The Great Ordovician Biodiversification Event: New York, Columbia University Press, p. 84-93.

Nordlund, U., 1989, Lithostratigraphy and Sedimentology of a Lower Ordovician Limestone Sequence at Hälludden, Öland, Sweden, Geologiska Föreningen, v. 111, p. 65-94.

Owen, A. W., Bruton, D. L., Bockelie, J. F., and Bockelie, T. G., 1990, The Ordovician Successions of the Oslo Region, Norway: Norsk Geoogisk, Special Publication 4, p. 3-54.

Péterffy, O., 2015, Sedimentology and Carbon Isotope Stratigraphy of Lower-Middle Ordovician Successions of Slemmestad (Oslo-Asker, Norway) and Brunflo (Jämtland, Sweden) [Master's Thesis]: Lund University, Lund, Sweden, 44p.

Peters, S. E., and Loss, D. P., 2012, Storm and Fair-Weather Wave Base: A Relevant Distinction? Geology, v. 40, n. 6, p. 511-514.

Phelps, R. M., Kerans, C., Scott, S. Z., Janson, X., and Bellian, J. A., 2008, Three-Dimensional Modelling and Sequence Stratigraphy of a Carbonate Ramp-to-Shelf Transition, Permian Upper San Andreas Formation, Sedimentology, v. 55, p. 1777-1813.

Philip, J. M., and Gari, J., 2005, Late Cretaceous Heterozoan Carbonates: Palaeoenvironmental Setting, Relationships with Rudist Carbonates (Provence, South-East France), Sedimentary Geology, v. 175, p. 315-337.

Pomar, L., Brandano, M., and Westphal, H., 2004, Environmental Factors Influencing Skeletal Grain Sediment Associations: A Critical Review of Miocene Examples from the Western Mediterranean, Sedimentology, v. 51, p. 627-651.

Rankey, E. C., 2004, On the Interpretation of Shallow Shelf Carbonate Facies and Habitats: How Much Does Water Depth Matter? Journal of Sedimentary Research, v. 74, n. 1, p. 2-6.

Rasmussen, J. A., 1991, Conodont Stratigraphy of the Lower Ordovician Huk Formation at Slemmestad, Southern Norway: Norsk Geologisk Tidsskrift, v. 71, p. 265-288.

Rasmussen, J. A., Bruton, D. L., and Nakrem, H. A., 2013, Stop 17. Tremadocian to Darwillian Units, Bjørkasholmen and Djuptrekkodden, Slemmestad, *in* Calner, M., Ahlberg, P., Lehnert, O., and Erlström, M., 2013, The Lower Paleozoic of Southern Sweden and the Oslo Region, Norway, Field Guide for the 3rd Annual Meeting of the IGCP Project 591: Geological Survey of Sweden, v. 133, p. 67-72.

Rasmussen, C. M. Ø., Kröger, B., Nielsen, M. L., and Colmenar, J., 2019, Cascading Trend of Early Paleozoic Marine Radiations Paused by Late Ordovician Extinctions, Proceedings of the National Academy of Sciences of the United States of America, v. 116, n. 15, p. 7207-7213.

Read, J., F., 1985, Carbonate Platform Facies Models, The American Association of Petroleum Geologists Bulletin, v. 69, n. 1, p. 1-21.

Reymond, C. E., Zihrul, K. S., Halfar, J., Riegl, B., Hunphreys, A., and Westphal, H., 2015, Heterozoan Carbonates from the Equatorial Rocky Reefs of the Galápagos Archipelago, Sedimentology, v. 63, p. 940-958.

Sanders, D., and Höfling, R., 2000, Carbonate Deposition in Mixed Siliciclastic-Carbonate Environments on top of an Orogenic Wedge (Late Cretaceous, Northern Calcareous Alps, Austria), Sedimentary Geology, v. 137, p. 127-146.

Schieber, J., 2003, Simple Gifts and Buried Treasures - Implications of Finding Bioturbation and Erosion Surfaces in Black Shales, The Sedimentary Record, v. 1, n. 2, p. 4-8.

Schieber, J., Southard, J., and Thaisen, K., 2007, Accretion of Mudstone Beds from Migrating Floccule Ripples, Science, v. 318, p. 1760-1763.

Schieber, J., Southard, J. B., Kissling, P., Rossman, B., and Ginsburg, R., 2013, Experimental Deposition of Carbonate Mud from Moving Suspensions: Importance of Flocculation and Implications for Modern and Ancient Carbonate Mud Deposition, Journal of Sedimentary Research, v. 83, p. 1026-1032.

Schmitz, B., Harper, D. A. T., Peucker-Ehrenbrink, B., Stouge, S., Alwmark, C., Cronholm, A., Bergström, S. M., Tassinari, M., and Xiaofeng, W., 2008, Asteroid Breakup Linked to the Great Ordovician Biodiversification Event: Nature Geoscience, v. 1, p. 49-53.

Schulz, M., and Schäfer-Neth, C., 1997, Translating Milankovitch Climate Forcing into Eustatic Fluctuations via Thermal Deep Water Expansion: A Conceptual Link, Terra Nova, v. 9, p. 228-231.

Seilacher, A., 1967, Fossil Behavior, Scientific American, v. 217, p. 72-83.

Sjøtun, K., Husa, V., Asplin, L., and Sandvik, A. D., 2015, Climatic and Environmental Factors Influencing Occurrence and Distribution of Macrolage – a Fjord Gradient Revised, Marine Ecology Progress Series, v. 532, p. 73-88.

Song, H., Wignall, P. B., Song, H., Dai, X., and Chu, D., 2019, Seawater Temperature and Dissolved Oxygen over the Past 500 Million Years, Journal of Earth Science, v. 30, n. 2, p. 236-243.

Størmer, L., 1953, The Middle Ordovician of the Oslo Region, Norway, Norsk Geologisk Tidsskrift, v. 31, p. 37-141.

Štorch, P., Mitchell, C. E., Finney, S. C., and Melchin, M. J., 2011, Uppermost Ordovician (Upper Katian-Hirnantian) Graptolites of North-Central Nevada, U.S.A., Bulletin of Geosciences, v. 86, n. 2, p. 301-386.

Taylor, A. M., and Goldring, R., 1993, Description and Analysis of Bioturbation and Ichnofabric, Journal of the Geological Society, London, v. 150, p. 141-148.

Tinn, O., and Meidla, T., 1999, Ordovician Ostracods from the Komstad Limestone: Bulliten of the Geological Society of Denmark, v. 46, p. 25-30.

Torsvik, T. H., and Rehnström, E. F., 2003, The Tornquist Sea and Baltica-Avalonia Docking: Tectonophysics, v. 362, p. 67-82.

Torsvik, T. H., Ryan, P. D., Trench, A., and Harper, D. A. T., 1991, Cambrian-Ordovician Paleogeography of Baltica: Geology, v. 19, p. 7-10.

Trilobites of Norway, 2020, Paleontology & Nature: Geology in Slemmestad: https://www.trilobitesofnorway.com/ (accessed June 2020).

Tucker, M. E., 1985, Shallow-Marine Carbonate Facies and Facies Models, Geological Society of London Special Publications, v. 18, p. 147-169.

Van Wagoner, J. C., Posamentier, H. W., Mitchum, R. M., Vail, P. R., Sarg, J. F., Loutit, T. S., and Hardenbol, J., 1988, An Overview of the Fundamentals of Sequence Stratigraphy and Key Definitions, SEPM Special Publication No. 42, p. 39-45.

Walker, J. D., Geissman, J. W., Bowring, S. A., and Babcock, L. E., compilers, 2018, Geologic Time Scale v. 5.0: The Geological Society of America.

Webby, D. B., Paris, F., Droser, M. L., and Percival, I. G., eds., 2004, The Great Ordovician Biodiversification Event: New York, Columbia University Press, 484 p.

Westphal, H., Munnecke, A., Pross, J., and Herrle, J. O., 2004, Multiproxy Approach to Understanding the Origin of Cretaceous Pelagic Limestone-Marl Alternations (DSDP Site 391, Blake-Bahama Basin), Sedimentology, v. 51, p. 109-126.

Wu, R. C., Calner, M., Lehnert, O., Peterffy, O., and Joachimski, M. M., 2015, Lower-Middle Ordovician $\delta^{13}C$ Chemostratigraphy of Western Baltica (Jämtland, Sweden), Palaeoworld, v. 24, p. 110-122.

Young, S. A., Saltzman, M. R., Ausich, Desrochers, A., and Kaljo, D., 2010, Did Changes in Atmospheric CO_2 Coincide with the Latest Ordovician Glacial-Interglacian Cycles? Palaeogeography, Palaeoclimatology, Palaeoecology, v. 296, p. 376-388.

Zaaur, S., Affek, H. P., and Brandon, M. T., 2013, A Revised Calibration of the Clumped Isotope Thermometer: Earth and Planetary Science Letters, v. 382, p. 47-57.

Zecchin, M., and Catuneanu, O., 2013, High-Resolution Sequence Stratigraphy of Clastic Shelves I: Units and Bounding Surfaces, Marine and Petroleum Geology, v. 39, p. 1-25.

Zeller, M., Verwer, K., Eberli, G. P., Massaferro, J. L., Schwarz, E., and Spalletti, L., 2015, Depositional Controls on Mixed Carbonate-Siliclastic Cycles and Sequences on Gently Inclined Shelf Profiles, Sedimentology, v. 62, p. 2009-2037.

Appendix A: Field Logs

KBH Field Log		Location: 59.794224°N, 10.502400°E
Outcrop: Kyststein Beach Penninsula (KBH)	By: James J. Van Hook	Date: 09-28-2018

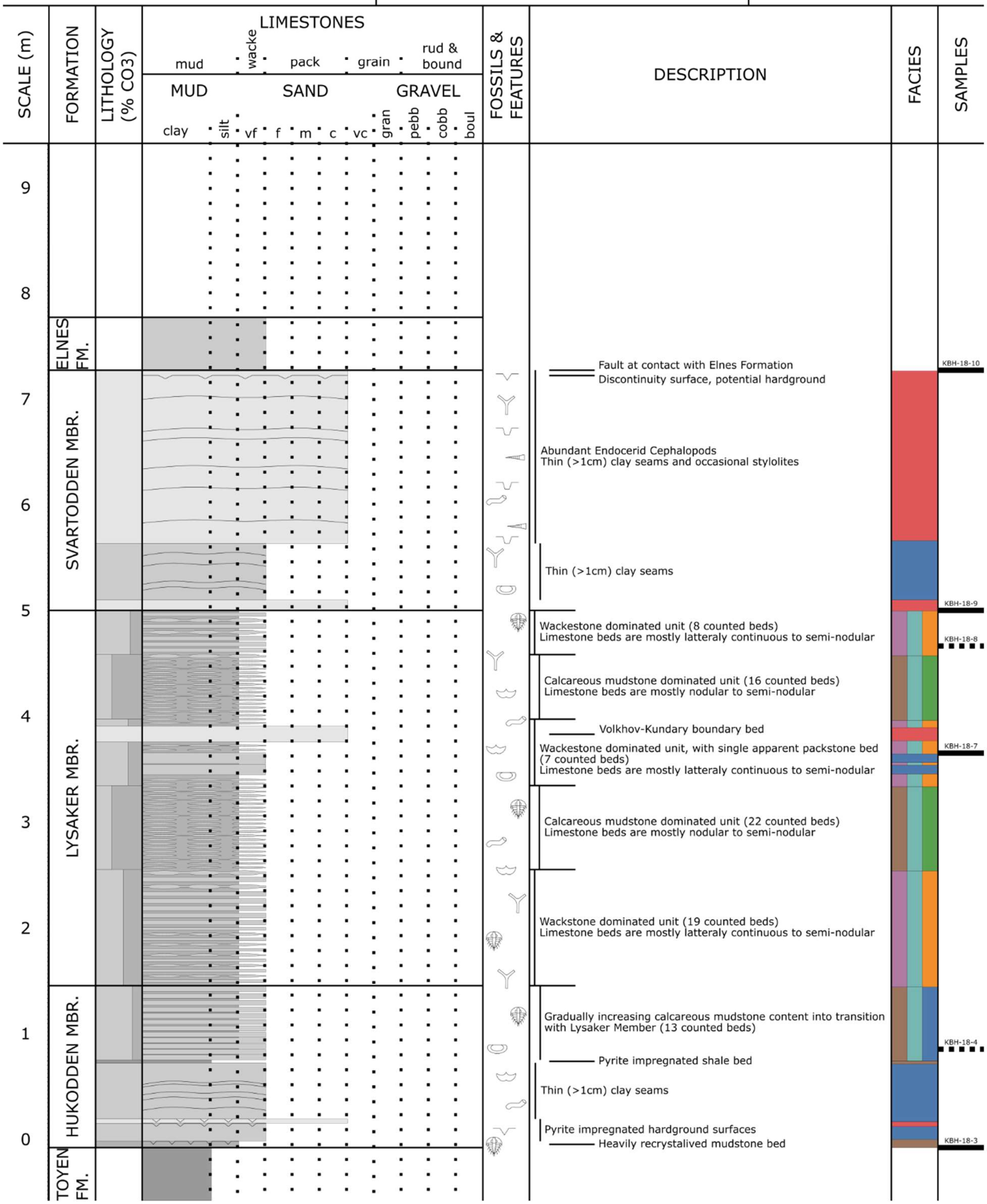

KYH Field Log		Location: 59.793863°N, 10.502873°E
Outcrop: Kyststein Trail Penninsula (KYH)	By: James J. Van Hook	Date: Date: 09-26-2018

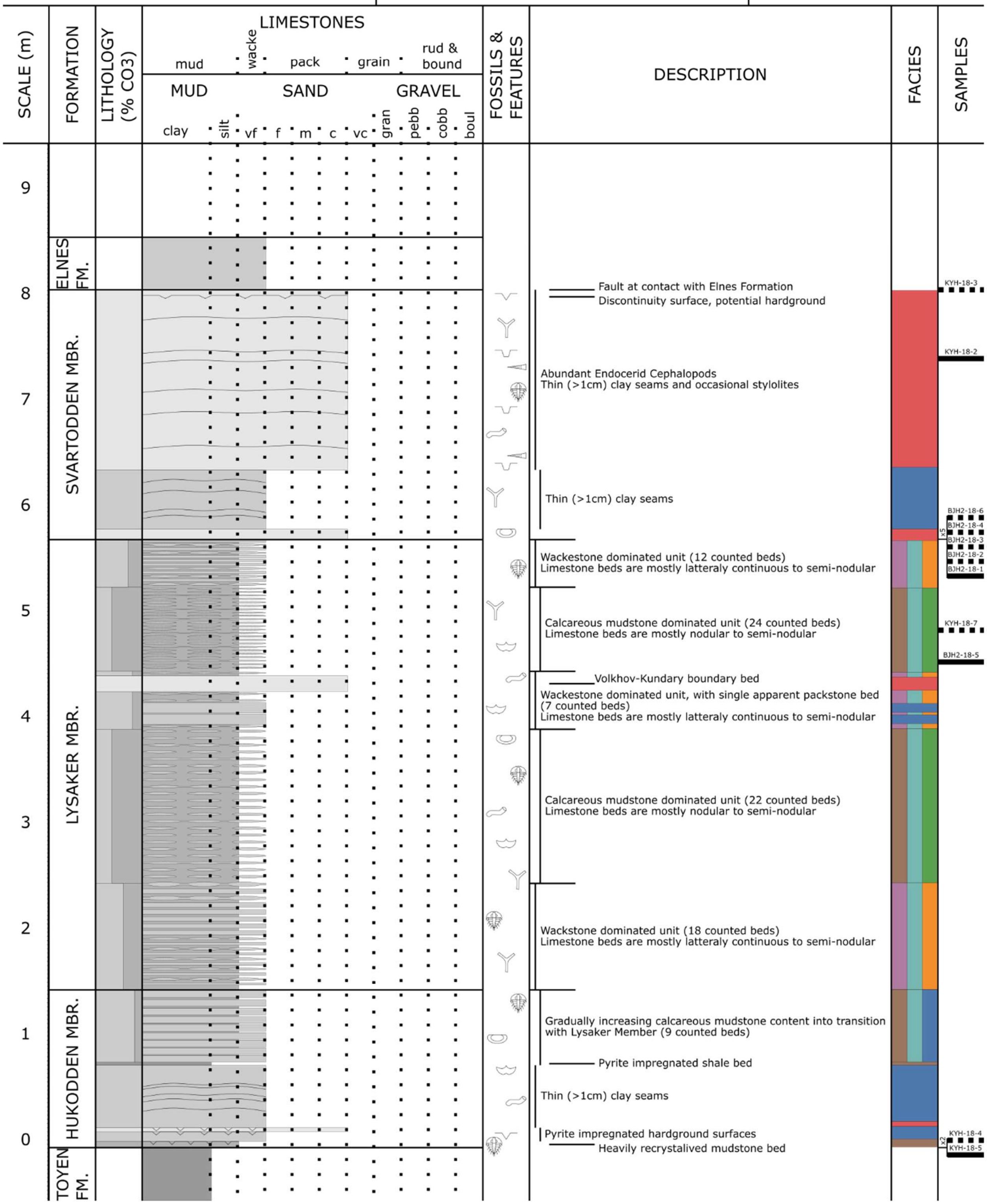

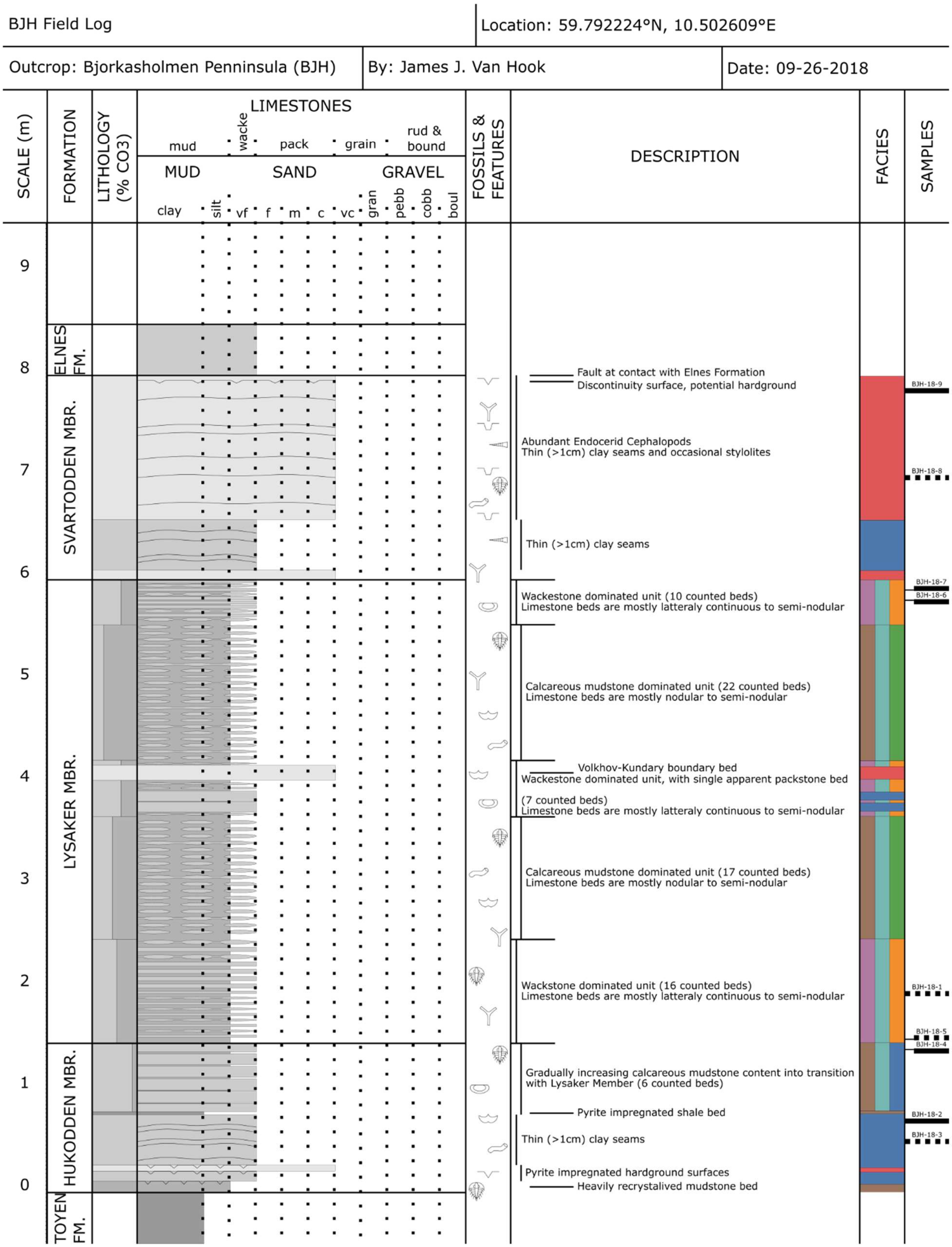

BJH Field Log
Location: 59.792224°N, 10.502609°E
Outcrop: Bjorkasholmen Penninsula (BJH)
By: James J. Van Hook
Date: 09-26-2018
SCALE (m)
FORMATION
LITHOLOGY (% CO3)
LIMESTONES
mud
wacke
pack
grain
rud & bound
MUD
SAND
GRAVEL
clay
silt
vf
f
m
c
vc
gran
pebb
cobb
boul
FOSSILS & FEATURES
DESCRIPTION
FACIES
SAMPLES
9
8
7
6
5
4
3
2
1
0
ELNES FM.
SVARTODDEN MBR.
LYSAKER MBR.
HUKODDEN MBR.
TOYEN FM.
Fault at contact with Elnes Formation
Discontinuity surface, potential hardground
Abundant Endocerid Cephalopods
Thin (>1cm) clay seams and occasional stylolites
Thin (>1cm) clay seams
Wackestone dominated unit (10 counted beds)
Limestone beds are mostly latteraly continuous to semi-nodular
Calcareous mudstone dominated unit (22 counted beds)
Limestone beds are mostly nodular to semi-nodular
Volkhov-Kundary boundary bed
Wackestone dominated unit, with single apparent packstone bed
(7 counted beds)
Limestone beds are mostly latteraly continuous to semi-nodular
Calcareous mudstone dominated unit (17 counted beds)
Limestone beds are mostly nodular to semi-nodular
Wackestone dominated unit (16 counted beds)
Limestone beds are mostly latteraly continuous to semi-nodular
Gradually increasing calcareous mudstone content into transition with Lysaker Member (6 counted beds)
Pyrite impregnated shale bed
Thin (>1cm) clay seams
Pyrite impregnated hardground surfaces
Heavily recrystalived mudstone bed
BJH-18-9
BJH-18-8
BJH-18-7
BJH-18-6
BJH-18-1
BJH-18-5
BJH-18-4
BJH-18-2
BJH-18-3

SLH Field Log	Location: 59.781272°N, 10.489550°E	
Outcrop: Slemmestad Road Cut (SLH)	By: James J. Van Hook	Date: 09-25-2018

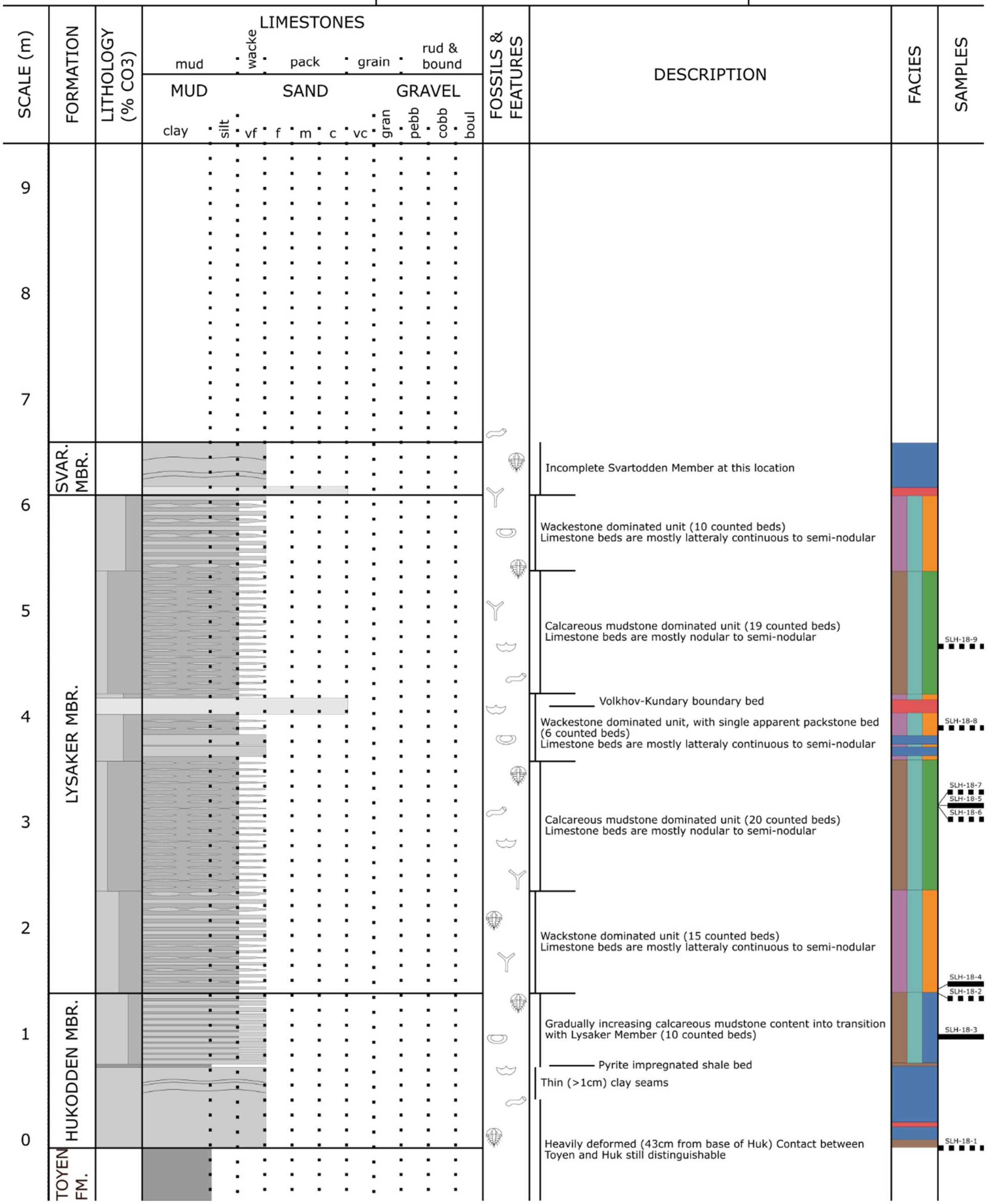

SFH Field Log		Location: 59.775949°N, 10.481403°E
Outcrop: Slemmestad Football Arena (SFH)	By: James J. Van Hook	Date: 09-27-2018

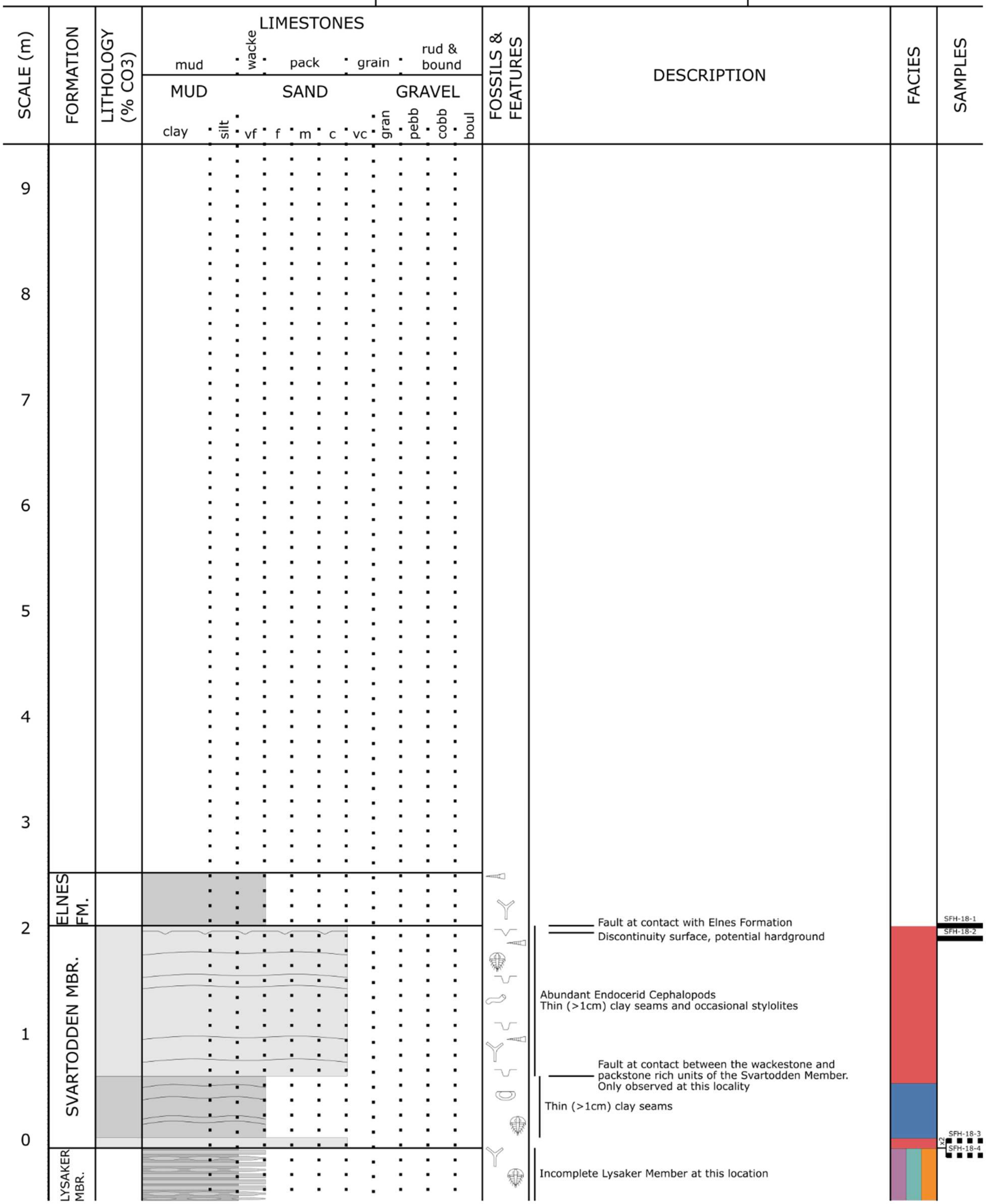

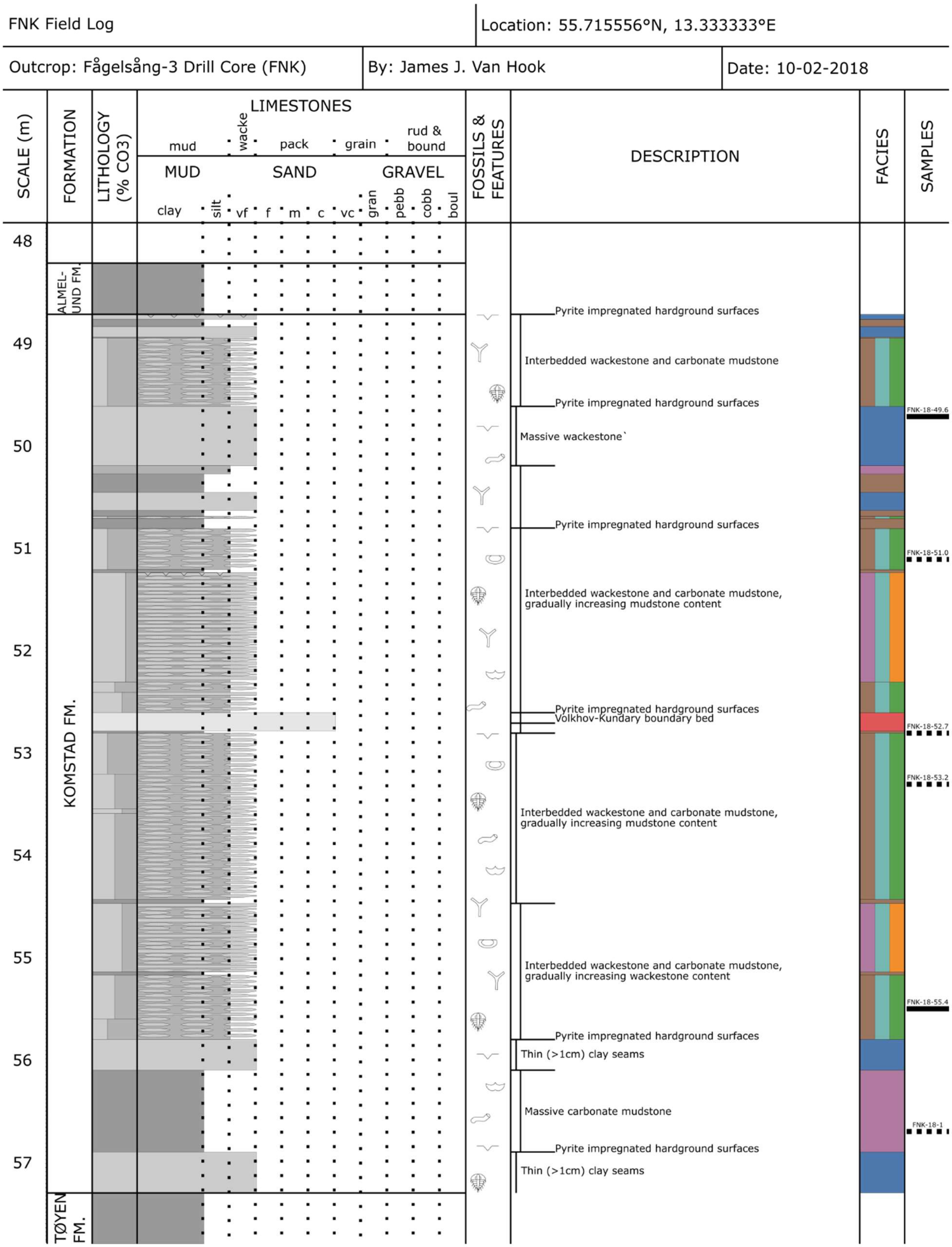

FNK Field Log
Location: 55.715556°N, 13.333333°E
Outcrop: Fågelsång-3 Drill Core (FNK)
By: James J. Van Hook
Date: 10-02-2018
SCALE (m)
FORMATION
LITHOLOGY (% CO3)
LIMESTONES
mud
wacke
pack
grain
rud & bound
MUD
SAND
GRAVEL
clay
silt
vf
f
m
c
vc
gran
pebb
cobb
boul
FOSSILS & FEATURES
DESCRIPTION
FACIES
SAMPLES
48
49
50
51
52
53
54
55
56
57
ALMEL-UND FM.
KOMSTAD FM.
TØYEN FM.
Pyrite impregnated hardground surfaces
Interbedded wackestone and carbonate mudstone
Pyrite impregnated hardground surfaces
Massive wackestone`
Pyrite impregnated hardground surfaces
Interbedded wackestone and carbonate mudstone, gradually increasing mudstone content
Pyrite impregnated hardground surfaces
Volkhov-Kundary boundary bed
Interbedded wackestone and carbonate mudstone, gradually increasing mudstone content
Interbedded wackestone and carbonate mudstone, gradually increasing wackestone content
Pyrite impregnated hardground surfaces
Thin (>1cm) clay seams
Massive carbonate mudstone
Pyrite impregnated hardground surfaces
Thin (>1cm) clay seams
FNK-18-49.6
FNK-18-51.0
FNK-18-52.7
FNK-18-53.2
FNK-18-55.4
FNK-18-1

Appendix B: Thin Section Micrographs

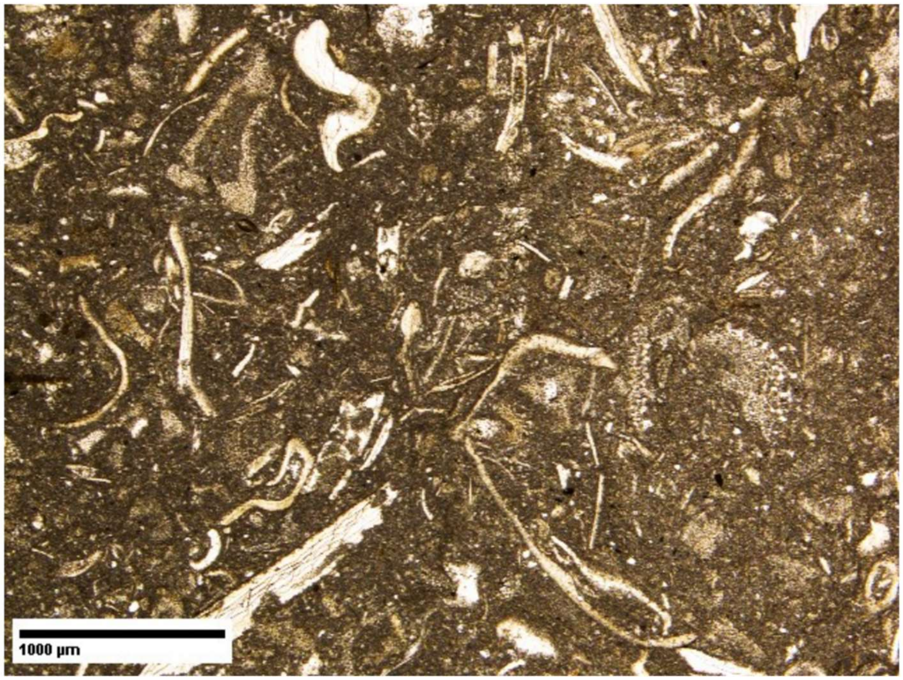

KBH-18-10: Huk Formation sample recovered from KBH 7.35m from base of outcrop (composite recovery height of 7.9m from base). Facies 4a.

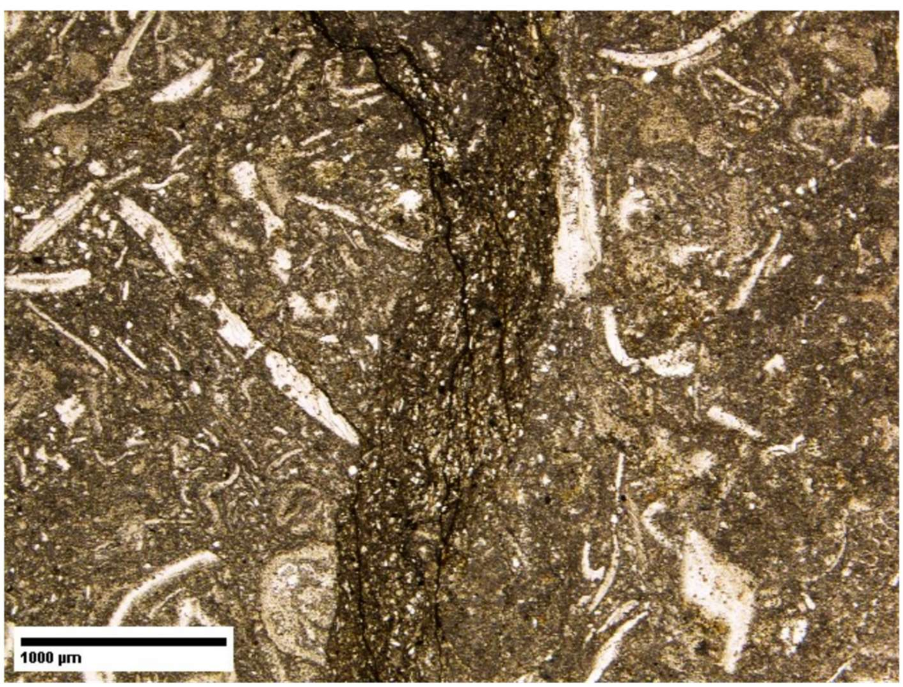

SFH-18-1: Huk Formation sample recovered from SFH 2.10m from base of outcrop (composite recovery height of 7.9m from base). Facies 4a.

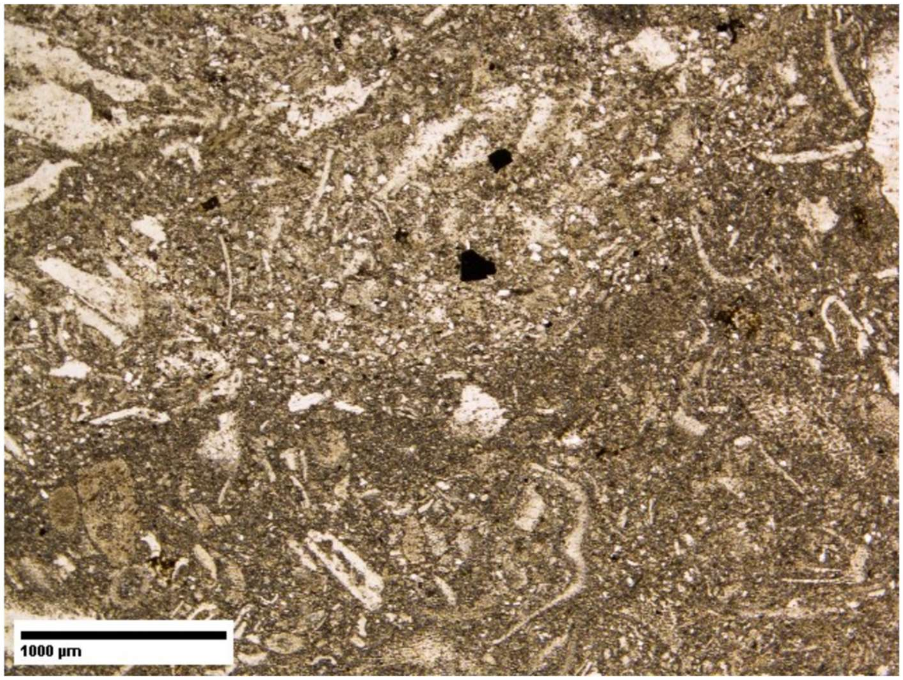

SFH-18-2: Huk Formation sample recovered from SFH 1.98mm from base of outcrop (composite recovery height of 7.8m from base). Facies 4a.

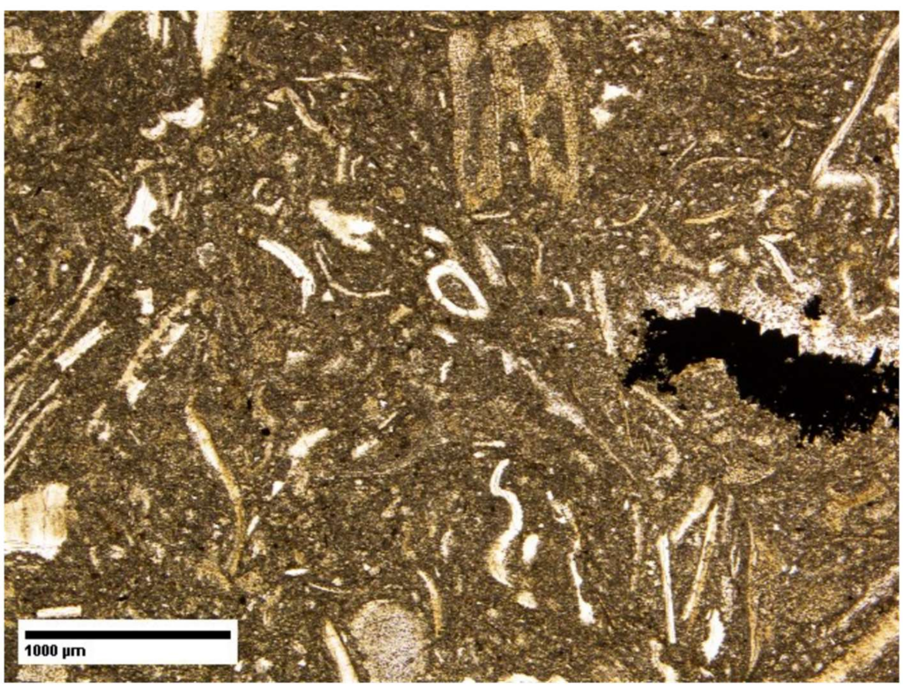

BJH-18-9: Huk Formation sample recovered from BJH 7.85m from base of outcrop (composite recovery height of 7.7m from base). Facies 4a.

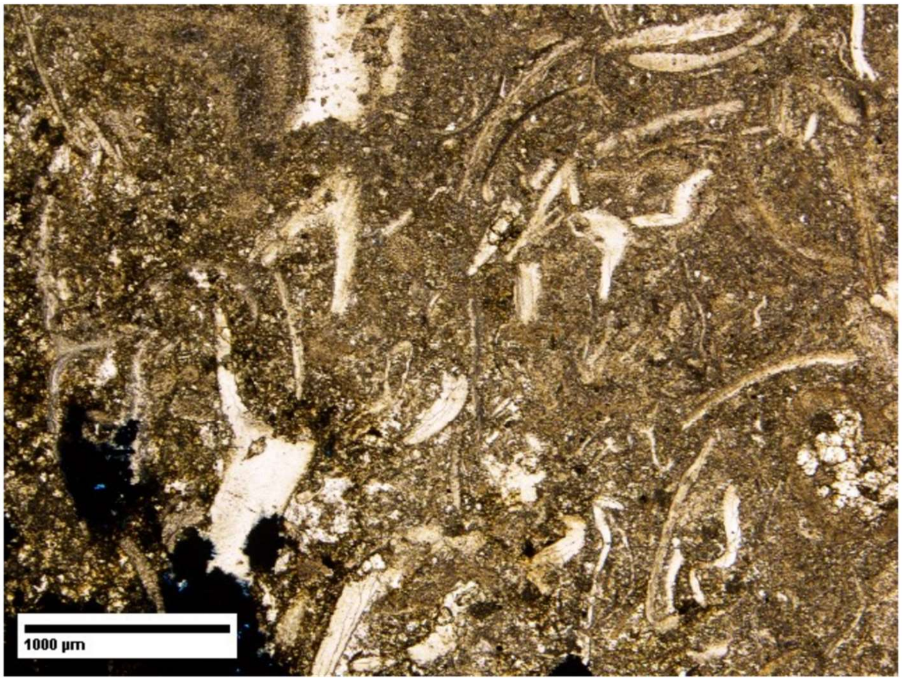

KYH-18-2: Huk Formation sample recovered from KYH 7.46m from base of outcrop (composite recovery height of 7.3m from base). Facies 4a.

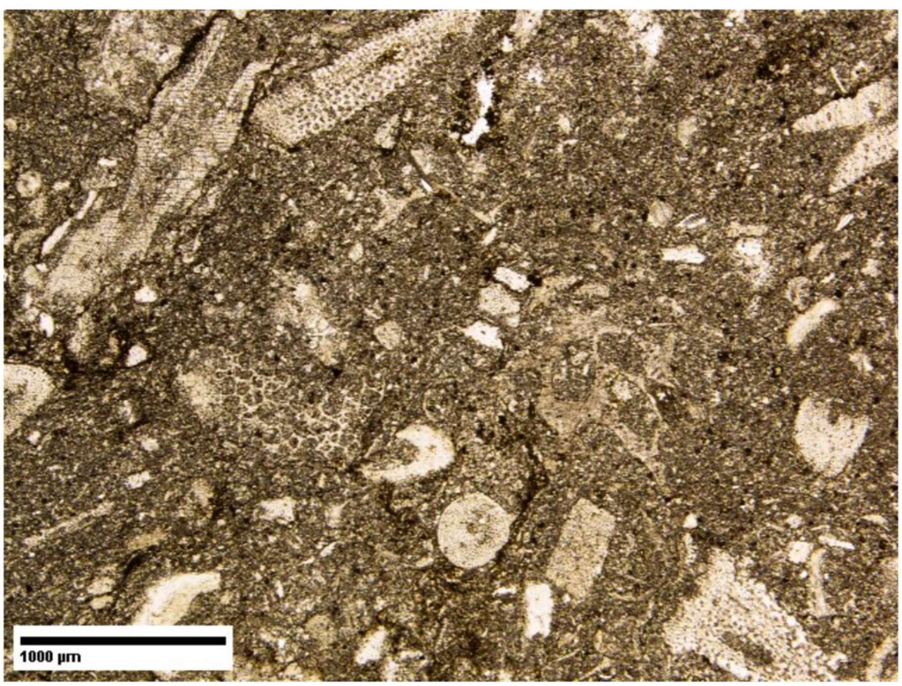

KBH-18-9: Huk Formation sample recovered from KBH 5.08m from base of outcrop (composite recovery height of 5.7m from base). Facies 4a.

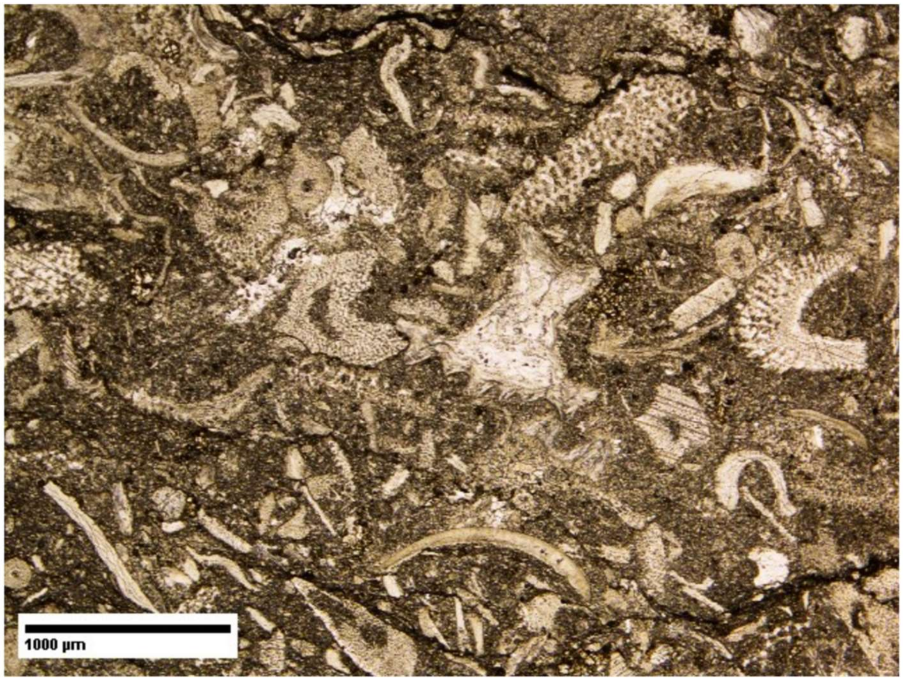

BJH2-18-1: Huk Formation sample recovered from KYH 5.75m from base of outcrop (composite recovery height of 5.7m from base). Facies 4a.

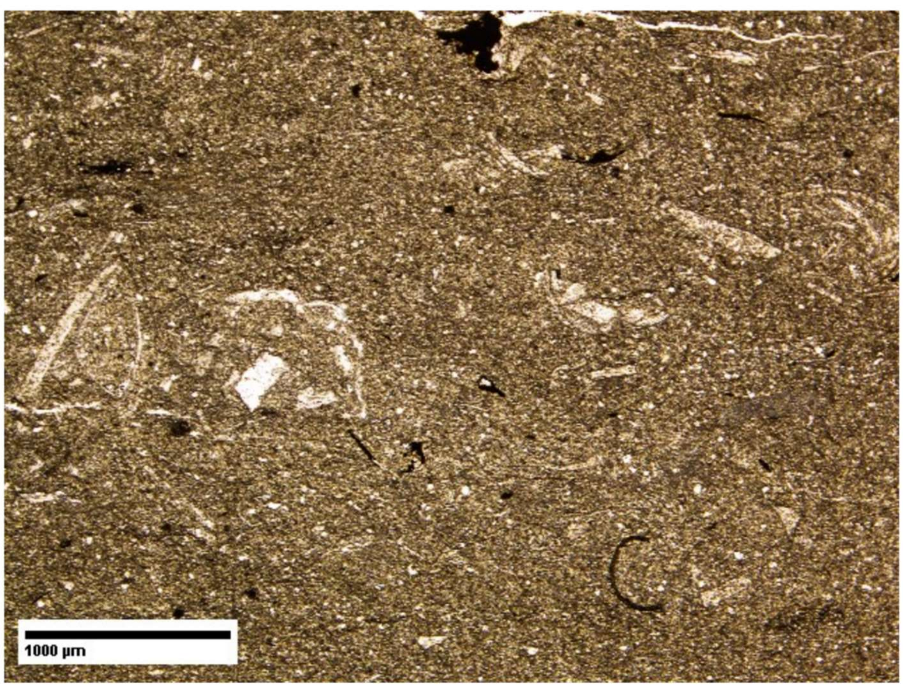

BJH-18-7: Huk Formation sample recovered from BJH 5.90m from base of outcrop (composite recovery height of 5.6m from base). Facies 1 with minor amounts of facies 2.

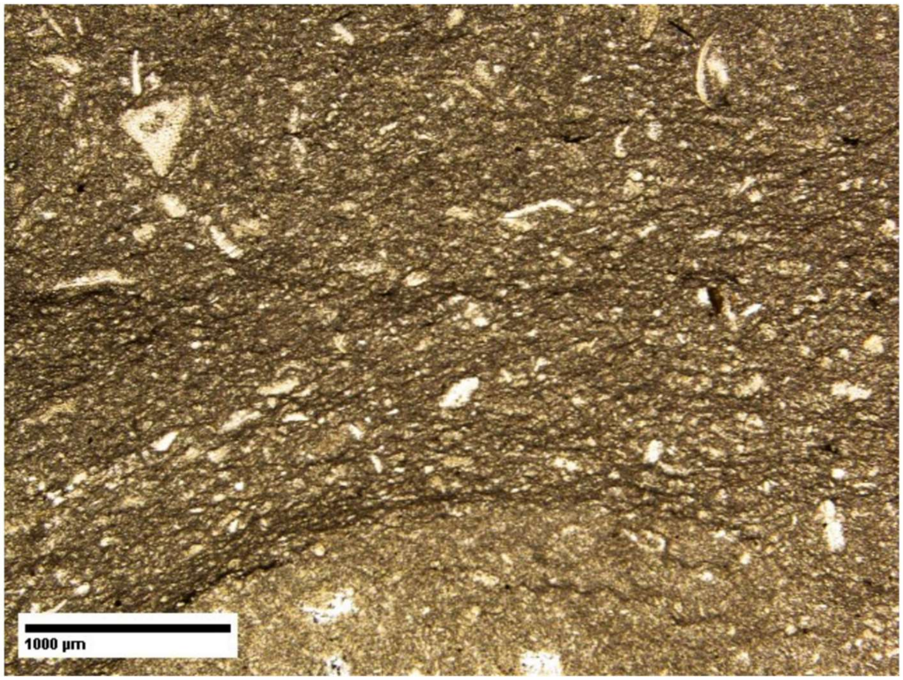

BJH-18-6: Huk Formation sample recovered from BJH 5.80m from base of outcrop (composite recovery height of 5.5m from base). Facies 2 with partial burrow at the bottom of the sample. Note preferential grain orientations and mud halos surrounding the burrow.

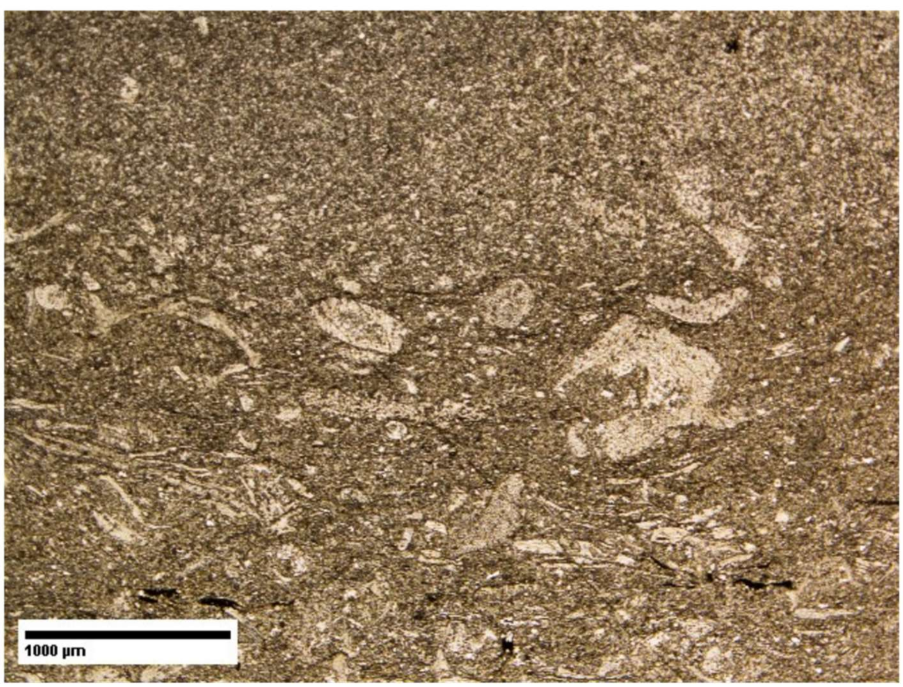

BJH2-18-5: Huk Formation sample recovered from KYH 4.59m from base of outcrop (composite recovery height of 4.6m from base). Facies 1 (top) and facies 3b (bottom).

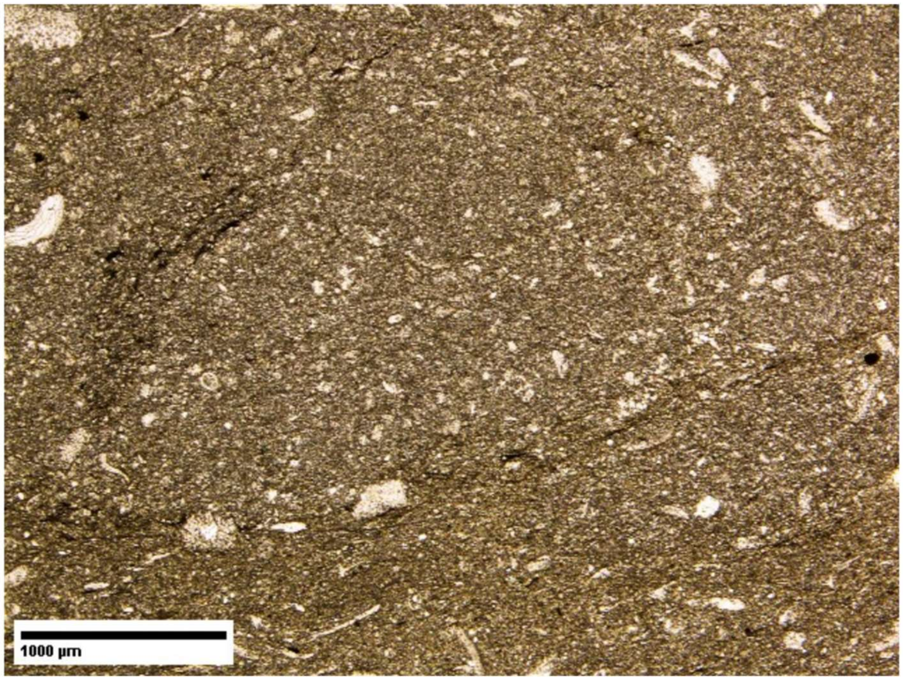

KBH-18-7:Huk Formation sample recovered from KBH 3.73m from base of outcrop (composite recovery height of 3.9m from base). Mixed facies 1 and facies 2. Note potential burrow with muddy halo in the center of the sample.

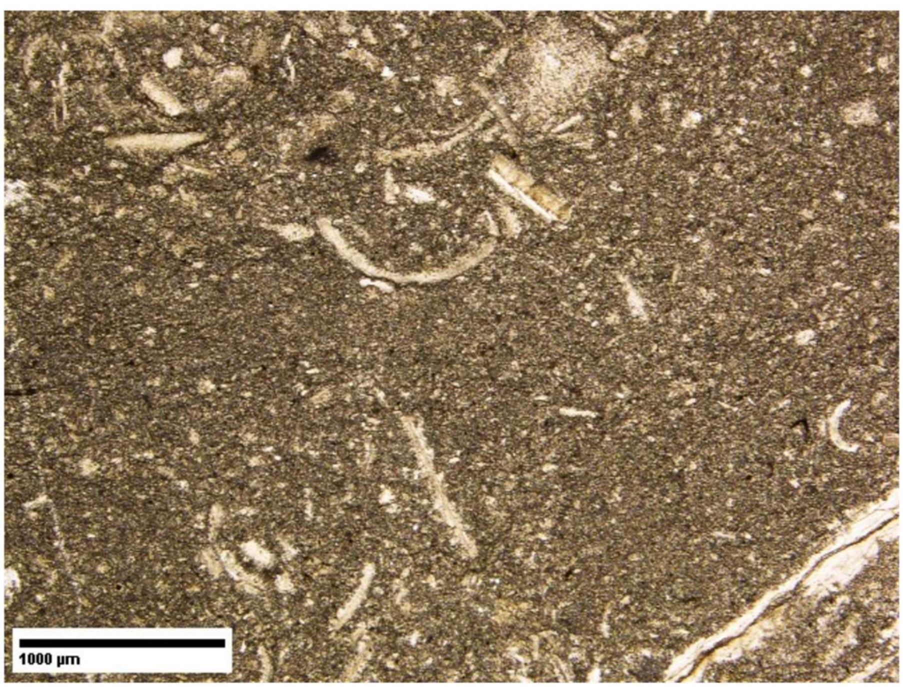

SLH-18-5: Huk Formation sample recovered from SLH 3.23m from base of outcrop (composite recovery height of 3.1m from base). Facies 3a.

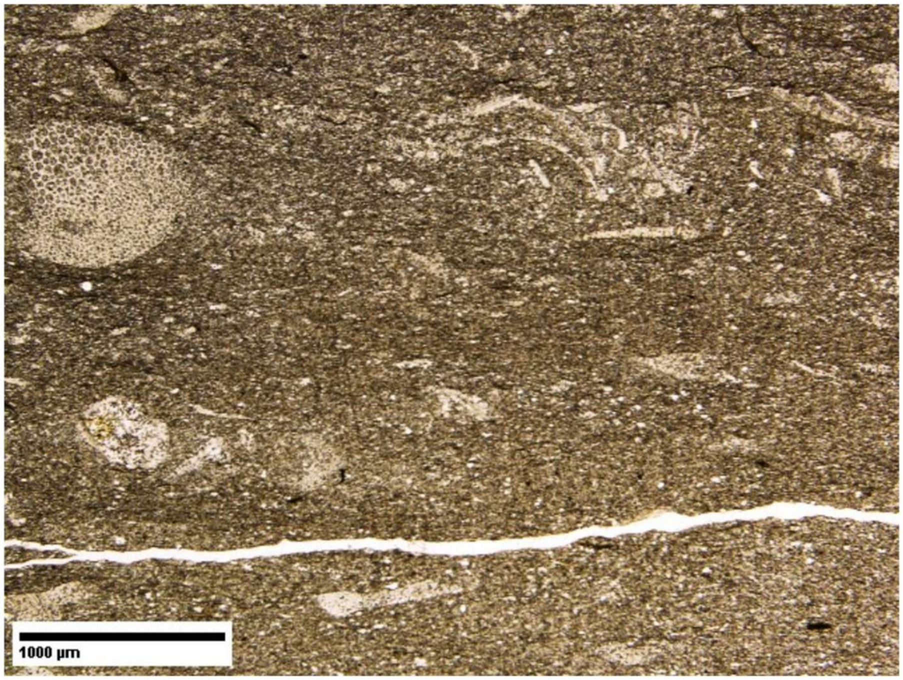

SLH-18-4: Huk Formation sample recovered from SLH 1.50m from base of outcrop (composite recovery height of 1.5m from base). Facies 1 near the bottom of the sample and facies 2 making up the top of the sample. Note calcite seam running across the bottom of the sample.

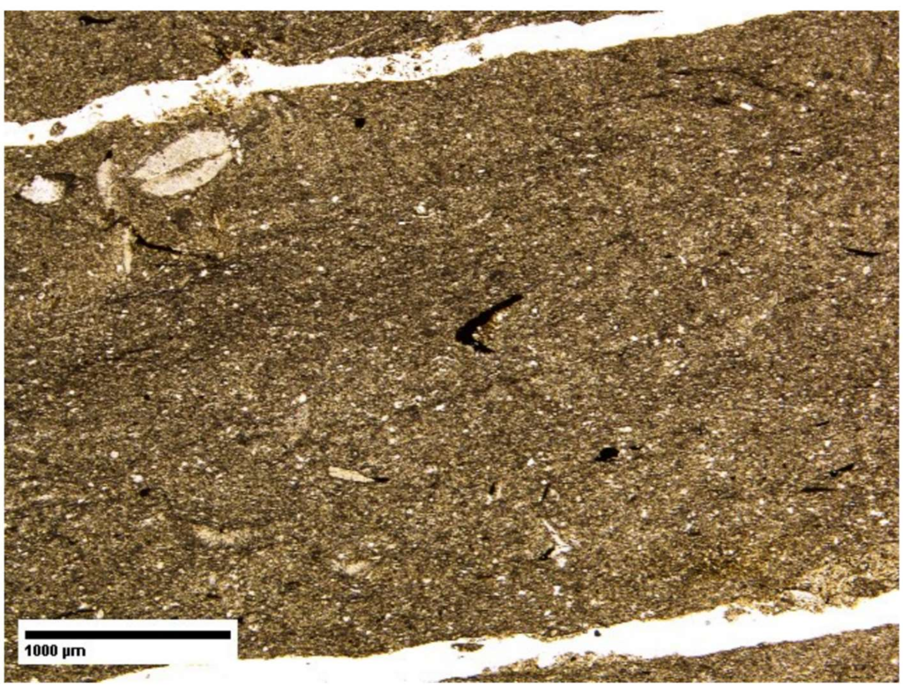

BJH-18-4: Huk Formation sample recovered from BJH 1.40m from base of outcrop (composite recovery height of 1.4m from base). Facies 2 with two parallel calcite seams.

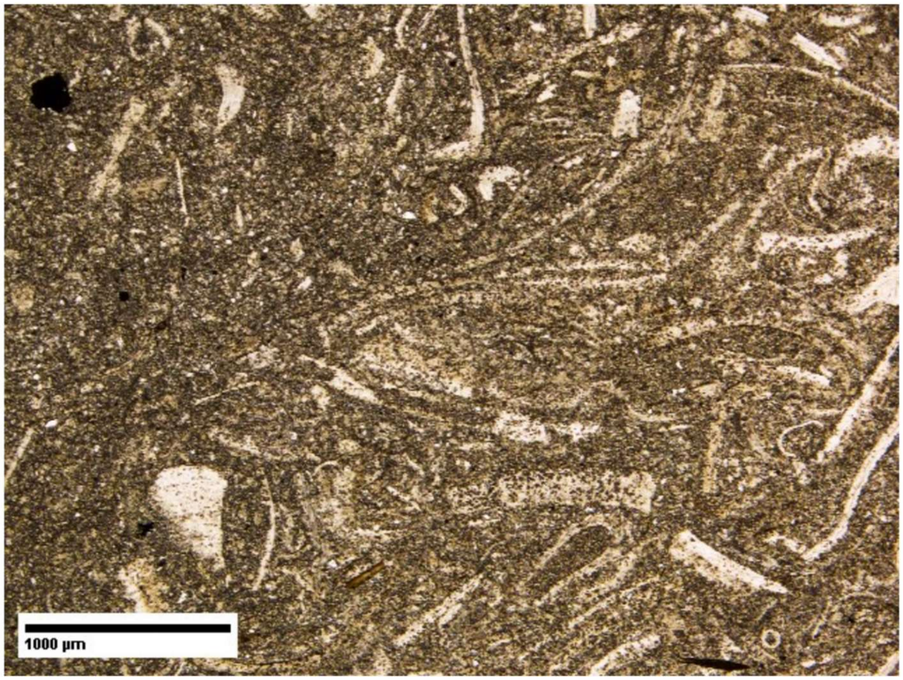

SLH-18-3: Huk Formation sample recovered from SLH 1.05m from base of outcrop (composite recovery height of 1.5m from base). Facies 3c.

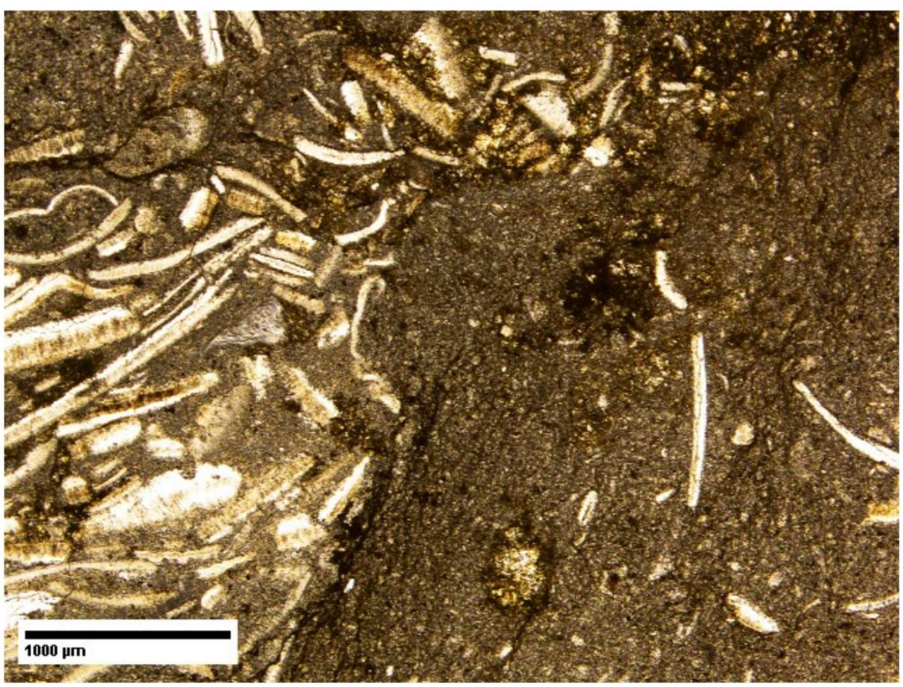

BJH-18-2: Huk Formation sample recovered from BJH 0.70m from base of outcrop (composite recovery height of 0.7m from base). Facies 4b packstone pocket within facies 1.

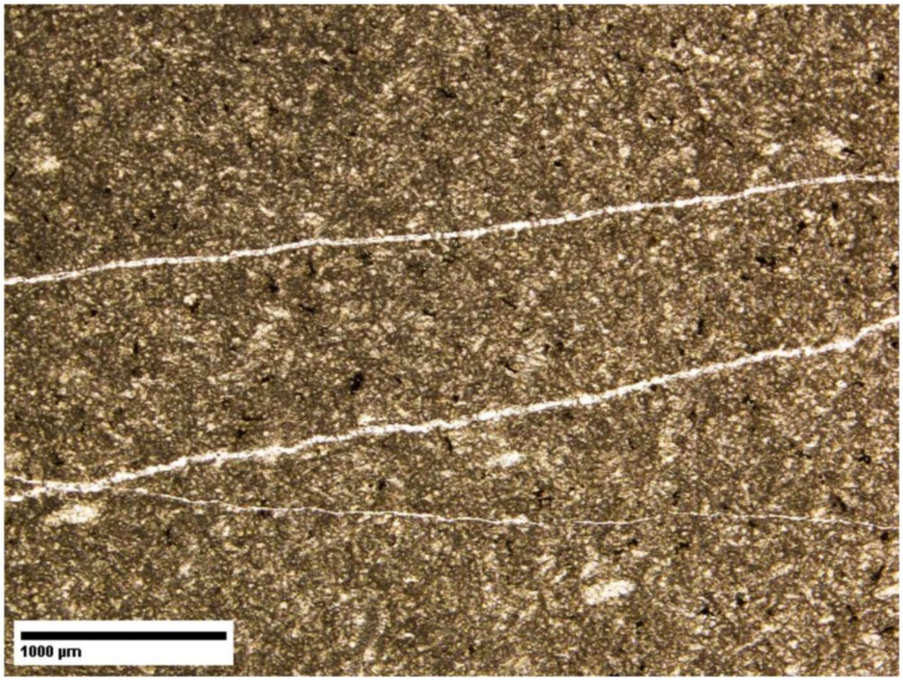

KBH-18-3: Huk Formation sample recovered from KBH 0.00m from base of outcrop (composite recovery height of 0.00m from base). Heavily recrystallized facies 1.

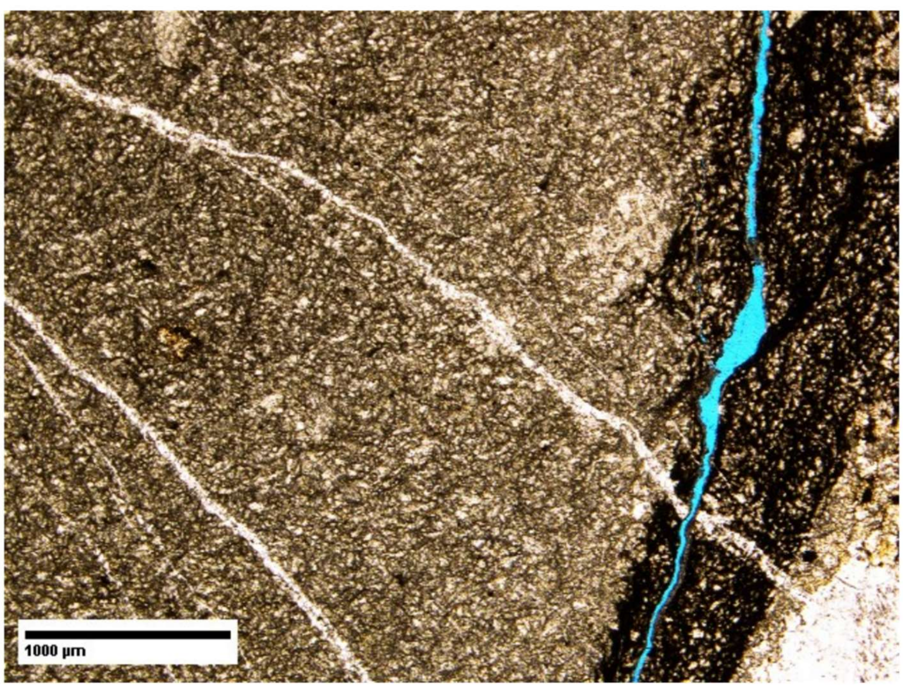

KYH-18-5: Huk Formation sample recovered from KYH 0.00m from base of outcrop (composite recovery height of 0.00m from base). Heavily recrystallized facies 1 with clay seam on the right side of the sample.

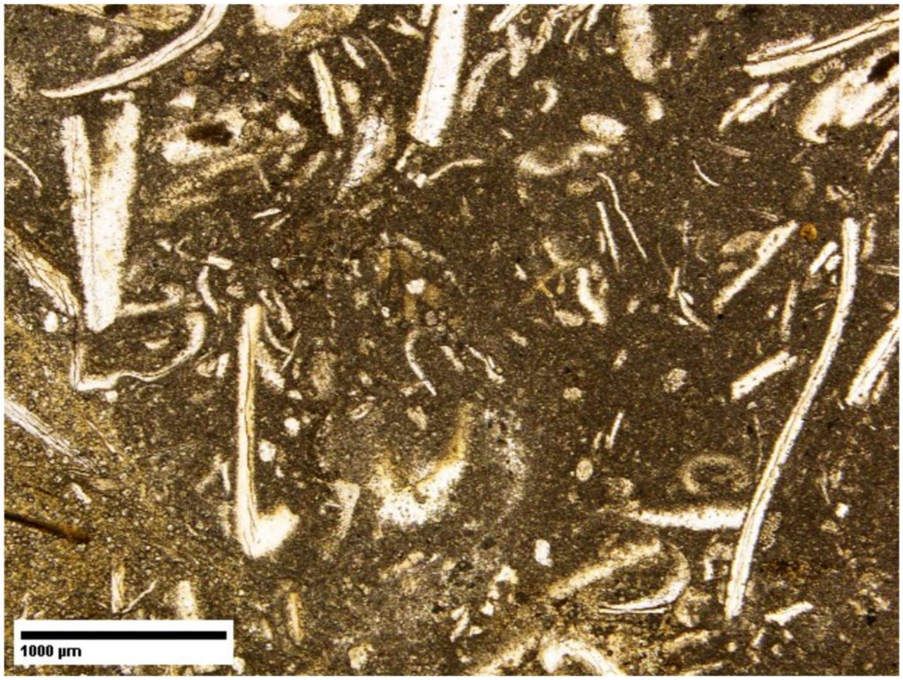

FNK-18-49.6: Komstad Formation sample recovered at a core depth of 49.6m. Facies 4a.

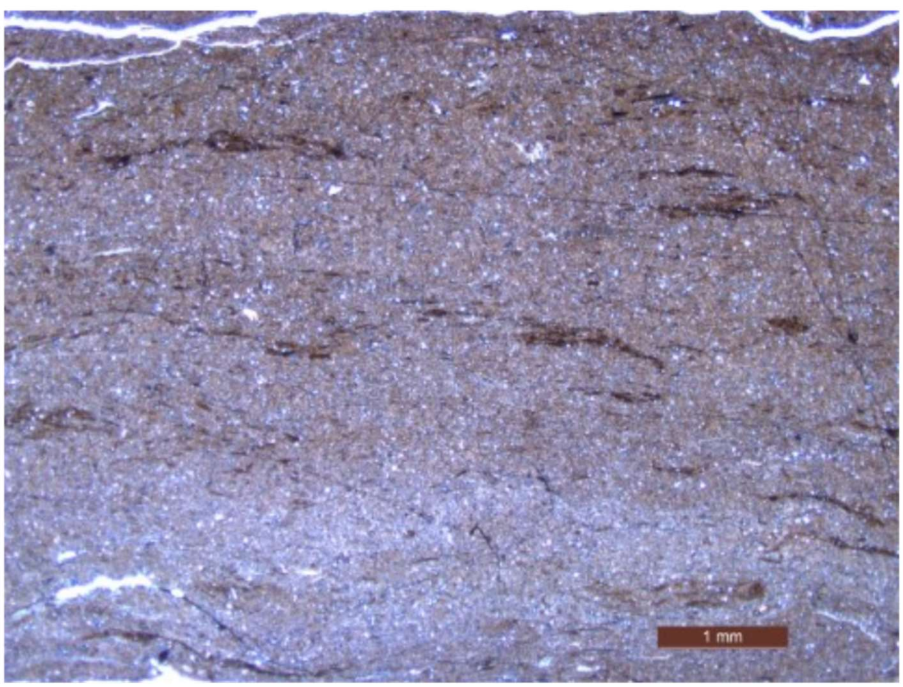

FNK-18-51.0: KomstadFormation sample recovered at a core depth of 51.0m. Facies 2. Note calcite seams at the topof the sample.

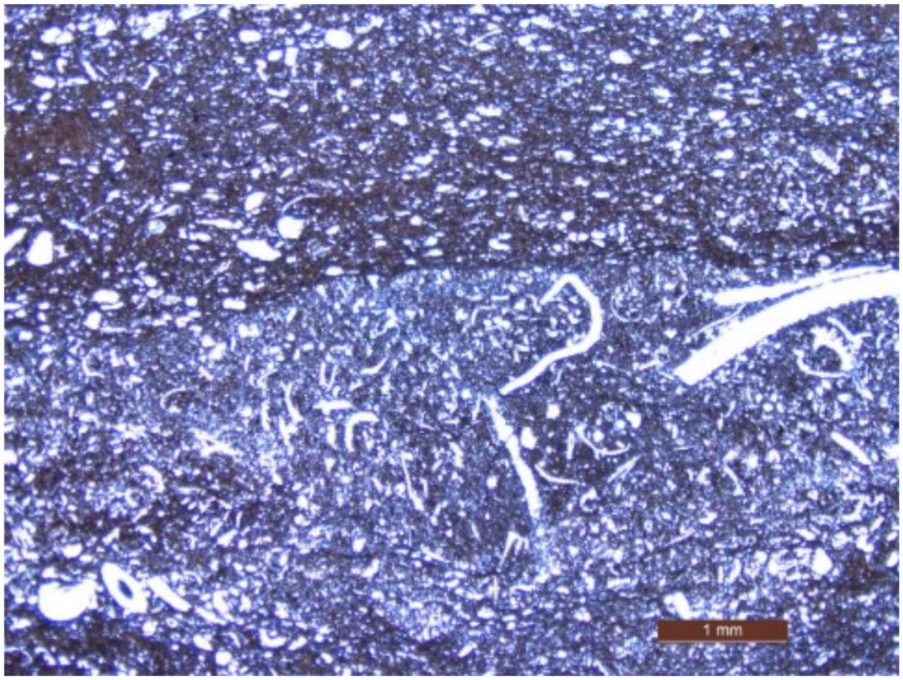

FNK-18-52.7: Komstad Formation sample recovered at a core depth of 52.7m. Facies 3c.

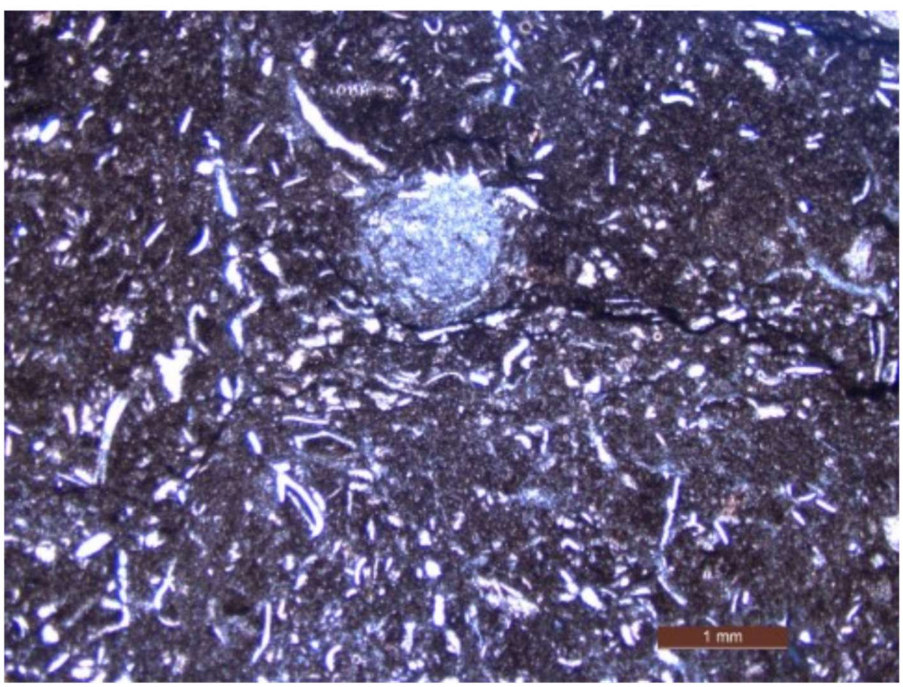

FNK-18-53.2: Komstad Formation sample recovered at a core depth of 53.2m. Facies 3a.

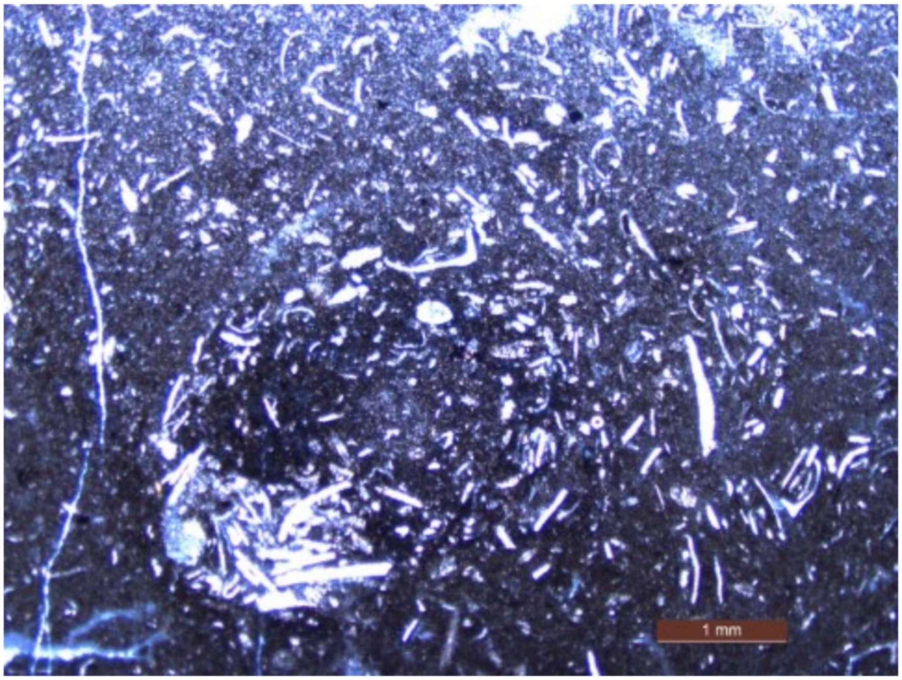

FNK-18-55.0: Komstad Formation sample recovered at a core depth of 55.0m. Facies 2 making up the majority of the sample mixed with facies 3a.

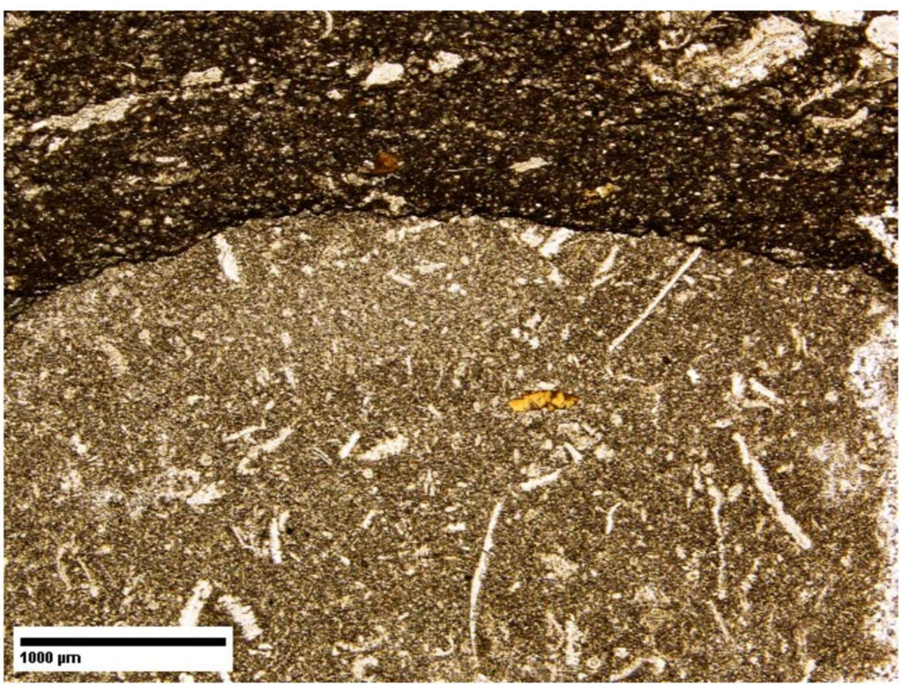

FNK-18-55.4: Komstad Formation sample recovered at a core depth of 55.4m. Contact with facies 1 (top) and facies 3a (bottom).

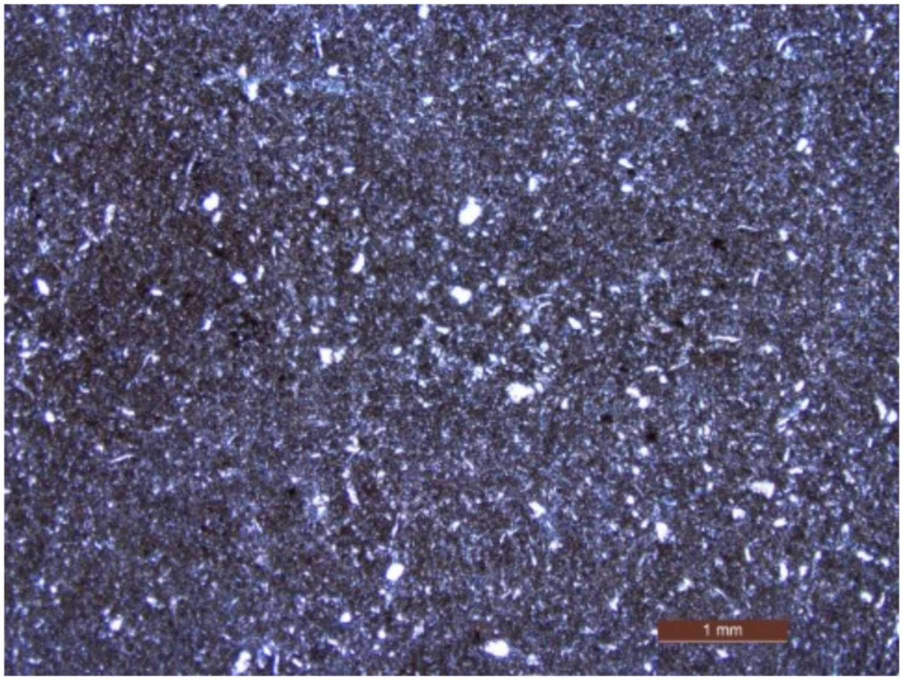

FNK-18-1: Komstad Formation sample recovered at a core depth of 57.4m. Facies 1.